Gerald Birngruber, B.Sc.

Digital Energy Twin: A data-driven approach to analyze and optimize industrial energy systems

Master's Thesis

to achieve the university degree of

Diplom-Ingenieur

Master's degree programme: Computer Science

submitted to

Graz University of Technology

Institute for Softwaretechnology

Supervisor
Univ.-Prof. Dipl.-Ing. Dr.techn. Wotawa Franz

Co-Supervisor
Mag.phil. Dr.techn. MA MA Schweiger Gerald

Graz, April 2021

Affidavit

I declare that I have authored this thesis independently, that I have not used other than the declared sources/resources, and that I have explicitly indicated all material which has been quoted either literally or by content from the sources used. The text document uploaded to TUGRAZonline is identical to the present master‘s thesis.

Date

Signature

Acknowledgements

I would like to thank my supervisor Franz Wotawa for the support by correcting my thesis and providing feedback for the work. A special thanks goes to Gerald Schweiger, my Co-Supervisor. He employed me in his research group and gave me tremendous background knowledge for the thesis. Further, he established connections to project partners of the Digital Energy Twin (DET) project. He spent endless hours correcting my thesis drafts, answering my questions, and supporting me wherever possible. Special mention goes to the members of my research group. Thomas Schranz and Thomas Schwengler helped me with my entrance into research and gave generous support in solving technical issues. A special thanks also goes to my colleague and lab partner Michael Grömer. With his help, it was possible to organize and perform the lab experiment at the TU Graz physics department. He also had good ideas for the data model creation. He was very pleasant to work with.

The lab experiment had some more supporters. In the first place, there was Markus Koch, who provided a laboratory room and equipment for the experimentation. He also helped with ideas for funding the experiment. The money was then offered by the NAWI Graz organization, which has a budget for student projects. Thank you, NAWI Graz, for the trust in our work and the funding. Some loaned equipment we borrowed from my former employers Greiner Bio-One Diagnostics GmbH and Genspeed Biotech GmbH. The equipment lent by you made our experiment possible in the first place, allowed us to do more precise measurements, and saved our budget.

The last words of gratitude go to the project partners of the DET project and first of all to the organizantion unit for the whole project AEE INTEC. Ahmed Junaid Tahir and Carles Ribas Tugores are enthusiastic about pushing the project forward. Many thanks to Carles Ribas Tugores for supporting me in the modeling part of the thesis and always took the time to answer my questions and debug my created models. Many thanks also to Ahmed Junaid Tahir for the organization of all the meetings, workshops, and submissions. He always tried to support me, and together we found the right solutions for upcoming problems. Another valuable partner is ENERTEC Naftz & Partner GmbH & Co KG, especially Eugen Naftz and Angelika Swatek. They have excellent knowledge about the processes and machines in the electroplating plant and spent hours patiently explaining many details for the modeling part.

Abstract

Climate change affects everyone. A primary culprit is CO_2 emission. Reduction of CO_2 emission could curb climate change. Process optimization can save energy and thereby reduce CO_2emission. In Industry 4.0, a digital twin (DT) is a key-enabler for process optimization. This work is part of an Austrian Research Promotion Agency (FFG) project. The FFG project aims to build a digital twin for an electroplating plant. Within this thesis, the main goals are the improvement, simplification, and extension of existing parts. This thesis consists of two parts. The first part is the extension of a DT model with control mechanisms for machines and processes. The second part describes the development of data models. The data models deliver data as input for the digital twin model. In the first place, the DT needs an approximation for the electroplating process. A lab experiment took place to collect data about the process. Data models are generated with the collected data, which delivers the energy consumption depending on various input parameters. Besides the electroplating, there are a lot of other components. The plant provides a massive amount of sensor data. However, it is too much data; thus, the computations for the DT get too time-consuming. An automated function-based approximation of the data solves the problem. The DT is implemented in Modelica. Modelica is a multidomain modeling language for physical models. The results of the modeling part are control extensions for the existing machines and processes. Various programming languages, such as Python, can provide input for the Modelica models. Thus all approximations and data models are Python programs. The lab experiment took place at the TU Graz physics department. The data models use various machine learning algorithms like polynomial regression, decision tree regression, random forest regression, and neural networks to generate input for the Modelica model. There is also a discussion about the machine learning methods and their performance to handle a problem and when it is better to find another prediction method, such as function-based

approximation. It uses optimizer functions to fit the given functions best to real data and return the functions' parameters. Thus the function predicts future events. The result is a framework that creates predictions for machine data in arbitrary time frames. Altogether the separately developed parts work well together. With the optimizations, the computations are faster. The predictions are not as exact as real data, but they approximate the real data well, and therefore, it is an excellent trade to lose a little precision but receive better computation times. This leads to faster development and has benefits for the progress of the whole project.

Contents

1. Introduction

> *Die Klimakrise ist im vergangenen Jahr durch die Pandemie aus den Schlagzeilen gerutscht. Sie ist aber deswegen nicht verschwunden - im Gegenteil. [...]*
> *Wir stehen vor der größten Herausforderung der Menschheit in diesem Jahrtausend. Einer größeren Herausforderung als jener durch die Pandemie. Und gegen die Klimakrise wird es keine Impfung geben. Da sind wir alle selbst gefordert. Es wird ein Wettlauf mit der Zeit. Aber wir können ihn gewinnen. Wir müssen ihn gewinnen, wollen wir diesen Planeten für uns Menschen gut bewohnbar halten.* - Alexander Van der Bellen (president of austria) in Austria's Virtual New Year's Reception 2021

Due to the presence of Sars-CoV-2 in the daily news, climate change has moved into the background again, but it is still essential and will affect our daily lives more and more - a few examples: Food prices rise because raw ingredients, like wheat, are threatened by heatwaves (Hasegawa et al., 2018). The number of natural disasters rose in the past few years (Wuebbles et al., 2017). Drinking water is becoming less and less, or more challenging to tap (Watts et al., 2016).

Greenhouse gases (GHG) are responsible for climate change. IPCC (Intergov. Panel Clim. Change), 2018 and Owusu and Asumadu-Sarkodie, 2016 define Carbon dioxide (CO_2), Methane (CH_4), Nitrous oxide (N_2O), Hydrofluorocarbons (HFCs), Perfluorocarbons (PFCs) and Sulphur hexafluoride (SF_6) as GHGs. The GHGs block the radiation from earth towards space. Thus more radiation stays within the atmosphere and raises the temperature on earth (El Zein and Chehayeb, 2015).

CO_2 has the greatest impact on the ozone layer. It has increased by more than 35% since the pre-industrial time (Reay et al., 2007; Owusu and

Asumadu-Sarkodie, 2016). As Reay et al., 2007 shows, the two main sectors of CO_2emission are energy production and industrial processes. Since these two sectors are the biggest CO_2producers, small reductions in these sectors have a massive impact on overall CO_2 emissions. Nowadays, the industry grows nearly every year, with two exceptions in the past twenty years. The first exception was the economic crisis in 2008 and the second exception is the current corona crisis. The crises had a massive impact on the industry and the gross domestic product (GDP). The GDP is an indicator of the development in industry and economy. Over the past ten years, the GDP grows by 0.7% every year on average in Austria (WKO Austria, 2020). A growing industry leads to increased energy consumption. Flauger et al., 2020 say that the need for energy will rise tremendously in the next years. They see one of the main reasons for the increasing consumption in the electrification of industrial processes. Instead of using coal, oil, and gas for heating, cooling, and energy-intensive processes, the industry uses electric energy to generate heat for processes. Currently, the primary sources of electric energy are coal, oil, and gas (International Energy Agency, 2019), but electricity can also be created from renewable sources like water, wind, or solar power. Then electric energy is renewable and CO_2-neutral energy. Forecasts say that the rise of renewable energy resources cannot cover the demand of energy needed in the next years. The world cannot achieve 100% renewable energy without (i) a decline in energy consumption, (ii) improvement of the efficiency in energy generation, and (iii) the increase of the share of renewable energy (Masson-Delmotte et al., 2018).

The growing industry does not only mean growing energy consumption. It also implies modernization, which newer plants reach. In contrast to earlier plants, newer ones use a massive number of sensors to collect data. The data is meaningful for the product's quality, process monitoring, energy supply monitoring, controlling, and various other parameters. The gathered data controls the machines' process and allows a fine-grained setting because the controller can react faster with the permanently added data. The permanent measurements and the resulting settings lead to products of higher quality and a lower rejection rate.
Digitization and the continuous increase of computational power are fundamental parts of Industry 4.0 (Lasi et al., 2014; Bendel, 2019). In Industry 4.0, machines and production equipment are capable of decision-making.

With the data from sensors, connections to other devices, and Artificial intelligence (AI), which processed the data, it is possible to autonomously monitor the system and support operators and decision-makers in defining the next steps. With continuous learning, AI can more and more make its own decisions.

System control and control optimization are important features in Industry 4.0 (Uhlemann, Lehmann, and Steinhilper, 2017). The first step requires a digital copy of the system. With the collected data, the digital copy can emulate the represented system, and in the last step, the digital system can control the real system. This system is called a Digital Twin (DT). For more details on DT, see Chapter 2.1. With a DT, it is possible to perform optimization on a digital level and simulate its new behavior. With this setup, it is easy to optimize the system for different parameters without affecting the real production system. One of these parameters is energy consumption and, in conclusion, the reduction of CO_2emissions.

There are multiple ways to reduce CO_2emissions. On the one hand, there is renewable energy, and on the other hand, there is energy optimization. Since the industry is strongly dependent on the environmental conditions, it is not always possible to rely on renewable energy, but reducing energy consumption by energy optimization is still a possibility. The optimization needs monitoring, screening, and data analysis to retrieve knowledge from the massive amount of data generated by sensors and measuring systems. The data elaboration is part of Industry 4.0. The amount of data also allows the creation of DTs. DTs are a key-enabler for optimization and, therefore, even an introductory module in CO_2 reduction.

This thesis is part of the Austrian Research Promotion Agency (FFG) project DigitalEnergyTwin in cooperation with AT&S Austria as industry partner. It is part of a vast project and tries to improve, simplify, and extend existing parts in a DT project. The thesis has two main parts. One part is the DT modeling of an electroplating plant, and the second part is data prediction as input for the DT model. The model was developed in cooperation with project partners within the FFG project. AEE INTEC provides a model of the general structure of the electroplating plant. This thesis adds the control logic for the machines, various processes, and safety measures in the plant. The prediction part is split up into two subparts. The first prediction part is the electroplating process. In this part, the electroplating process from the electroplating plant is recreated in a lab experiment. During the experiment, data about the process is collected. With the gathered data, various machine learning algorithms are trained and tested. The primary purposes are to understand the electroplating process, collect data for data models, and develop them. The output of the models is then input for the DT model. This part is a collaboration with Michael Grömer from the physics department at TU Graz. The second prediction part is about the approximation of sensor data. The plant operators collect a massive amount of sensor data from their plants. This amount of data is too big, so it is impossible to process this in the DT model. A lightweight alternative is needed to get results without loading all the data at once. The result is an algorithm to approximate the outcome. Further, it also allows predicting data in the future.

The thesis is divided into five chapters. Chapter 2 describes the basics of used methods and implementations. It furthermore links the independent parts together to create an overview of the work. The chapter is about Digital Twins, the modeling language Modelica, and its user interface Dymola. Further, it holds information about electroplating, various data models, and approximation methods. Afterwards, Chapter 3 presents the evaluation and the individual components' results. Chapter 4 is about the current status of the project and how the thesis results work are included. It also contains personal assessments and interpretations. Chapter 5 completes the work and gives an outlook on further work and upcoming issues based on the thesis. Appendix A contains the overview of energy flows which is the basis for the DT model. For the sake of completeness and traceability, Appendix B and Appendix C hold the handwritten and digitized data of the lab experiments.

2. Methods

2.1. Digital Energy Twin

2.1.1. Digital Twin

> *A Digital Twin is an integrated multiphysics, multiscale, probabilistic simulation of an as-built vehicle or system that uses the best available physical models, sensor updates, fleet history, etc., to mirror the life of its corresponding [. . .] twin.* (Glaessgen and Stargel, 2012)

A Digital Twin (DT) uses a real-world object as an example and mimics it. The first definition was given by Grieves, 2002 during a presentation for the product lifecycle management and was then defined by Tao et al., 2018. It is a digital counterpart to the physical object. Instead of a controller in the physical object, algorithms replace the control logic. The algorithms mirror the behavior. The mirroring uses an "as best as possible" approach, where the algorithms are optimized to act like they can replace the real-world controller. The use of digital twins can have different purposes. A primary goal is the accurate and precise representation of the behavior of the physical object. A further objective is to decouple the digital object from the real-world object, do experiments on it, and see the influence of various changes on the system's different parameters without bothering the real-world processes. The experiments can have multiple purposes of use. Optimization is one of them. The main targets for optimizations are energy optimizations, duration reduction, lower costs, or CO_2 reduction. DT allows investigating different control strategies that minimize energy consumption (thus CO_2). Duration improvement reduces the needed time to produce output with consistent quality (Gaul, 2018).

Kritzinger et al., 2018 has created an overview of different papers aiming at the DT and gives a classification for different categories of DTs. Figure 2.1 shows these classifications. The DT has several classes. The basic class is the Digital Model (DM). The DM has a physical object and a digital object, which represents the physical object. Data exchange between the two objects works manually. The user both extracts the physical object's data and after that inserts it into the digital object by hand. It has the advantage that the user can check inserted data beforehand, so no damage to the physical object happens. Checking data from the physical objects also has the advantage that the user gets an overview of the data and detects failed measurement. The user can use the knowledge to improve the digital object and make it more fault tolerant. This is the first stage in the development process. It helps to improve the safety of the digital object cleverly. A Digital Shadow (DS) is a more advanced model. There is also a physical object and a digital object in the DS, but data transfers are different. The data from the physical object to the digital object works automatically. Thus, the objects have a common interface which they use to transfer data to the digital object. Various patterns fulfill automatic data transfer. A simple approach is a file-based transfer, where the physical object writes to a file, and the digital object reads the file and processes the data. A more advanced approach is a sender and receiver pattern where the physical object sends data, and the digital object receives it. The digital object returns the processed data manually to the physical object. Thus, the digital object computes suggestions, depending on the physical object's data, but the decision of implementing them is up to the operator. The most advanced class in this classification is the Digital Twin (DT). This class transfers all data automatically. In extension to the DS, the DT also has automatic data transfer from the digital object to the physical object. It means that the digital object is aware of control for the physical object. The computed data controls the physical object actively. With a DT, the digital object has huge power over the physical object.

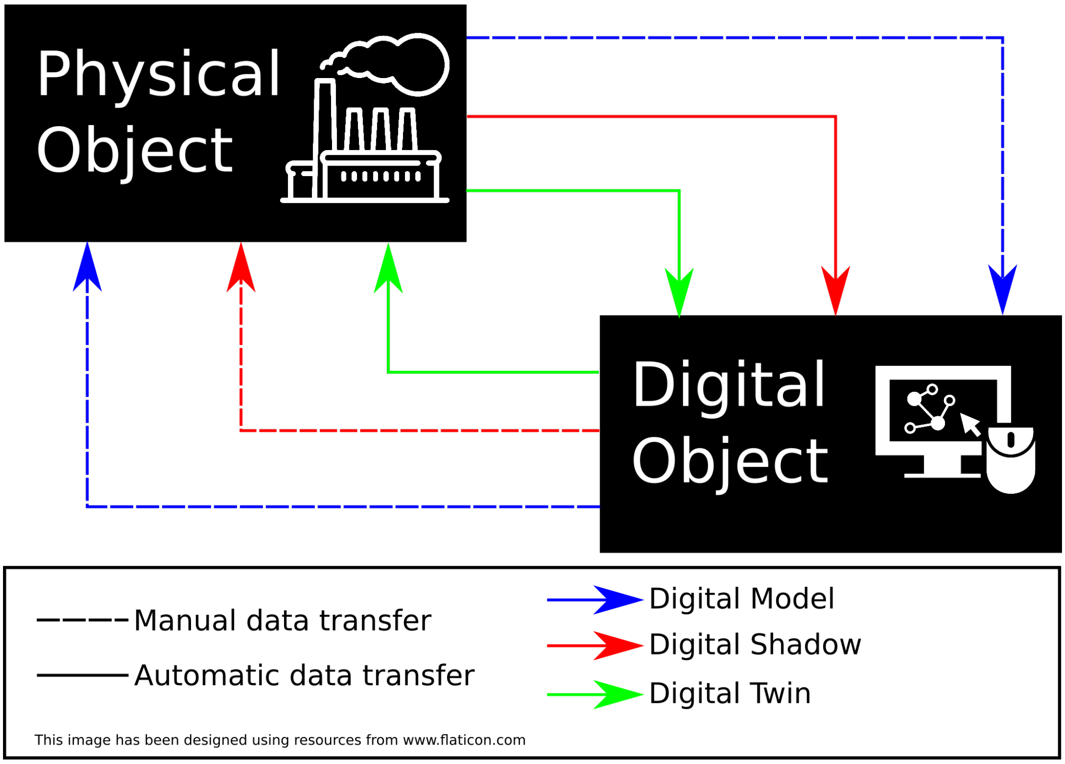

Figure 2.1.: Digital Twin vs. Digital Shadow vs. Digital Model (Kritzinger et al., 2018) Digitization has a physical object as a role model. The digital object tries to reproduce the behavior of the physical object. Depending on the way of data transfer, it is possible to distinguish between 3 types:
In a **Digital Model**, the data transfer is completely manual. Data from the physical object are transferred by hand to the digital object and vice versa. With a **Digital Shadow**, the transfer from the physical object to the digital object is automated. Still, the transfer back to the physical object has to be done by hand. A **Digital Twin** automates every connection between the physical and the digital object.

2.1.2. From Digital Twin to Digital Energy Twin

A DT represents a physical object in various ways. A special derivate is the Digital Energy Twin (DET). As the name already says, the main target of the DET is energy. First, it simulates the energy consumption of a physical object with given data of any kind. The data can be energy consumptions or any process data, enabling energy consumption calculation or prediction.

In the course of this thesis, the electroplating process is of special importance. The computations of the energy consumption for an electroplating plant need current, voltage, and plating duration. Computing energy consumption of pumps needs information about workload, degree of efficiency, and a function mapping to energy consumption. Secondly, the comparison between the plant's calculated energy consumption and the real measured energy consumption happens. When there are several measuring points, the process is more straightforward because a divide and conquer approach is used by dividing the whole energy consumption into smaller chunks and compare these chunks with the calculated one. This approach finds errors in the calculations more quickly.

2.2. Modelica and Dymola

This section is about Modelica, Dymola, and the implementation of an electroplating plant using these tools. The combination of Chapter 2.1 and Chapter 2.2 create a functional simulation of the plant. For results, see Chapter 3.1.

2.2.1. Modelica

Modelica (Ramírez et al., 2017) is an open-source, object-oriented modeling language for physical systems. Modelica compiles models into C-code. Thus, models are computed efficiently on the CPU. Modelica uses acausal modeling; this means that the system is described via differential-algebraic equations (DAE). A equation has the form $F(\dot{x}(t), x(t), y(t)) = 0$. With given conditions, Modelica solves the equations for unknowns. This acausal approach supports the user by focusing on the modeling part rather than on Modelica's background. Variables have a special syntax, which allows adding further information to them. The listing below shows a definition of a parameter with details describing the unit of the parameter and an explanation of the parameter.

```
parameter Real duration(unit="s")"Duration time in process X";
```

The unit system enables Modelica to evaluate given equations for correctness. By default, Modelica supports a vast set of physical models. The standard library contains elements to model mechanical, electrical, thermal, fluid, and many other physical systems (Modelica Association, 2020). Furthermore, a lot of free libraries provided by the community are available. This project mainly uses the opensource library *Buildings* (Wetter et al., 2014). The library offers great support for every kind of heating, cooling, and general energy supplies in any existing kind.

2.2.2. Dymola

Modelica has multiple graphical user interfaces (GUI). Widely used GUIs are Dymola[1], SimulationX[2], Wolfram SystemModeler[3], and Openmodelica[4]. This project uses Dymola as its GUI. Peter Fritzson, 2011 and Fritzson and Thiele, 2016 explain Modelica and present details about the langauge. Modelica is text-based. The GUI adds graphical elements for coding. The user can place blocks on the program surface. The blocks act as placeholders for classes. Wires connect blocks in a bi-directional way. The connectors are inputs and outputs simultaneously, which is useful for physical models when for example, two containers connected via a pipe exchange a fluid. When the fluid flows from container A to container B, the connector at container A works as output, and the connector at container B works as input. Vice versa, when the fluid flows from container B to container A, B's connector is the output, and A's connector works as input. The GUI also has an interface for simulation. This section shows the simulation results in graphs and can display the results of a simulation. Figure 2.2 shows a screenshot of the Dymola GUI with a loaded example program.

[1] https://www.3ds.com/de/produkte-und-services/catia/produkte/dymola/
[2] https://www.simulationx.de/
[3] https://www.wolfram.com/system-modeler/
[4] https://www.openmodelica.org/

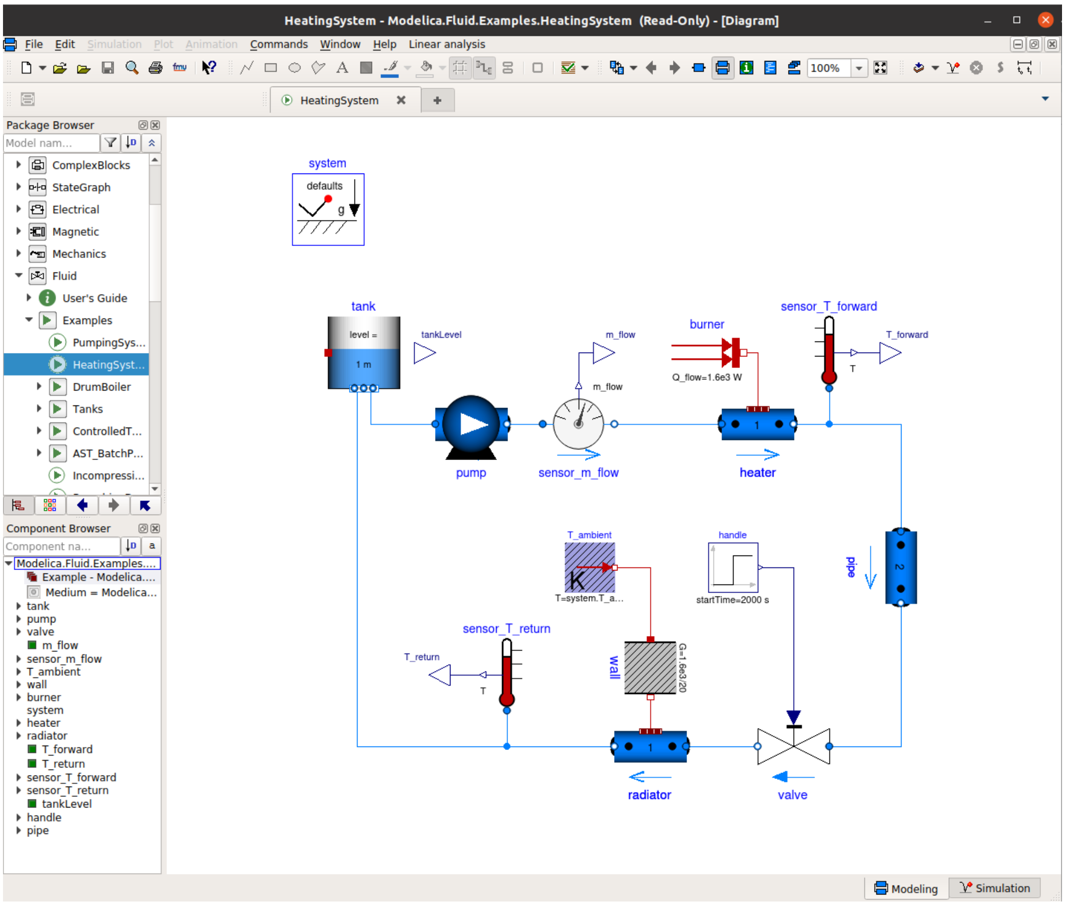

Figure 2.2.: A screenshot of the Dymola GUI
On the left side, the GUI shows the package browser, where all available packages and modules are listed. The main windows show a heating system model. In the right bottom corner is the switch between the modeling interface and the simulation interface.

2.3. Electroplating

Electroplating (Jelinek, 2013; Kanani, 2009; Unruh, 2016) is the electrochemical process of deposing metal ions on a conductive material. Figure 2.3 shows a basic setup for electroplating. The main components are an energy source, a cathode, an anode, and an electrolyte. The energy source must be direct current (DC). Alternating current (AC) would reverse the ongoing electrochemical process twice per swinging period. The anode consists either of the material which plates the cathode or of inert material. Inert material does not dissolve during the electroplating process. It is just a tool to close the electric circuit. In this case, the dissolved metal ions in the electrolyte plate the cathode. The concentration of deposing metal ions in the electrolyte determines the maximum plating thickness. When the anode is a non-inert material, it dissolves during the process. In this case, the anode and the electrolyte must match. The electrolyte must have the same ions dissolved as the anode delivers when it dissolves. When the anode is copper, the electrolyte also must be made of a copper ion. Thus a copper(II) sulfate ($CuSO_4$) solution suits well. One would use silver nitrate ($AgNO_3$) as an electrolyte for a silver anode. The electrolyte's main purpose is the transportation of ions to the cathode, where they got deposited. When there is a dissolvable anode, the concentration of metal ($ME^{+/2+}$) ions stays constant during the process. The electrolyte creates a concentration gradient from the anode to the cathode because the anode adds ions to the solution, and the cathode removes them. Mixing the liquid reduces this counterproductive effect. Metal ions deposit on the cathode. The process plates every part of the cathode's surface, which is in touch with the electrolyte. The plating's quality measurements are the surface quality, the plating thickness, and the layer's ionic structure. Electric field lines, the current density, process duration, and temperature are responsible for the plating quality. The temperature influences the ionic structure of the electroplated layer. It does not have an impact on the plating thickness. Current density and the process duration mainly define the plating thickness. Straight field lines are essential for an even overall layer thickness.

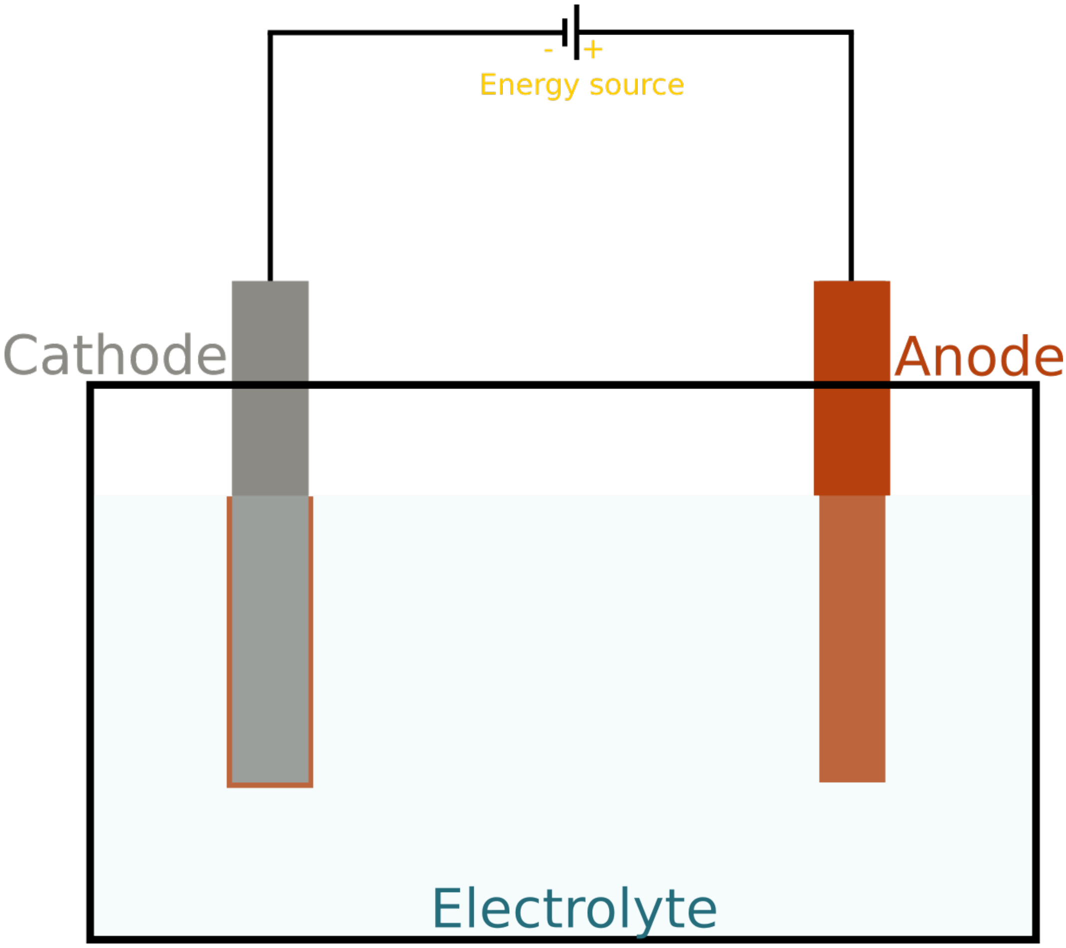

Figure 2.3.: Schema electroplating
Electroplating has four main parts. The energy source delivers direct current electricity for the reaction. The anode dissolves or is inert to the electrochemical process, while on the cathode, the material deposits. The electrolyte dissolves the metal ions and is responsible for the ion transport to the cathode, where the ions solidify. Adapted from Unruh, 2016.

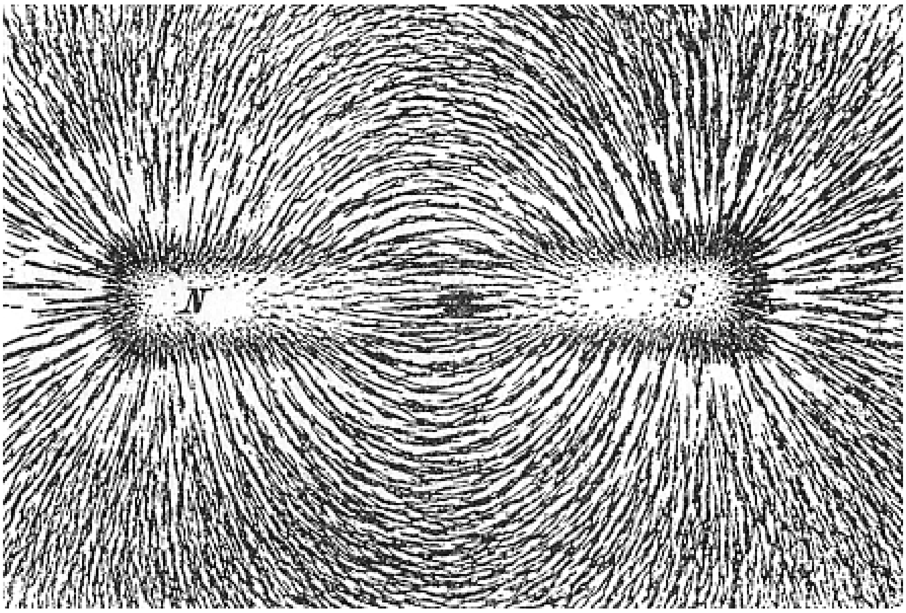

Figure 2.4.: Field lines experiment
The experiment shows field lines in a magnetic ambient. The experiment uses a magnet with north-pole (-) and south-pole (+) and iron filings. The iron filings are magnetized and align themselves according to the field lines. Figure 2.5 vividly illustrates the result of the experiment. (Black and Davis, 1922)

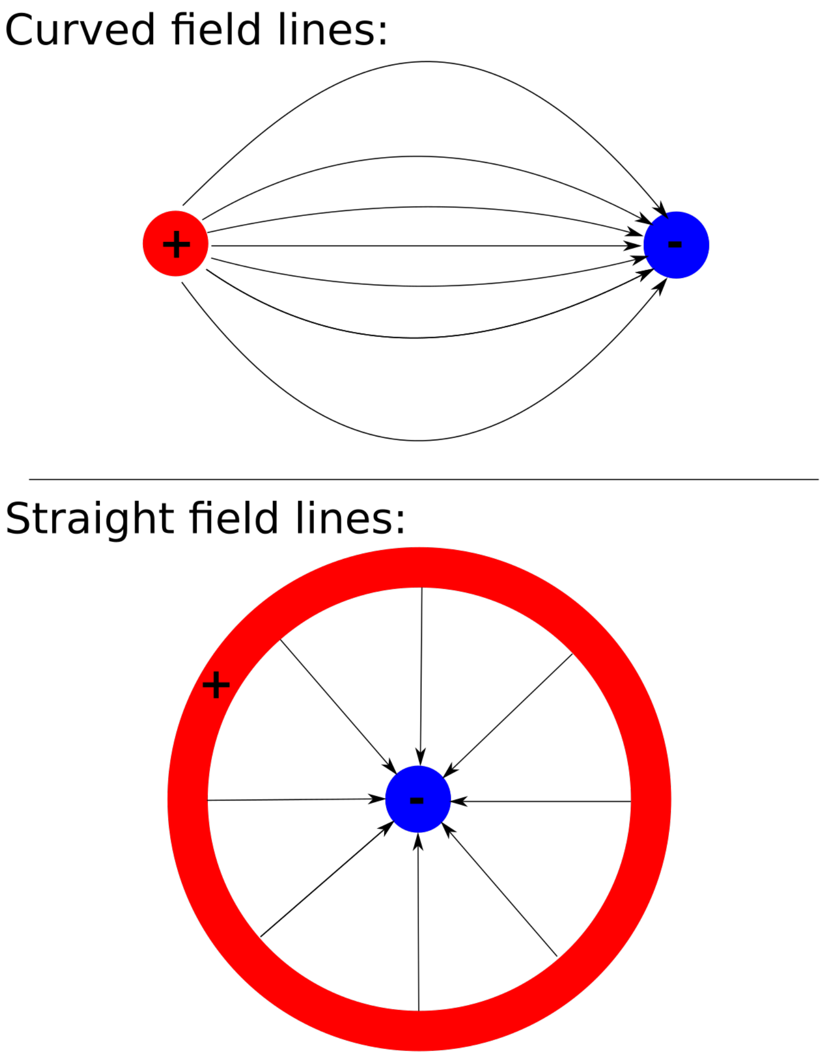

Figure 2.5.: Electric field lines schema
Electric field lines emerge between a positive and a negative electric charge and represent the Coulomb force. They always flow from the positive to the negative pole in a directed way. Electroplating needs as many straight field lines as possible. Curved field lines generate edge cases where more material deposits and result in an uneven layer. Adapted from Black and Davis, 1922; Unruh, 2016.

Figure 2.4 shows field lines in an experiment. The iron filings align themselves according to the field lines. The curvature of the field lines leads to an uneven distribution of the iron filings on the poles' edges. The same effect also takes place in electroplating. In areas where many field lines hit, more material deposits than in areas where fewer field lines hit. Figure 2.5 shows a comparison between straight and curved field lines. The upper case represents the experiment in Figure 2.4. The lower case is an ideal setup for an even deposition of material on a workpiece. The lab experiment (see Chapter 2.3.1) and the industrial process aim to have straight field lines. Both cannot use the ideal setup because of various reasons. On the one hand, a workpiece does not always have a cylindric shape, and on the other hand, it is way more expensive to build the anode as a cylinder and fill it with electrolyte. It is also hard to transfer the workpiece through the cylindric anode in an automated, continuous way.

The base of electroplating are redox reactions. Redox reactions are a combination of reduction reactions and oxidation reactions. Redox reactions include the movement of electrons (e^-) from the reduction reaction to the oxidation reaction. In electroplating, the reduction reaction takes place on the cathode. Reaction R1 shows the general reaction of deposing a metal ion. $X \in \mathbb{N}$ is the number of charges. For metal ions, it is usually 1 or 2. For example copper is a doubly positively charged ion Cu^{2+}, here $X = 2$.

$$Me^{X+} + X \cdot e^- \longrightarrow Me \qquad [R1]$$

On the anode, the oxidation reaction takes place. Reaction R2 shows the general reaction of dissolving metal.

$$Me \longrightarrow Me^{X+} + X \cdot e^- \qquad [R2]$$

In sum, both reactions take place at the same time. The redox reaction is the resulting reaction. Reaction R3 shows the whole redox reaction.

$$Me \longrightarrow Me \qquad [R3]$$

The reactions do not work automatically, they need an additional energy source. Figure 2.3 shows the energy source. Electroplating uses a direct current energy source, which transfers the electrons from the anode to the cathode. In other words: Transfering the electrons from the oxidation reaction to the reduction reaction. The plus pole of the energy source is an electron sink, and the minus pole is an electron source. This explains why the layer thickness depends on the time and the Amperage. The longer the process lasts, the longer electrons can move, and the higher the amperage, the more electrons move in a specific time interval.

2.3.1. Lab-scale experiment

The lab experiment aims to understand the electroplating process, the influence of various parameters on the layer thickness, and the layer quality. With the gathered data, a data model is created to describe the electroplating process. All these steps help to better understand the process on an industrial scale. The experiment took place at the department of experimental physics at TU Graz. Within three weeks, over 200 electroplating experiments took place. The experiment uses copper as anode and as cathode. Resulting, the electrolyte is a $CuSO_4$ solution. The energy source is a laboratory power supply. To keep a constant temperature, water baths are used.

The varied parameters are duration time (t), temperature (T), and current density ($\vec{j}$). Duration time and current density directly impact the coating thickness, while temperature does not directly impact the coating thickness. Temperature influences the structure of the crystal lattice. Its results are smoother and trouble-free surfaces and layers. Equation 2.1 (Unruh, 2016) shows the influence of the parameters on the coating thickness and Equation 2.2 explains the term current density.

$$t_e = \frac{Ae}{\varrho} * \vec{j} * t * \eta_i \tag{2.1}$$

where:

t_e = Coating thickness
Ae = Electrochemical equivalent, $Ae(\mathrm{Cu}) = 1.19\,\mathrm{g\,A^{-1}\,h^{-1}}$
ϱ = Density of the layer material, $\varrho(Cu) = 8.96\,\mathrm{g\,cm^{-3}}$
$\vec{j}$ = Current density, see Equation 2.2
t = Duration time
η_i = Current efficiency, $\eta_i(Cu) \sim 0.97$

$$\vec{j} = \frac{I}{A} \tag{2.2}$$

where:

$\vec{j}$ = Current density
I = Current
A = Coating area

2.4. Data models

2.4.1. Machine learning

Machine learning (ML) (Aggarwal, 2020) is a method to generate knowledge from existing data. During training, machine learning algorithms learn parameters for statistic models using training data. After the training, the ML algorithm can predict further unknown data and does not need the training data anymore. During the training phase, the algorithm finds patterns and correlations in the given data. The project uses supervised learning for the training phase. It means that the training data consists of input values and the corresponding output value (= result), and the algorithm tries to fit the data in the best possible way. A problem of ML is overfitting. Figure 2.6 shows an example of overfitting. Here, a linear and a polynomial model approximate a noisy linear function. While the polynomial function has excellent results on the training set by overfitting the values, it fails on the test data set. There are various models for ML. The next sections give an overview of the used models in this thesis.

Neural Networks

> *The neural network is this kind of technology that is not an algorithm, it is a network that has weights on it, and you can adjust the weights so that it learns. You teach it through trials.* – Howard Rheingold (M. B. Patel, J. N. Patel, and Bhilota, 2020)

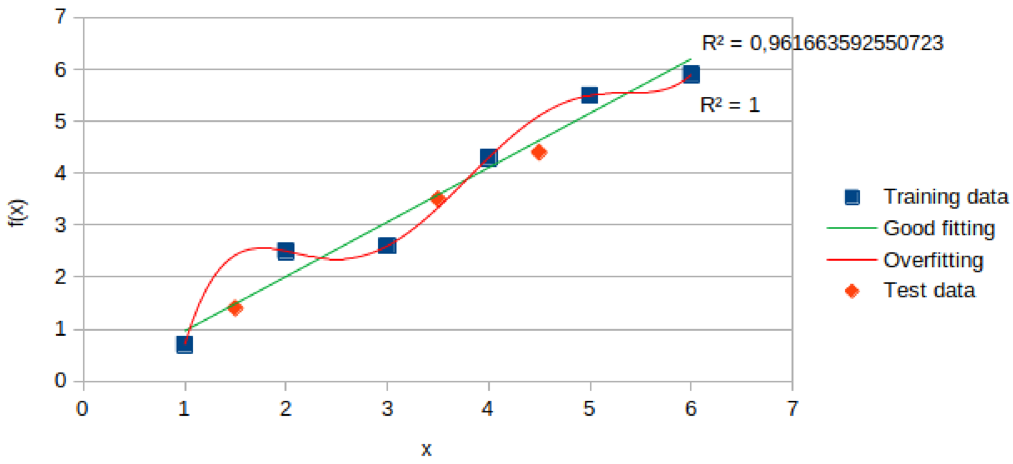

Figure 2.6.: Overfitting
The data (blue and orange dots) shows a noisy linear function. The blue dots represent the training data set, and the orange dots represent the test set. With the training set, two models are trained. The green line represents the linear model, and the red line represents a polynomial model. The linear model has a R^2 of 0.96 on the training data, while the polynomial model fits the data perfectly and has a R^2 of 1. But when the models apply to the test data, the R^2 differ a lot. The R^2 of the linear model is 0.99, while the R^2 of the polynomial model drops to 0.84. It is a typical case of overfitting. The model fits the training data without having the background of the data in mind, and so it fails on further data.

The idea of Neural Networks (NN)(Rojas, 1996; Rashid, 2017; Yiu, 2019a; Sai Ajay, 2020) is based on the way the human brain works. Neurons send signals when they are triggered. But instead of chemical reactions triggering the signal, mathematical equations are the reason for the reaction.

A NN has an input layer, an output layer and arbitrary many hidden layers. The input layer takes the input to the NN. The inputs are called features. A feature can be a measurement when we want to do regression, or it can be a pixel of an image for classification. The output layer represents the result of the prediction from the NN. In regression, the output layer consists of one neuron, which holds the result. In classification, the output layer has n neurons, where n is the number of classes. Each of the n neurons then holds the probability that the input matches the represented class. Each neuron in a layer is connected with each neuron in the next and the previous layer. Each connection has a weight, which is multiplied by the value of the outgoing neuron before it comes to the incoming neuron. A neuron holds a bias, which is added to the incoming values, and the result is then the input parameter for a non-linear function that produces the output of the neuron. The non-linear function can, for example, be a sigmoid function.

The training of the NN is based on forward propagation and backward propagation. During the learning phase, the features traverse the NN, and the output is compared to the set's label using a cost function. Adapting the weights and biases can minimize the cost function. So backward propagation uses the result of the cost function to traverse the neural network backward from the output to the input. In the backward propagation, the algorithm adapts the weights and biases to minimize the cost function. For the implementation, scikit-learn (Pedregosa et al., 2011) as one of the most popular and established Python packages is used.

Linear regression

Linear regression (LR) (Rohith, 2018) is a statistical method used in ML. The main goal is to fit given data with a linear function. The primary condition is to minimize the mean square error (MSE) between the predicted value and the real data. The LR uses a cost function and minimizes it. The cost function (= MSE)

$$J = \frac{1}{n} \sum_{i=1}^{n} (pred_i - y_i)^2 \tag{2.3}$$

where:

n = Number of data points
$pred_i$ = Predicted value, see Equation 2.4
y_i = Data point

describes the error between the prediction and the real data. The predicted value ($pred_i$) is calculated by a linear function.

$$pred_i = d + \sum_{j=1}^{m} w_j * x_j \tag{2.4}$$

where:

w = Weight of the parameter
x = Dependend variables
d = Initial value

The LR uses the equations and finds the best fitting parameters (w_j, d) to minimize the MSE. For this, it uses a gradient descend method.

Polynomial regression

Polynomial regression (PR) (Nocedal, 2006) uses the same methods as LR, but instead of a linear function, it uses a polynomial function as a cost function. The degree of the polynomial is a choosable parameter. The choice of the degree determines whether the calculated function overfits or not. Choosing the degree in about the number of variables leads to a well-fitting polynomial. If the degree is 1, the polynomial regression becomes a linear regression.

Decision tree regression

Decision tree regression (DTR) (Li, 2019) is also a supervised machine learning algorithm. During the training phase, the algorithm builds a binary tree with the decision results in the leafs. Each node has a true/false question, which is answered with the given data to create a prediction. The information gained by the split determines the splitting of the data in the left or right subtree. The algorithm maximizes the information gain (IG) for each split. For this, it optimizes the objective function.

$$IG(D_p, f) = I(D_p) - \left(\frac{N_l}{N_p} I(D_l) + \frac{N_r}{N_p} I(D_r) \right) \tag{2.5}$$

where:

IG = Information gain
I = Impurity function
f = The feature for the node's criterion
D_p = Dataset in the parent node
D_l = Dataset in the left child node
D_r = Dataset in the right child node
N_p = Number of data points in the parent node
N_l = Number of data points in the left child node
N_r = Number of data points in the right child node

This means that the higher the parent node's impurity and the smaller the child node's impurity, the higher the information gain. In regression, the impurity function is the MSE between the real and the predicted value, as it was already in LR and PR. The DTR regression also gives information about the importance of the features. Figure 2.7 shows a decision tree of depth 2 for the lab experiment. It shows that the most important features are the current density and duration. The DTR is likely to overfit, so the tree's maximal depth is an important parameter to reduce this error. Figure 2.8 shows the result of the decision tree from Figure 2.7. All predictions are in one of the four possible categories. Deeper trees result in more categories and subsequently also in more precise predictions. The bucket behavior of the DTRs leads to a further disadvantage. It is impossible to detect correlations between the data; the model can only make new predictions within the training data set. Outliers are always assigned to the nearest bucket.

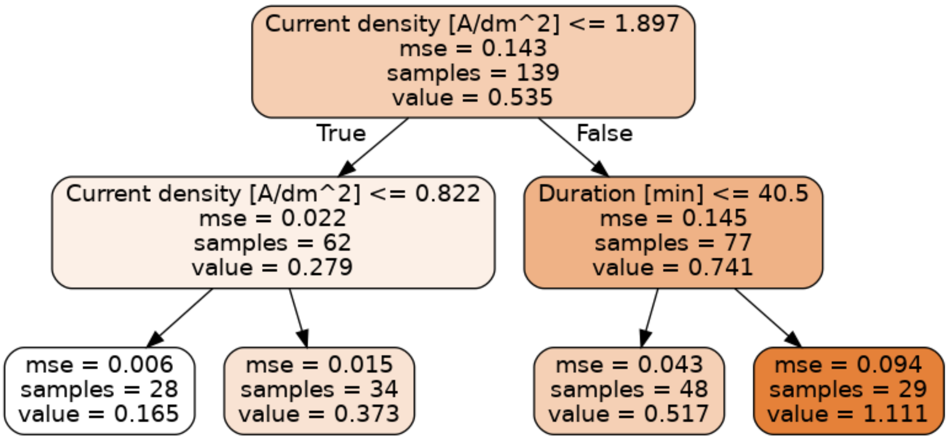

Figure 2.7.: Decision tree
The tree has a maximal depth of 2. In each node, the first line shows the condition, the second line shows the calculated MSE, and the third line shows the number of samples. The last line is the corresponding value.

Random forest regression

Random forest regression (RFR) (Yiu, 2019b) is a successor of DTR. It uses many uncorrelated DTR trees to vote for a result. The significant advantage is that this algorithm uses the wisdom of the crowd as a key feature. It means that there are many votes for the result, and when there is a maleficent vote, it is overruled by many other correct votes. The single DTR trees are uncorrelated. This ensures the statistical correctness of the algorithm. Two mechanisms grant it. The first one is Bootstrap Aggregation (Bagging). Small changes in training data lead to a totally different tree. When the training data consists of N data points, each tree chooses a random set of the training data. The newly selected data set has a size of N again; it also means that some of the new data sets contain the same data points multiple times. With many different training sets, many varied decision trees are generated. The second mechanism also builds on the sensitivity of the trees. Feature randomness lets each of the trees choose features randomly for all

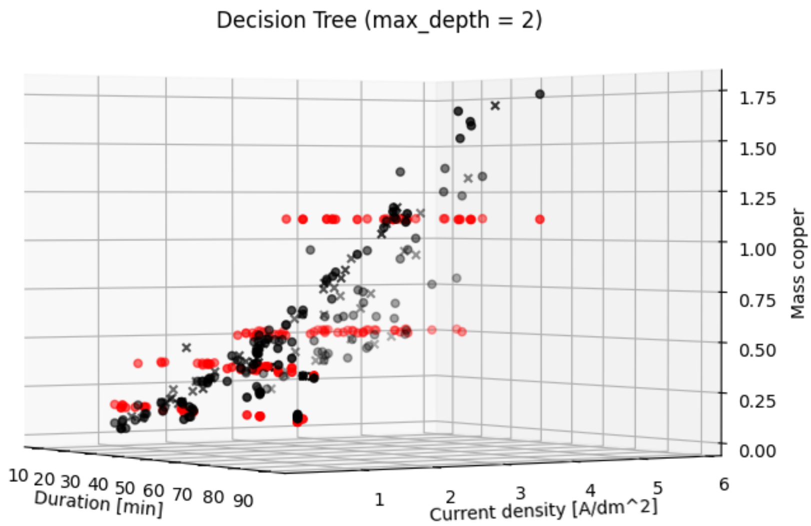

Figure 2.8.: DTR data and predictions
The black dots represent the training data. The black crosses stand for the test data. Training data trains a DTR model of depth 2. The red dots represent the predictions of the model. The R^2 is 0.72 on the training set and 0.59 on the test set. The model is not very accurate, but it shows the concept of DTRs quite well. Deeper DTRs are more accurate.

existing features. So various combinations of features a tree can choose from are created.

2.5. Function-based approximation of data

During the project, the partners had recorded an enormous amount of data, which is used in the DT models. Most of the data describe temperature curves, voltage, and amperage values. All the values follow a specific pattern influenced by the laws of physics and the plant's control strategy. For example, the temperature curves are nearly constant during production. They only vary slightly around the set temperature. When the plant gets turned off, the temperature falls according to the cooling curve of fluids

$$T(t) = T_A + (T_0 - T_A) * e^{-c_c t}. \tag{2.6}$$

where:

$T(t)$ = Temperature at a given time t
t = The time to calculate the temperature
T_A = The temperature of the ambient
T_0 = The temperature of the fluid at the beginning of the cooldown
c_c = A coefficient affected by the volume of the fluid, the surface, thermal capacity, and the density of the fluid

When production starts again, a linear function describes a head up

$$T(t) = T_0 + c_h t. \tag{2.7}$$

where:

$T(t)$ = Temperature at a given time t
t = The time to calculate the temperature
T_0 = The temperature of the fluid at the beginning of the head up
c_h = A coefficient affected by the volume of the fluid, the surface, thermal capacity, and the density of the fluid

Using the given data for further processing leads to a massive computing overhead. The shown equations serve the same purpose but have a lot less computing overhead. The collected data are still in use. With the data, the functions are parametrized. The parametrization is a one-time overhead that can be reused. For results see Chapter 3.3.

3. Results

3.1. Digital Energy Twin Model

3.1.1. The Digital Twin of an electroplating plant

This Section represents the results of Chapter 2.1 and Chapter 2.2. The model is based on the scheme from Appendix A (ENERTEC Naftz & Partner GmbH & Co KG, 2020). Figure 3.1 shows the created model in Dymola. The energy scheme describes the flow of energy in the system. The scheme has two parts. On the left-hand side, it shows the first plant (Werk 1), and on the right-hand side, it shows the second plant (Werk 2). This thesis deals only with the left-hand side because it is the central part of its development. The colors of the connections stand for the pipes' temperatures, where red connections mean hot fluid and blue connections mean cold fluid.

The central parts of the scheme are the two tanks. One contains cold water (KW Becken Werk 1), and the other contains warm water (WW Becken Werk 1). Whenever the warm water level rises too high, the water dumps into the nearby river (End-Kontrolle KW 1). The cold water tank stores water for the process. When the water level gets too low, it adds water from a well (Brunnenwasser) and tempers it with water from the warm water tank. The cold water tank delivers the water for process cooling, and the warm water tank provides rinsing water. A hydraulic separator generates hot water. It mainly uses waste heat from the other machines for the heat up. If not enough waste heat is present, the plant has a few options to generate heat. It can activate a heat pump (WP) and cool down warm water from the warm water tank and bring it to the cold water tank. In the last instance, natural gas is used to heat the hydraulic separator.

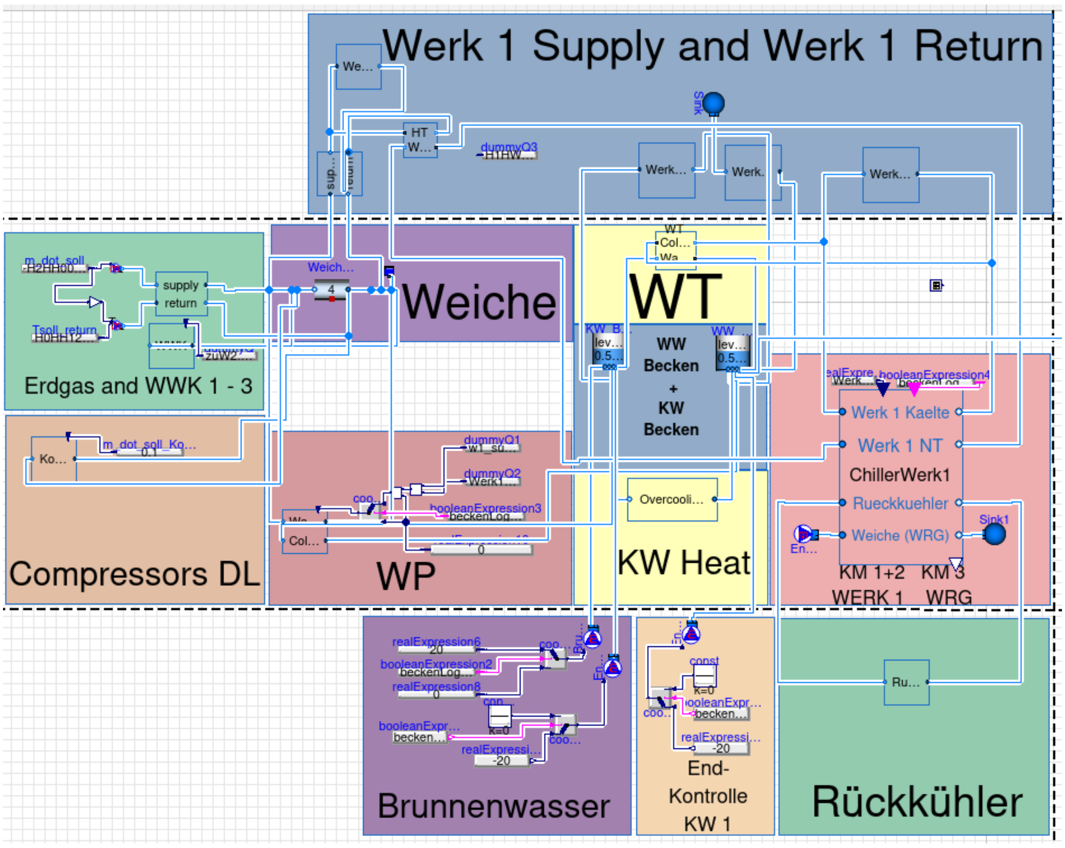

Figure 3.1.: Energy flow model in Modelica

The Modelica model in Figure 3.1 aims to imitate the energy scheme, the control of the machines, and the security mechanisms. It also uses the collected data from the real plant for the simulations. One of the main advantages of Modelica is visualization. After studying the energy scheme, the Modelica model looks similar to the real plant, and it is easy to navigate in the model and find the components. The next part shows the implemented control mechanisms. All implementations are designed as state machines to avoid chattering. Chattering is a misbehavior in numerical methods. At a specific point, the calculation jumps between multiple states within milliseconds. A specific point can be a threshold determining on or off, for example. State machines also use delays before they change to the next state. That avoids chattering and is also used to simulate the start-up time and the switch-off time.

Security mechanism - Overflow detection

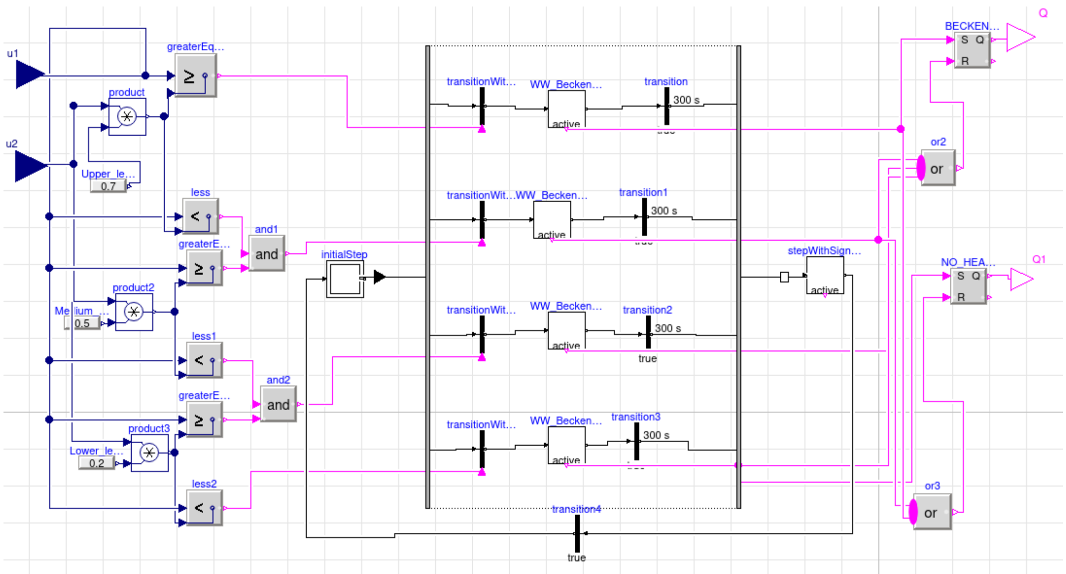

Figure 3.2.: Overflow detection model
On the left-hand side, the model shows the inputs. The dark blue painted arrows are the inputs and hold values for the current water level and the maximum water level in the tank. The model has three thresholds (Overflow, Normal, Empty) determining the four possible levels. Logical equations transform the input values and the thresholds into four boolean signals for the state machine in the middle of the picture. Depending on the state machine's boolean input, the state, and the delays, the state machine can produce an overflow alert. The alert is represented by a boolean signal and stored in a flip-flop register. The right-hand side shows the outputs of the overflow detection.

Overflow detection is a safety mechanism. It controls the water level in the tanks. When the level rises too high, it directs water into the nearby river. Figure 3.2 shows the overflow detection. The core component is the state machine in the middle of the model. It has six states. The initial state is the starting point for the calculations. After the initial state, the machine has four alternating states. In each iteration, only one of the four possible states is active. By definition of the module, the first state that gets activated is the prior one used in the current iteration. The four alternating states all have a separate boolean output. It determines whether the output shows an overflow alert or not. The last state is an end state. It does not have any effect. It is needed for the completeness of the program. Each state has a transition block (black vertical bar) in front and behind it. Transitions serve two purposes. At first, they release or block a path depending on the boolean input they receive. If there is no input, they always release the path. The second purpose is to introduce delays. As otherwise, the chattering effect would happen. From the data around the water tanks, it is clear that an overflow takes several minutes to happen, and it is not necessary to react to an overflow within seconds. It is sufficient to respond within a few minutes. So the transition between the last state and the initial state has a delay of five minutes. The following equations describe the input for the transitions.

$$\sigma_{FULL} = l_{curr} \geq (l_{max} * t_{FULL}) \tag{3.1}$$

$$\sigma_{A.FULL} = (l_{curr} < (l_{max} * t_{FULL})) \wedge (l_{curr} \geq (l_{max} * t_{NORMAL})) \tag{3.2}$$

$$\sigma_{A.EMPTY} = (l_{curr} < (l_{max} * t_{NORMAL})) \wedge (l_{curr} \geq (l_{max} * t_{EMPTY})) \tag{3.3}$$

$$\sigma_{EMPTY} = l_{curr} < (l_{max} * t_{EMPTY}) \tag{3.4}$$

where:

σ_{FULL} = Signal (Boolean value) determing if tanks is full
$\sigma_{A.FULL}$ = Signal (Boolean value) determing if tanks is almost full
$\sigma_{A.EMPTY}$ = Signal (Boolean value) determing if tanks is almost empty
σ_{EMPTY} = Signal (Boolean value) determing if tanks is empty
l_{curr} = Current water level of the tank
l_{max} = Maximal water level of the tank
t_{FULL} = Threshold for full water level
t_{NORMAL} = Threshold for normal water level
t_{EMPTY} = Threshold for low water level

A flip-flop register stores the result of the overflow detection. For the flip-flop register following equations hold.

$$S = s_{FULL} \tag{3.5}$$
$$R = s_{A.FULL} \vee s_{A.EMPTY} \vee s_{EMPTY} \tag{3.6}$$

where:

S = Signal to trigger the set of the flip-flop register
R = Signal to trigger the reset of the flip-flop register
s_{FULL} = Signal determing if state FULL is active
$s_{A.FULL}$ = Signal determing if state ALMOST FULL is active
$s_{A.EMPTY}$ = Signal determing if state ALMOST EMPTY is active
s_{EMPTY} = Signal determing if state EMPTY is active

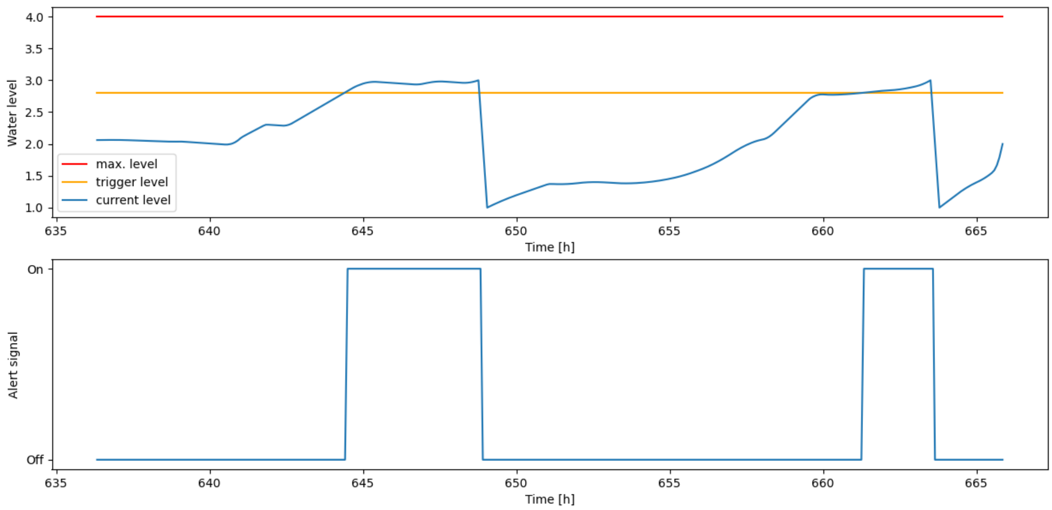

Figure 3.3.: Overflow detection result
The upper figure shows the current, maximum, and trigger level of the overflow detection. Every time the current level goes above the trigger level (at hour 644 and hour 662), the lower figure switches from off to on. When the level falls below the trigger level (at hour 648 and hour 664), also the signal turns off.

Figure 3.3 shows the result of the overflow detection. The overflow detection works as expected. Whenever the water level rises above the trigger level, the signal turns on, and then the water level drops again. Modelica models crash if there is an overflow in a component. This security mechanism saves the model from crashing and also imitates the real object well.

Process mechanism - Compressor control

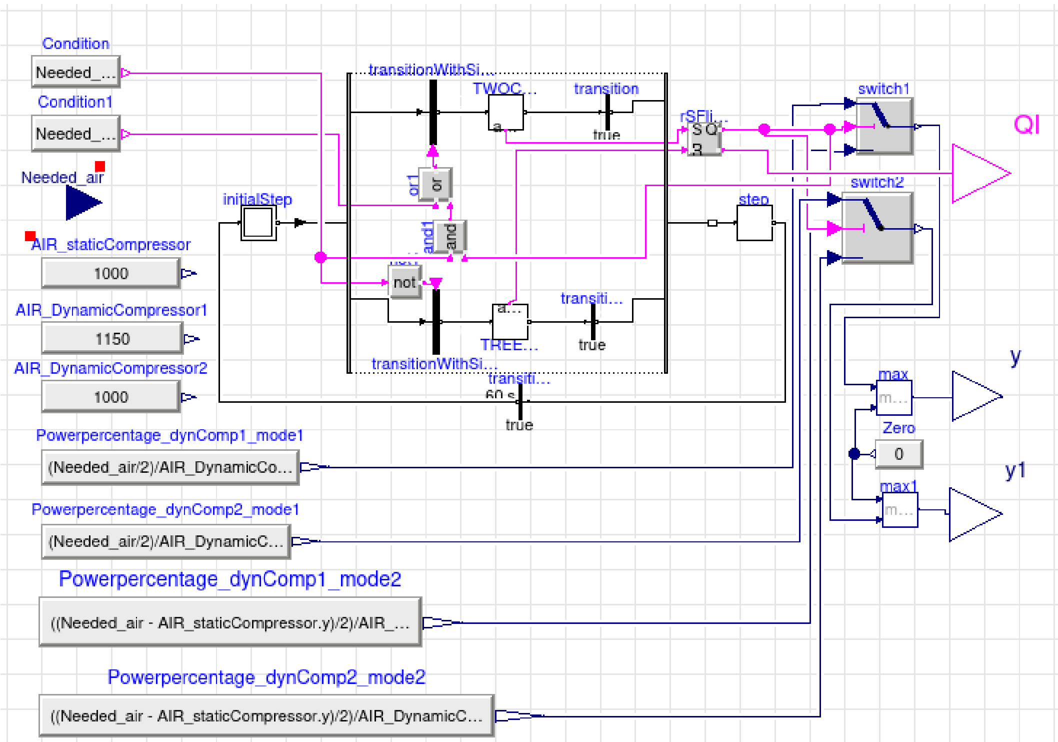

Figure 3.4.: Compressor control model
The model only has one input, which is the current air consumption of the plant. There are also parameters for the power of the compressors. The state machine in the middle of the figure has two states. One represents the first production mode, where two dynamic compressors handle the compressed air production. The second state takes the case when the two dynamic compressors do not have enough power to handle the required air, and the third compressor needs to be activated. Depending on the state, the model calculates the dynamic compressors' power level and the static compressor's control signal.

The plant uses compressed air to drive drilling machines. Depending on the capacity utilization of the drilling machines, the compressed air consumption varies. The plant uses three compressors to produce compressed air. Two compressors are dynamic compressors with dynamic rotation speed. The compressors are more energy-efficient than the third compressor, which is a static one. It can only be turned on or off. It is desired that the dynamic compressors run as much as possible, and that the static compressor is only active when the dynamic compressors cannot handle the current air consumption. Figure 3.4 shows the compressor control model. It has an input for the current air consumption and uses maximal producible air amount as parameters. A central part is a state machine. In total, it has four states. An initial state, which is the entry for the model. Two states represent the production modes. The first mode handles the case that the dynamic compressors have enough power to produce the required air consumption. The second state assumes that all three compressors must be in operation to fulfill the compressed air needs. The program needs the last state for correctness reasons. To decide which state is active, the transitions (vertical black bars) have the following conditions.

$$\sigma_{2C} = (\eta_A < 0.95 * (2 * \min(p_{C1}, p_{C2})))\vee \\ ((\eta_A < 0.75 * (2 * \min(p_{C1}, p_{C2}))) \wedge s_{2c}) \quad (3.7)$$

$$\sigma_{3C} = \neg(\eta_A < 0.95 * (2 * \min(p_{C1}, p_{C2}))) \quad (3.8)$$

where:

σ_{2C} = Signal (Boolean value) determining if 2 compressors needed
σ_{3C} = Signal (Boolean value) determining if 3 compresser needed
η_A = The current compressed air consumption
$\min()$ = A function returning the minimal value of its parameters
p_{C1} = Power of dynamic compressor 1
p_{C2} = Power of dynamic compressor 2
s_{2C} = Boolean value determing if 2 compresser mode active

Depending on which transition is activated, a flip-flop register R stores the result. If R is one, then two compressors are active; otherwise, all three compressors are used. The flip-flop register directly influences the static compressor. If R is one, then the static compressor is off and if R is zero, then the static compressor is on. The power level for the dynamic compressors calculates as following.

$$pl_{C1} = \begin{cases} (\frac{\eta_A}{2}) * p_{C1}^{-1} & \text{2 compressor mode} \\ (\frac{\eta_A - p_S}{2}) * p_{C1}^{-1} & \text{3 compressor mode} \end{cases} \quad (3.9)$$

$$pl_{C2} = \begin{cases} (\frac{\eta_A}{2}) * p_{C2}^{-1} & \text{2 compressor mode} \\ (\frac{\eta_A - p_S}{2}) * p_{C2}^{-1} & \text{3 compressor mode} \end{cases} \quad (3.10)$$

where:

pl_{C1} = Power level of compressor 1
pl_{C2} = Power level of compressor 2
η_A = The current compressed air consumption
p_{C1} = Power of dynamic compressor 1
p_{C2} = Power of dynamic compressor 2
p_S = Power of static compressor

Figure 3.5 shows the result of the implemented algorithm. As the requirements request, the dynamic compressors run as much as possible. Only in peak times, the static compressor runs.

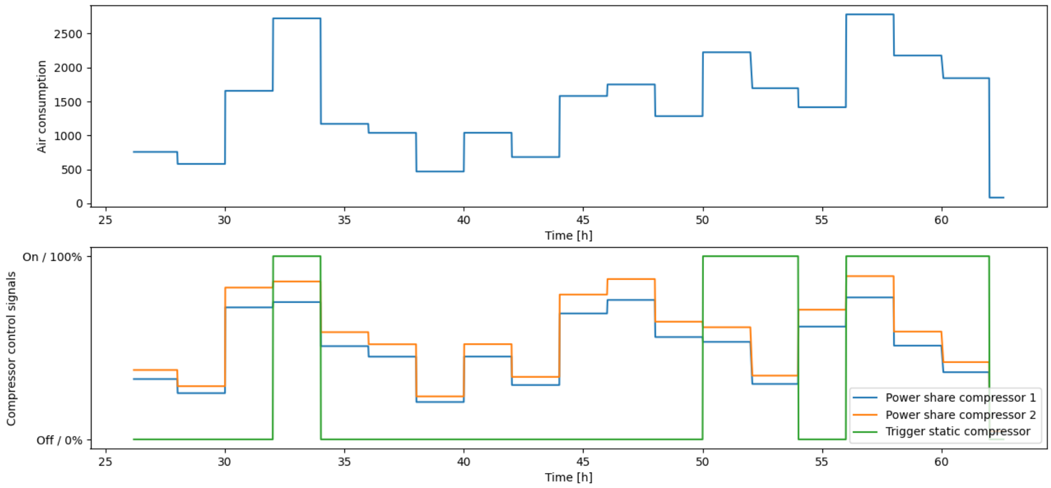

Figure 3.5.: Compressor control result
The upper figure shows the current air consumption. The data are randomly generated values from a test suit. The below figure shows the control signals for the compressors. The static compressor has a fixed rotational speed and has only two operating modes. It can be on or off. The dynamic compressors can vary the rotation speed. So the control signal is the share of the maximum power of the compressors. As long as the dynamic compressors can handle the air consumption, the static compressor is off (for example, between hours 34 - 50). But when the air consumption rises and the dynamic compressors reach their limits, the static compressor turns on and supports the compressed air production (e.g., hour 50).

Process mechanism - Tank logic

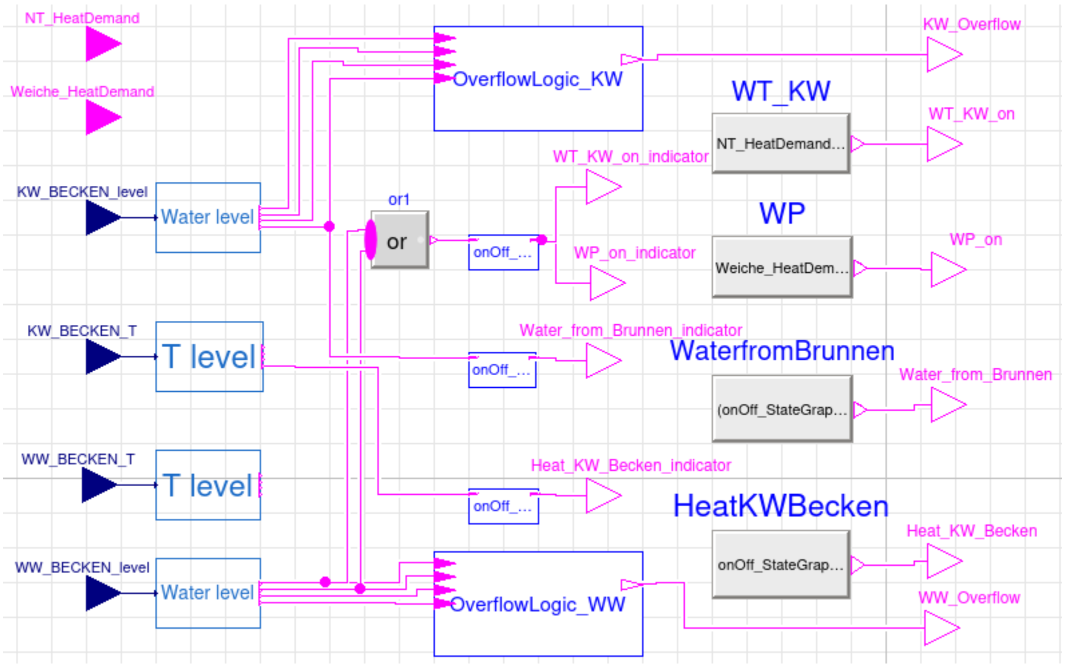

Figure 3.6.: Tank logic model
The tank logic module contains the logic for triggers depending on the tanks' water level and the water temperature. It includes the overflow logic from Figure 3.2 as modules twice - one time for the cold water tank and one time for the warm water tank. Additionally, there are logical equations for heat pumps and heat exchangers switches. The module also decides if water from the well is needed and if the water in the cold water tank needs to heat up.

As shown in the overflow detection chapter, the tank levels are critical measurements for the control logic, but there is more information within the tank levels. The control state of other machines like heat exchangers or heat pumps depends on the tank levels. Figure 3.6 shows the tank logic module, which controls several devices based on the tank levels. The inputs are temperatures and the water levels of the tanks. Additionally, boolean inputs determine the need for heat for the hydraulic separator and the low-temperature sector. As Appendix A shows, there are many devices connected to the water tanks. A heat pump (WP) uses warm water to generate extra heat for the hydraulic separator by cooling the warm water down and deliver it to the cold water tank. Another device is the heat exchanger (WT KW), which creates load for the chillers (KM 1-3), producing more waste heat, which heats the hydraulic separator. The last control unit is the refilling of the tank. There is also a control part for the inlet of well water and the cold water tank's tempering.

The following equations describe the state of the heat pump and the heat exchanger.

$$r_{HP} = \eta_{HS} \wedge \lambda_{WW} \wedge \neg\omega_{KW} \tag{3.11}$$
$$r_{HE} = \eta_{LT} \wedge \lambda_{WW} \wedge \neg\omega_{KW} \tag{3.12}$$
$$\lambda_{WW} = s_{FULL} \vee s_{A.FULL} \tag{3.13}$$

where:

r_{HP}	=	On/off status of the heat pump
r_{HE}	=	On/off status of the heat exchanger
η_{HS}	=	Heat demant in the hydraulic seperator
η_{LT}	=	Heat demant in the low temperature section
ω_{KW}	=	Overflow detection in the cold water tank
λ_{WW}	=	Warm water tank contains enough water
$s_{FULL,WW}$	=	State FULL in the warm water tank
$s_{A.FULL,WW}$	=	State ALMOST FULL in the warm water tank

The following equations describe the water level and the water temperature in the cold water tank.

$$r_{FT} = \epsilon_{KW} \wedge \neg r_{HP} \wedge \neg r_{HE} \tag{3.14}$$
$$r_{HC} = \tau CW < t_{TEMP,LOW} \wedge \neg r_{HE} \wedge \neg r_{HP} \tag{3.15}$$

where:

r_{FT}	=	On/off status of the well inlet
r_{HC}	=	On/off status of the cold water tank heat
ϵ_{KW}	=	Cold water tank level EMPTY
τCW	=	Temperature of the cold water tank
$t_{TEMP,LOW}$	=	Threshold for low temperature

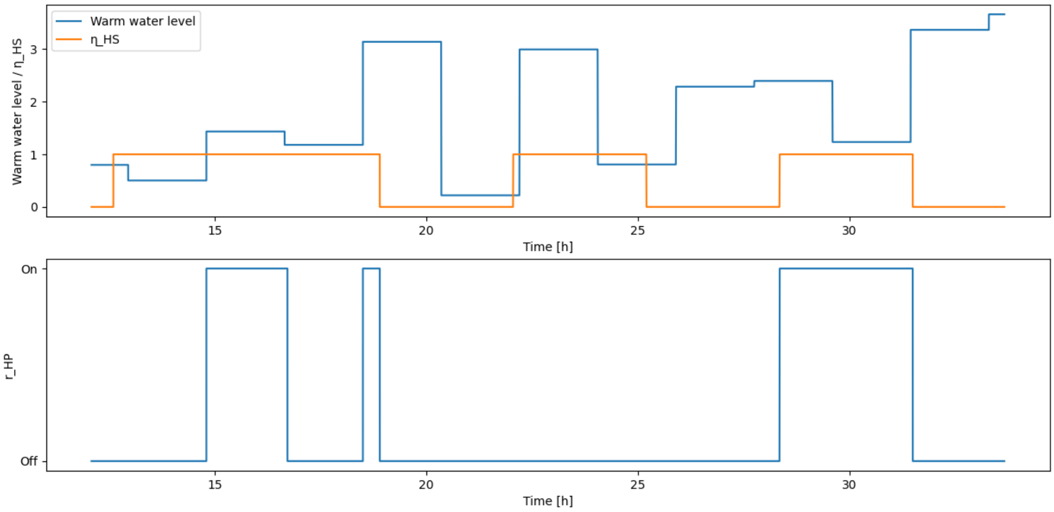

Figure 3.7.: Heat pump result
The heat pump is only active if the warm water level is high enough and the hydraulic separator needs the energy. The upper chart shows the warm water level and the control signal from the hydraulic separator. The lower graph shows the resulting control signal for the heat pump. The first on-phase (hour 14 to hour 18) of the heat pump shows the case where the hydraulic separator would need energy earlier, but there is too little water in the tank, and the controller cannot turn on the heat pump. After a while, the water level rises, and the heat pump turns on. The last on-phase shows the case where all conditions meet, and the heat pump is on.

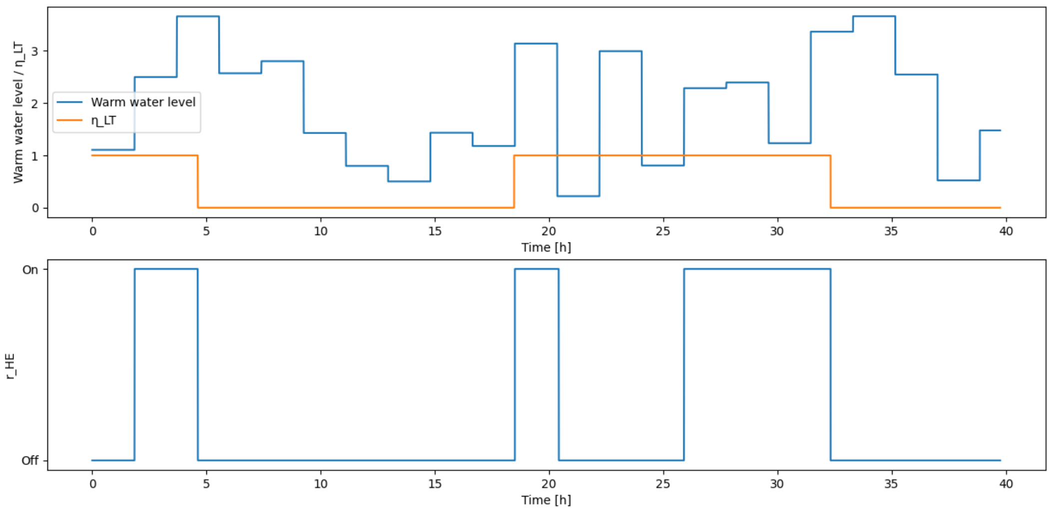

Figure 3.8.: Heat exchanger result
The heat exchanger only works when the low-temperature sector needs coldness and the warm water level is high enough. The first on-phase shows the case where all conditions meet (hour 2 to hour 5). The second and the third on-phase show that the low-temperature sector needs more cold energy, but the water tank level is too low, so it is not always possible to provide.

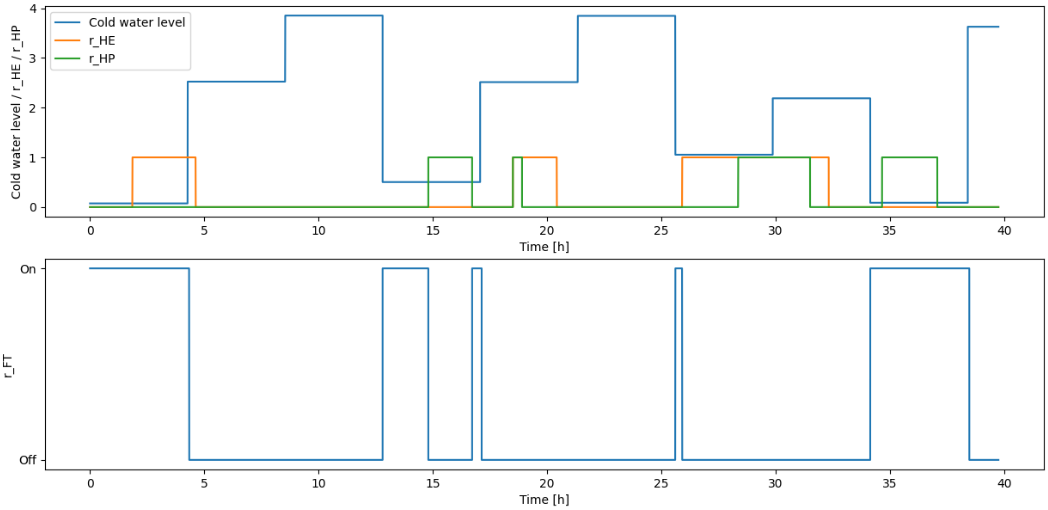

Figure 3.9.: Well inlet result

The well inlet is responsible for the refilling of the cold water tank. While the heat pump or the heat exchanger is running, it is not needed to use well water to refill the cold water tank because the two devices feed the cold water tank with water. If the cold water level is shallow, the well inlet is active no matter whether the heat exchanger or the heat pump runs. This the case for the last on-phase in the lower chart (hour 34 to hour 38). All the other cases do not have an urgent need, so the water feed from the heat pump and heat exchanger are sufficient. The upper chart shows the cold water level and the control signals for the heat pump and the heat exchanger's control signal.

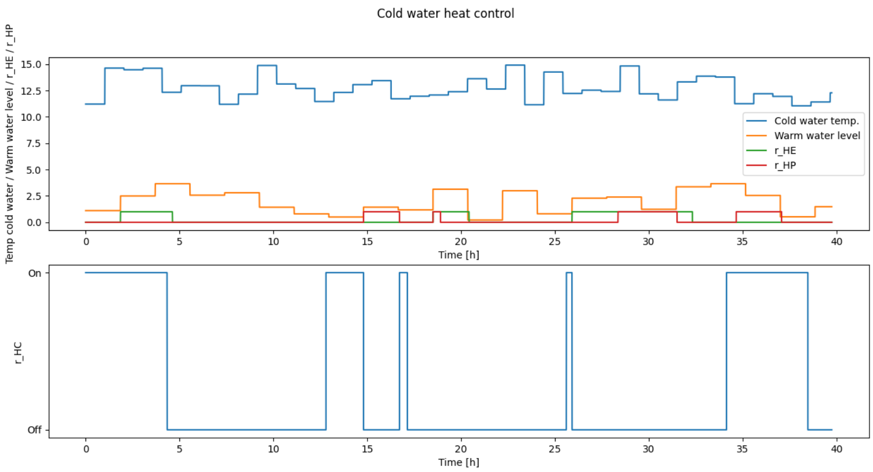

Figure 3.10.: Cold water heater result
If the cold water gets too cold, the warm water tank heats it if some conditions meet. The cold water tank must not have an overflow, and the warm water tank must contain enough water. Further, the heat exchanger and the heat pump should also be off, because otherwise they would produce tempered water. If the cold water temperature is far too low from production set temperature, it is acceptable to use the heat pump, the heat exchanger, and the warm water to heat the cold water tank. The first and the last on-phase in the lower chart show this behavior. The upper chart shows the necessary values for decision-making.

Figure 3.7, Figure 3.8,Figure 3.9, and Figure 3.10 show the results of the control strategies. The inputs are generated to test all possible operating modes and edge cases.

List of devices (In cooperation with Grömer, 2021)

Table 3.1.: Lab experiment: Equipment and devices

ID	device	producer	specification
3.1.1	Water bath 1 (55°C/60°C)	Lauda	Aqualine AL 12
3.1.2	Water bath 2 (40°C)	Grant JB series	-
3.1.3	Water bath 3 (25°C)	-	-
3.1.4	Water bath 4 (45°C/50 °C)	Harry Gestigkeit GmbH	W16, 1480202
3.1.5	Lab power supply 1	Volttech	RNG 3003 (1)
3.1.6	Lab power supply 2	Volttech	RNG 3003 (2)
3.1.7	Lab power supply 3	GW DC Power Supply	GPR-3030 D
3.1.8	Lab power supply 4	ELV	PS 7030
3.1.9	Multimeter	Keithley	179A TRMS Multimeter
3.1.10	Thermometer	Voltcraft Datalogger	K 204, Inv. Nr: 060600503
3.1.11	Magnetic Stirrer	Carl Roth	R 1000
3.1.12	Scales	Ikea	Drycken
3.1.13	Hair dryer	-	-
3.1.14	Ultrasonic bath	Bandelin Sonorex	0146799
3.1.15	Thermal element	-	-
3.1.16	KPG stirrer	Janke&Kunkel	Inv.Nr: 0175973
3.1.17	Copper Substrate	-	-
3.1.18	Caliper	-	-
3.1.19	Beaker Glass	Carl Roth	volume: 1 l
3.1.20	Tweezer	-	-
3.1.21	Crocodile clip	-	-

List of chemicals and materials (In cooperation with Grömer, 2021)

Table 3.2.: Lab experiment: Materials and chemicals

ID	material/chemical	producer	specification
3.2.1	Copper sulfate pentahydrate	Carl Roth	Copper(III) sulphate pentahydrate
3.2.2	Copper sheet	-	-
3.2.3	Sulfuric acid	Carl Roth	25 %
3.2.4	Destillated water	-	-
3.2.5	Perfume-free soap (tenside)	-	-

Copper sulfate pentahydrate[1]

H302: Harmful if swallowed.
H318: Causes serious eye damage.
H410: Very toxic to aquatic life with long lasting effects.
P273: Avoid release to the environment.
P280: Wear protective gloves/protective clothing/eye protection/face protection.
P305 + P351 + P338: IF IN EYES: Rinse cautiously with water for several minutes. Remove contact lenses, if present and easy to do. Continue rinsing.
P313: Get medical advice/attention.

Sulfuric acid[2]

H290: May be corrosive to metals.
H314: Causes severe skin burns and eye damage.
P280: Wear protective gloves/protective clothing/eye protection/face protection.
P301 + P330 + P331: IF SWALLOWED: rinse mouth. Do NOT induce vomitting.
P303 + P361 + P353: IF ON SKIN (or hair): Remove/Take off immediately all contaminated clothing. Rinse skin with water/shower.
P305 + P351 + P338: IF IN EYES: Rinse cautiously with water for several minutes. Remove contact lenses, if present and easy to do. Continue rinsing.

[1] http://gestis.itrust.de/nxt/gateway.dll/gestis_de/491473.xml
[2] http://gestis.itrust.de/nxt/gateway.dll/gestis_de/001160.xml

3.2. Electroplating and Predictions

3.2.1. Lab-scale experiment

The lab-scale experiment is a cooperation with Grömer, 2021.

Lab preparation

The first thing to do in the lab is the setup of the heated water baths (Table 3.1.1, Table 3.1.2, Table 3.1.3, Table 3.1.4). They need up to 20 minutes to reach and stabilize the set temperature. The second step is to clean the utilities such as beaker glasses (Table 3.1.19), stirrer (Table 3.1.16), and tweezers (Table 3.1.20).

Production of the electrolyte

According to Jelinek, 2013, the electrolyte should have a mass concentration of $100\,\mathrm{g\,L^{-1}} < \beta(\mathrm{CuSO_4}) < 200\,\mathrm{g\,L^{-1}}$. A batch of electrolyte has 760 mL. This is enough liquid to do four electroplatings parallely. First, $m(\mathrm{CuSO_4} \cdot 5\,\mathrm{H_2O}) = 133.5\,\mathrm{g}$ copper sulfate pentahydrate (Table 3.2.1) are weighed. In a second step the $\mathrm{CuSO_4} \cdot 5\,\mathrm{H_2O}$ is dissolved in $m(\mathrm{H_2O}) = 750\,\mathrm{g}$ destilled water (Table 3.2.4). The solution homogenizes for 10 minutes using a magnetic stirrer (Table 3.1.11). By adding $V(\mathrm{H_2SO_4}) = 10\,\mathrm{mL}$ sulfuric acid (Table 3.2.3) the pH-value is set to $pH = 4$. After a further homogenization the electrolyte was divided into beakers and tempered in the heated water baths.

Prepare the copper plates

The copper plates need a few cleaning steps each time before electroplating. In the first step, the copper plates are cleaned with a sponge combined with a scouring pad. It is a mechanical cleaning step to remove copper patina and anode sludge. The copper patina is the product of the natural aging of copper, depending on weather conditions. It is a copper-(carbonate-sulfate-chloride)-hydroxide mixture. Anode sludge contains all non-dissolvable contaminations of the copper plate. The mechanical cleaning with the sponge takes about five minutes per copper plate. The best indicator is when the whole plate has a light copper color (pale pink color). Then the copper plates are rinsed with water. The second cleaning step is ultrasonic cleaning in a ultrasonic bath (Table 3.1.14). Perfume-free soap (Table 3.2.5) is added to the bathwater as a tenside to remove grease residues. Then the copper plates are rinsed with water again. The last step is the acid cleaning step. Sulfuric acid (Table 3.2.3) cleans the copper plates' surfaces and dissolves surface contaminations. Calculating the current density (Equation 2.2) needs the coated copper plate area. Insulation tape swathed the copper plate to have a defined area. The area is then measured with a caliper (Table 3.1.18). The last step is the labeling and the weighting of the copper plates.

Electroplating

After preparation, labeling, and documentation, the electroplating can start. Crocodile clips (Table 3.1.21) connect the copper plate with the cables. The lab power supplies (Table 3.1.5, Table 3.1.6, Table 3.1.7, Table 3.1.8) deliver the energy for the electroplating process. The tempered beaker glasses hold the copper plates separated from each other. Thus they do not touch each other and produce a short circuit. The electrolyte must cover the marked area where the material should deposit. Figure 3.11 shows the schematic representation of the setup. The lab power supplies produce the energy for the reaction. The parameters are set according to the experiments' plan. Each experiment has its own duration time, current density, and temperature. During the electroplating process, measurements take place. For description, see the Documentation section below. After the duration time, the process stops by turning off the lab power supply. The operator removes the copper plates from the beaker glass, rinses them with water, and dries them with a hairdryer (Table 3.1.13). Figure 3.12 and Figure 3.13 show pictures taken in the lab.

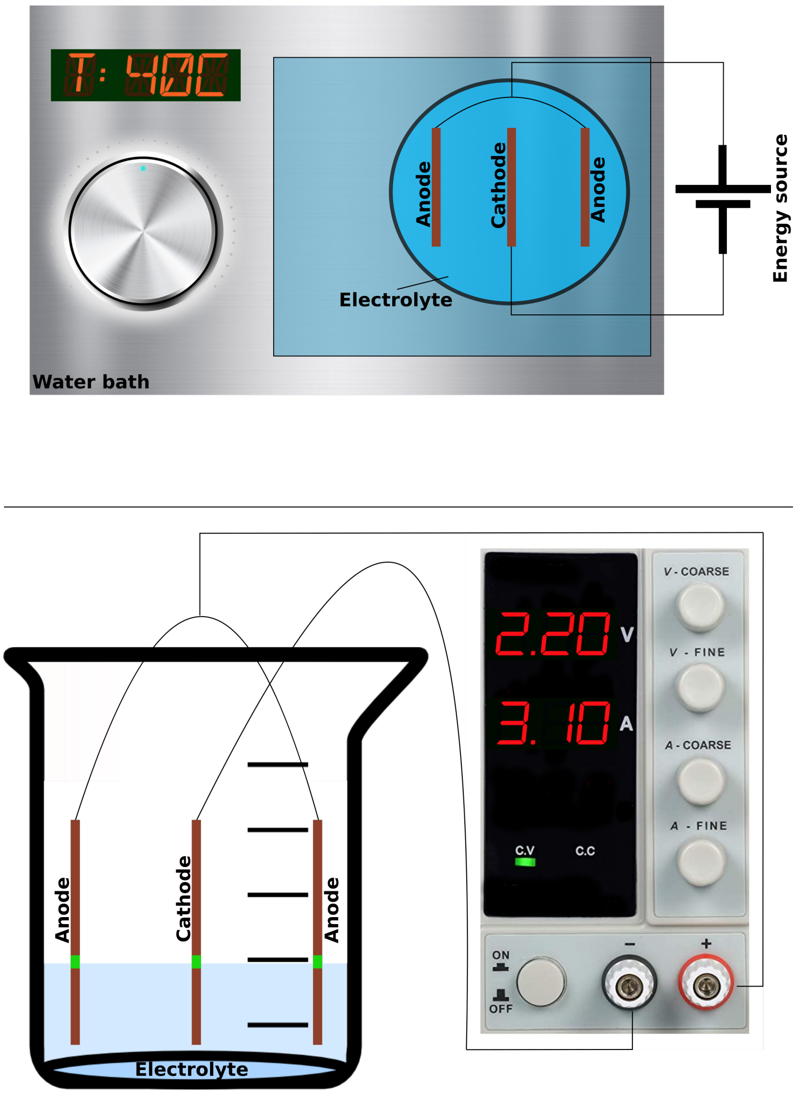

Figure 3.11.: Experimental setup scheme
The upper part shows a view from above. It shows a heated water bath containing the beaker glass where the electroplating takes place. It also shows the arrangement of the copper plates and the wiring. The second figure shows a frontal view of the electroplating process. On the left-hand side, it shows the beaker glass with the copper plates and the wiring. It also shows the isolation tape in green, which separates the processed copper area from the rest of the plate. The right-hand side shows a state-of-the-art lab power supply and the connections to the copper plates.

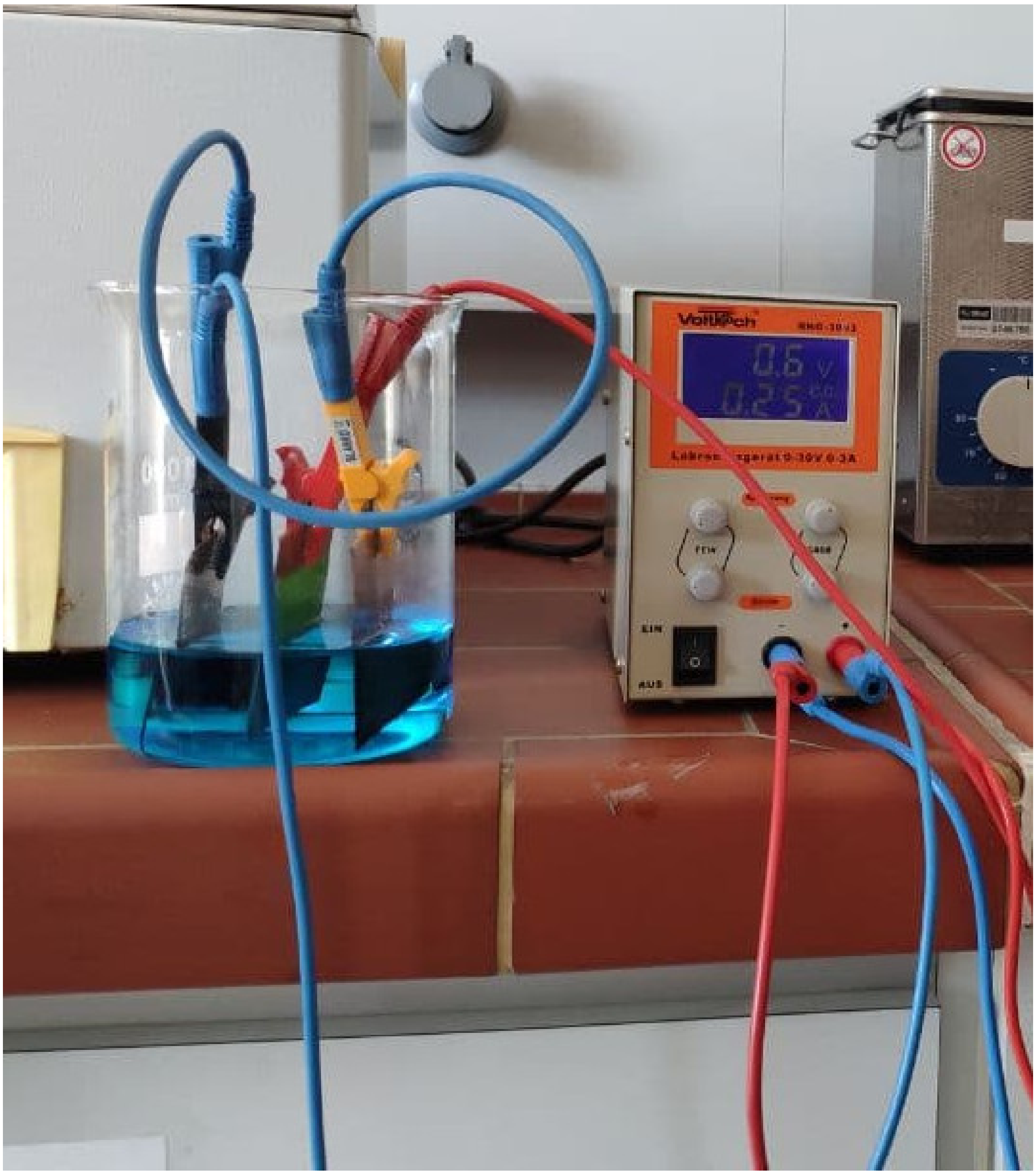

Figure 3.12.: Experimental setup
The picture shows the setup from Figure 3.11 in the lab.

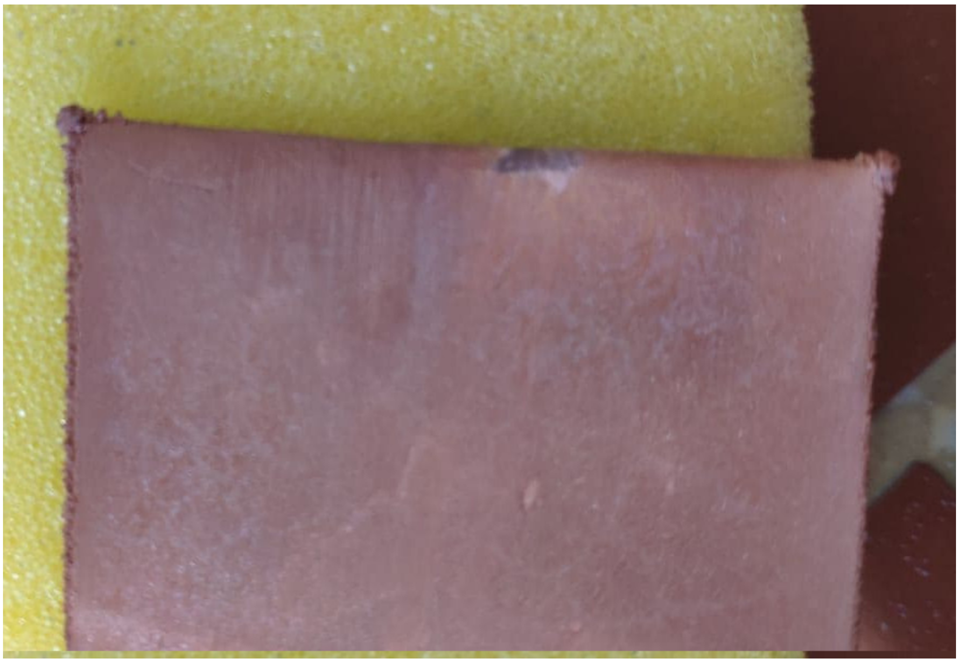

Figure 3.13.: Electroplating result
The picture shows the result of the electroplating. In the top mid, it shows the imprint of the holder. At the edges, non-perfectly linear field lines produce a higher deposition than on the surfaces. On the surface is plane and equally distributed deposition.

Documentation

VersuchNr.						
SOLL		min.		°C		A/dm^2
						A
	Nummer	Masse Start [g]	Masse Ende [g]	Fläche Kathode [cm^2]		
Kathode						
Anode 1						
Anode 2						
Temp_1 [°C]		Temp_2[°C]		Temp_3 [°C]		
I_1 [A]		I_2 [A]		I_3 [A]		
U [V]						
Startzeit			Endzeit			
			Dauer [min-]			
Netzteil						

Figure 3.14.: Documentation template

Figure 3.14 shows the template for the documentation. It contains all relevant information for the evaluation. The experiment number (VersuchsNr.) is a sequential number to identify and separate the individual experiments. In the target (SOLL) row, the parameters for the experiment are entered. It holds the duration time (min.), the temperature (°C), and the current density($A/dm^\wedge 2$). The current density depends on the area and the current (see Equation 2.2) and cannot be set directly. Thus the current must be calculated. The table in the middle of the template holds relevant information about the copper plates. It holds the label (Nummer) of the plates, their start (Masse Start [g]), and end (Masse Ende [g]) mass, and the area (Fläche Kathode [$cm^\wedge 2$]) which is in contact with the electrolyte. The copper plate area's length and width are used to calculate the area which is in contact with the electrolyte. The last six lines hold information for the electroplating process. It holds the electrolyte's temperature at the beginning (Temp_1[°C]), in the middle (Temp_2[°C]), and at the end (Temp_3[°C]) of the process. The same holds for the amperage (I_1[A], I_2[A], I_3[A]). Further, the template has a field for the voltage (U [V]), the number of the lab power supply (Netzteil), the start (Startzeit) and end (Endzeit) time, and the duration (Dauer [$min-$]) as a result of them. The results of the experiment are in Appendix C (original values) and in Appendix B (processed values).

Evaluation

The evaluation uses different methods to calculate the layer thickness and the energy consumption of the electroplating process. The original data (see Appendix C) are transferred to a spreadsheet. The transfer is validated by reference calculations, which are in a certain range or calculated from the data. Per definition of the experiment criteria the current density must be in range of $0.5\,\mathrm{A\,dm^{-2}}$ to $5\,\mathrm{A\,dm^{-2}}$ (Unruh, 2016). The plating area is also a fixed value and is between $25\,\mathrm{cm^2}$ and $35\,\mathrm{cm^2}$. The last criterion is the mass difference. Optimally it is zero, but caused by measuring errors, this does not always hold. So an epsilon $\varepsilon = 0.07\,\mathrm{g}$ is added to compensate for the errors.

Figure 3.14 shows the distributions of the influencing parameters in seperated charts. Each parameter has its own bar chart. Figure 3.15(a) shows the distribution of the current density. The value should be between $0.5\,\mathrm{A\,dm^{-2}}$ and $5\,\mathrm{A\,dm^{-2}}$. 18 results ($\sim 9\%$) are out of range. They are still used in the evaluation because they are valid results. The boundaries were set in the lab experiment preparations to get a rough idea of the values. The boundaries for the duration are 10 min as the minimum and 90 min as the maximum. Figure 3.15(b) shows the distribution of the duration. The data set has 4 out layers ($\sim 2\%$). The results are valid and used in the evaluation. The temperature distribution does not have any out layers. Figure 3.15(c) shows its distribution. During the experiments, only three results are invalid. One was a documentation error, and two results are invalid because of technical issues.

The valid data sets are the basis for further calculations and evaluations. The first approach is to use Equation 2.1 to calculate the layer thickness from the parameters and compare them to the gathered data. The coefficient of determination R^2 (Rinne and Ickler, 1986) determines the comparison.

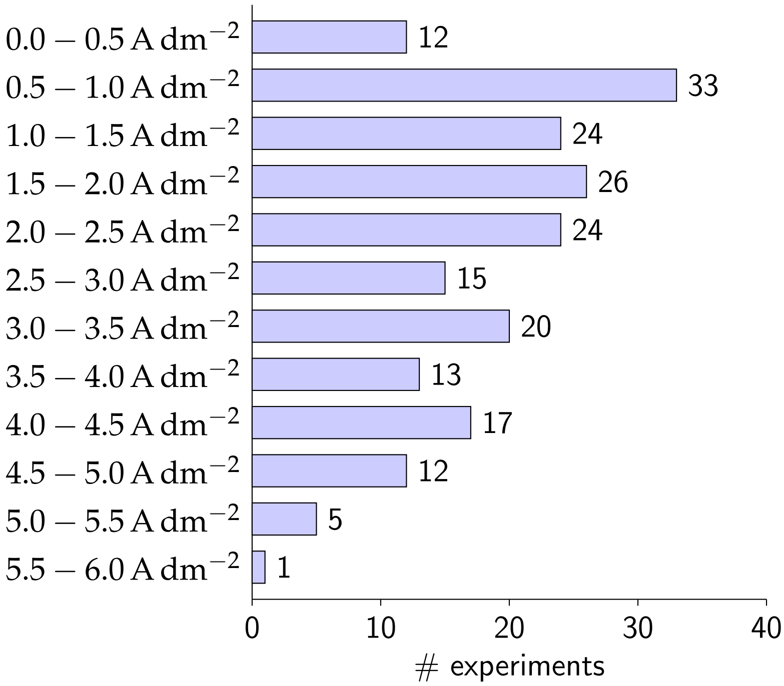

(a) Current density distribution

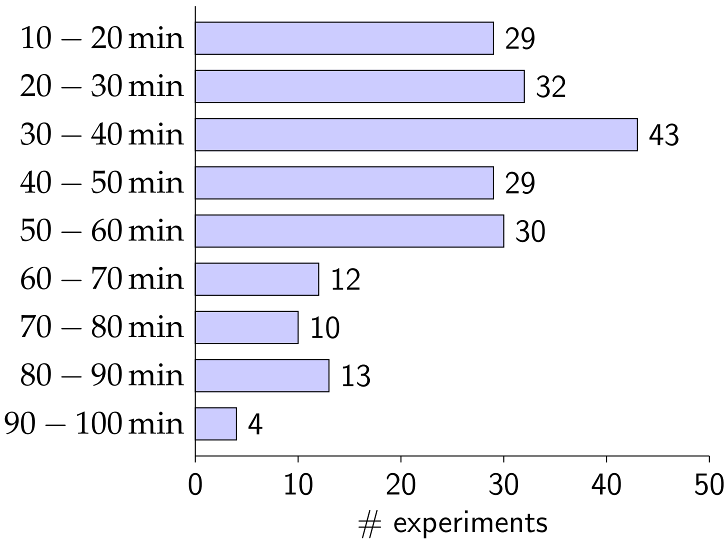

(b) Duration distribution

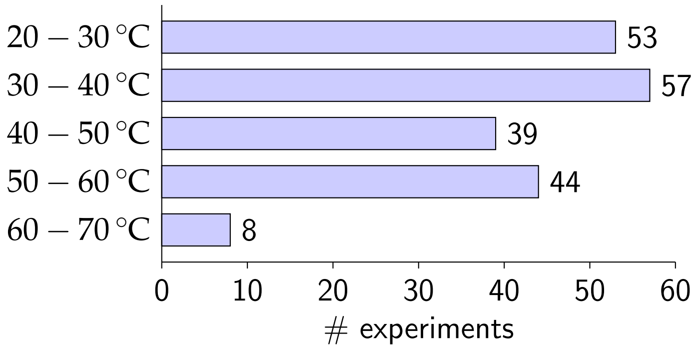

(c) Temperature distribution

Figure 3.14.: Distribution of experiment parameters
The lab experiments consist of over 200 experiments. In each experiment, the duration, the current density, and the temperature are chosen randomly within given boundaries. The bar charts show the distribution of the parameters.

$$R^2 = \frac{\sum (\hat{y}_i - \bar{y})^2}{\sum (y_i - \bar{y})^2} \tag{3.16}$$

where:

$\hat{y}_i$ = Predicted measurement
y_i = Single measurement
$\bar{y}$ = Mean of y

A further step uses neural networks and other machine learning methods to predict the layer thickness. Chapter 2.4 gives an overview of the used methods. The methods take the duration, temperature, and current density as input. All methods use supervised learning, so the layer thickness (resp. the mass of deposit copper) is also a parameter for the training. The trained models are used to predict further measurements. The results of the models can be found in Chapter 3.2.2. The methods described map the process well. The last step is the calculation of the needed electric energy for the procedure. The electric power P, and the electric potential energy W (Plamann and Schulz, 2016) can be calculated from the existing data.

$$W = P * t \tag{3.17}$$

where:

W = Electric potential energy
P = Electric power, see Equation 3.18
t = Duration time

$$P = U * I \tag{3.18}$$

where:

P = Electric power
U = Voltage
I = Electric current

The measurements and the calculated data are used to train a model, as well. This time the predicted value is the electric potential energy. The results of these models are in Chapter 3.2.3.

3.2.2. Coating thickness prediction

Appendix B shows 2 tables. The first table contains the documented data from the lab experiment. The second table contains the calculated values from the first table. The first evaluation of the data is the calculation of the coating thickness in two ways. The first approach is the expected coating thickness t_e, using Equation 2.1. The second approach is to calculate the real coating thickness t_r from the deposit mass of copper and the coating area.

$$t_r = \frac{\Delta m_C}{\varrho * A} \tag{3.19}$$

where:

t_r = Real coating thickness
Δm_C = Mass of deposit copper
ϱ = Density of copper
A = Coating area

In more than 90 % of the experiments, the deviation between the real and the expected coating thickness is smaller than 15 %. The R^2 over the whole data set is 0.98, which is very close to 1 and, therefore, excellent. The calculated real coating thickness t_r is the label for the documented data. With data and the corresponding label, models are trained to predict the coating thickness. The data set is divided and 70% of the data are used as training data. The used models are described in Chapter 2.4.

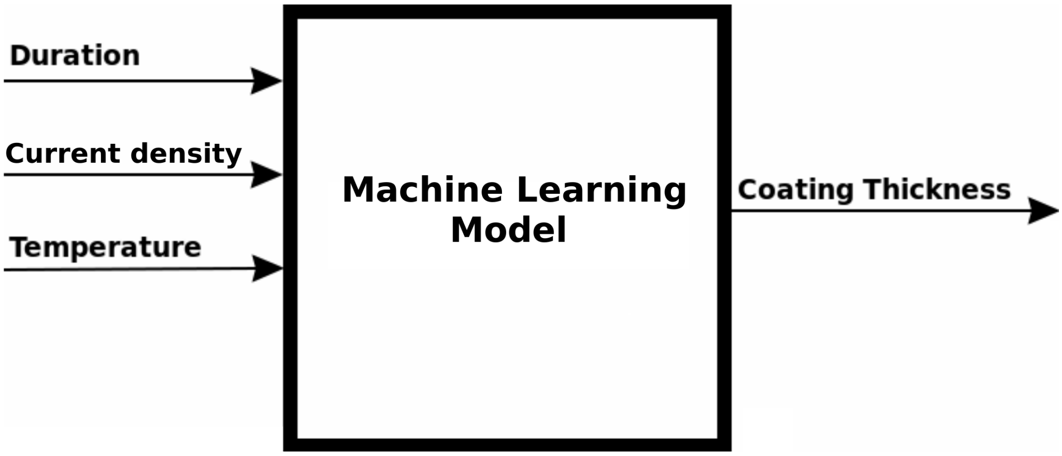

Figure 3.15.: Coating thickness model
A machine learning model needs the duration, the current density, and the temperature to predict the coating thickness.

Figure 3.15 shows the input features and the output/label for the created models. Chapter 4.2.1 holds the interpretation of the coating thickness prediction results. To get comparable and reproducible results, the random state is fixed for all methods which use it.

Linear regression

The linear regression does not need any further information than the data as input. The R^2 value determined the similarity between the predicted and the real values. It is applied to the test set and the training set. Table 3.3 shows the results on the test set and the training set.

Table 3.3.: Coating thickness prediction: Linear regression model

	R^2 on test set	R^2 on training set
Linear regression	0.812	0.777

Polynomial regression

The polynomial regression needs the maximal degree of the polynomial as an additional parameter. The model is created seven times with different maximal degree parameters. Setting the degree to one, the polynomial regression model becomes a linear regression model. Table 3.4 shows the results on the test set and the training set. With a degree of 7 the R^2 becomes negative. This happens when the model is worse than the null hypothesis. This means that the model fits the data worse than a straight line.

Table 3.4.: Coating thickness prediction: Polynomial regression models

Maximal degree	R^2 on test set	R^2 on training set
1	0.812	0.777
2	0.982	0.974
3	0.977	0.979
4	0.975	0.983
5	0.974	0.986
6	0.898	0.989
7	-1.357	0.993

Decision tree regression

The Decision tree regression needs the maximal depth of the tree as an additional parameter. The model is created 19 times with different maximal depth parameters. Table 3.5 shows the results on the test set and the training set.

Table 3.5.: Coating thickness prediction: Decision tree regression models

Maximal depth	R^2 on test set	R^2 on training set
1	0.385	0.370
2	0.596	0.725
3	0.730	0.845
4	0.869	0.944
5	0.914	0.977
6	0.922	0.993
7	0.940	0.997
8	0.931	0.999
9	0.933	1.000
10	0.932	1.000
11	0.938	1.000
12	0.937	1.000
13	0.930	1.000
14	0.936	1.000
15	0.929	1.000
16	0.931	1.000
17	0.938	1.000
18	0.931	1.000
19	0.937	1.000

Random forest regression

The random forest regression does not need any further information than the data as input. Table 3.6 shows the results on the test set and the training set.

Table 3.6.: Coating thickness prediction: Random forest regression model

	R^2 on test set	R^2 on training set
Random forest regression	0.959	0.994

Neural networks

The neural network consists of three hidden layers with 30 neurons each. The input layer is also a 30 neurons layer. Table 3.7 shows the results on the test set and the training set.

Table 3.7.: Coating thickness prediction: Neural network

	R^2 on test set	R^2 on training set
Neural network	0.946	0.991

3.2.3. Electric potential energy prediction

To calculate the real electric potential energy Equation 3.17 and Equation 3.18 are used. The results are the labels for the data models. Further, the data models get the duration, the temperature, the amperage, and the coating area as inputs. Each model used 70% of the data as training data. Figure 3.16 shows the structure of the data model. Chapter 4.2.2 holds the interpretation of the power prediction results. To get comparable and reproducible results, the random state is fixed for all methods which use it.

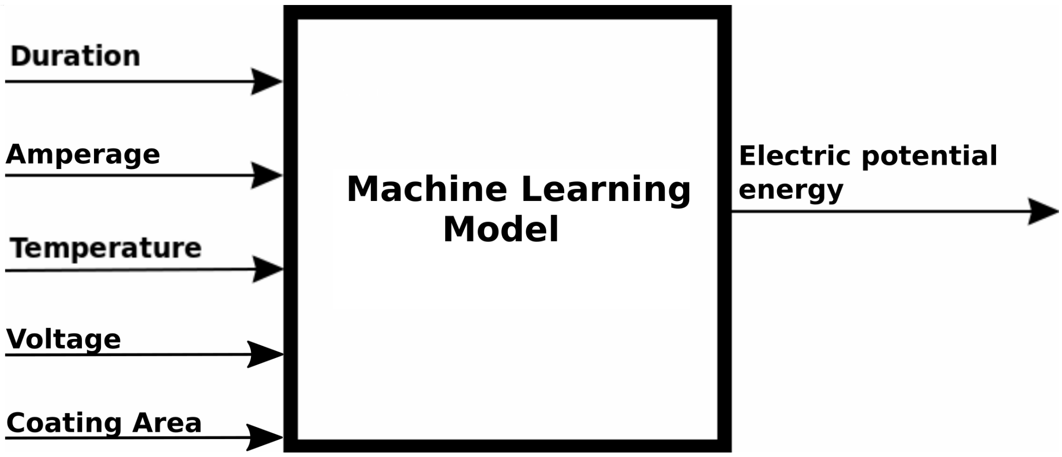

Figure 3.16.: Electric potential energy model
A machine learning model needs the duration, the amperage, the voltage, the coating area, and the temperature to predict the electric potential energy.

Linear regression and Polynomial regression

As stated in the last Chapter, linear regression is the same as a polynomial regression with one as its maximal degree. Thus both evaluations are combined in one section. The maximal degree parameter is varied from one to eight. Table 3.8 shows the results for varying degrees.

Table 3.8.: Electric potential energy: Linear regression and polynomial regression models

Maximal degree	R^2 on test set	R^2 on training set
1 = Linear regression	0.816	0.813
2	0.973	0.988
3	0.999	1.000
4	1.000	1.000
5	1.000	1.000
6	0.997	1.000
7	0.959	1.000
8	-0.694	1.000

Decission tree regression

The Decision tree regression needs the maximal depth of the tree as an additional parameter. The model is created 19 times with different maximal depth parameters. Table 3.9 shows the results on the test set and the training set.

Table 3.9.: Electric potential energy: Decision tree regression

Maximal depth	R^2 on test set	R^2 on training set
1	0.574	0.474
2	0.574	0.726
3	0.728	0.863
4	0.718	0.931
5	0.758	0.978
6	0.789	0.993
7	0.842	0.997
8	0.801	0.999
9	0.895	1.000
10	0.857	1.000
11	0.885	1.000
12	0.774	1.000
13	0.884	1.000
14	0.782	1.000
15	0.788	1.000
16	0.854	1.000
17	0.869	1.000
18	0.847	1.000
19	0.859	1.000

Random forest regression

The random forest regression does not need any further information than the data as input. Table 3.10 shows the results on the test set and the training set.

Table 3.10.: Electric potential energy: Random forest regression model

	R^2 on test set	R^2 on training set
Random forest regression	0.887	0.987

Neural network

The neural network consists of three hidden layers with 30 neurons each. The input layer is also a 30 neurons layer. Table 3.11 shows the results on the test set and the training set.

Table 3.11.: Electric potential energy: Neural network

	R^2 on test set	R^2 on training set
Neural network	0.939	0.990

3.3. Function-based approximation of data

This section presents the structure of the program and its results. The approximation is written in Python. The script has the following steps:

- Load data
- Calculate function parameters
- Calculate off-times
- Predict data for the future

Load data

In the course of this thesis, a program was developed to perform the function-based approximation automatically. The program has to load two files. The first file is a comma-separated values file (CSV file). It contains the data and the corresponding timestamps. The program uses this file to calculate the parameters for the approximation functions and to draw compare graphs. The second file contains information about the off times of the plant. The program uses this data to decide whether the plant is in production mode or turned off. Further, the data is needed to determine the point when the plant has to start heating, so it reaches production temperature when production begins.

Calculate function parameters

In the first place, the program calculates the default value for production. This value is the set point of the plant. The only known fact at this point is that the plant is mostly in production mode and only in about 15% (Weekend and Maintenance) off. So the program calculates the median M and the standard derivation SD of the data from the CSV-file. The median method sorts all n values from lowest to highest and picks the value located at index $n/2$ as its result. It is very likely to choose a value that belongs to the production phase because the production phase is about 85% of the time. To be sure that the value is a production phase value, the standard deviation is calculated, and then the program filters the whole data set and removes every value which is not in the range $M \pm SD$. On the filtered data set, the median is again calculated. This double-check removes every value which does not belong to the production phase and results in a value used as set point SP and the corresponding SD. In a second step, the variation around the SP is modeled. The deviation around the SP is shaped like a sine function. When the value gets too low, the bath starts heating and stops when it reaches a turn-off value. This up and down makes the data look like they are oscillating, and the sine function represents this behavior. The program used a general sine function

$$f(t) = A * \sin(\omega * t + \phi) + \alpha \tag{3.20}$$

where:

$f(t)$ = Value at a given time t
A = The amplitude of the sine function
ω = Correction factor for t
ϕ = The shift of the phase
α = Offset in y direction

The program fits the parameters to the given data using Scipys (Virtanen et al., 2020) optimization functions. This results in parameters A, ω, ϕ, and α to describe the sine function. In the last step, the parameters for the cooldown and the heat up are calculated. This step aims to find parameters for the Equation 2.6 and Equation 2.7. It first identifies the sequences where the cooldown and the heat up happen by filtering the data and removing the data at the $SP \pm SD$ and then finds the most prolonged phase where it happens. This way it gets the most precise values for the parameter calculation. Then the program again fits the equations to the data using the Scipy package. By doing this, the parameters for cooldown and heat up are determined.

Calculate off-times

The off-times are mostly determined by the maintenance and the weekends. During the creation of the offtime-object, the program calculates already the point when heat up has to start. For this it solves Equation 2.6 and Equation 2.7 for the time when they meet at the same point. It results in

$$t = \frac{\mathcal{W}\left(\frac{e^{\frac{c_c*(T_X-T_A)}{c_h}}*c_c*(T_0-T_A)}{c_h}\right)*c_h - c_c*(T_X-T_A)}{c_c*c_h} \tag{3.21}$$

where:

t = Time where the two functions are equal
T_0 = The temperature of the fluid at the beginning of cooldown
T_A = The temperature of the ambient
T_X = Fictive temperature where heat up has to start at begin of cooldown
c_c = A coefficient affected by the volume of the fluid, the surface, thermal capacity, and the density of the fluid
c_h = A coefficient affected by the volume of the fluid, the surface, thermal capacity, and the density of the fluid
$\mathcal{W}$ = Lambert $\mathcal{W}$ function

The precalculation makes the prediction less compute intensely. Instead of checking each time in which phase of the off-time a given timestamp is, the program has to check if the timestamp is smaller than t, then it is in the cooldown phase; otherwise, it is in the heat-up phase.

Predict data for the future

After all the preparations, the prediction is an easy task. For each given timestamp, the program checks if it is in an off-time or not. If it is not, then it uses the calculated sine parameters to get the prediction value. If it is an off-time phase, then the program checks if it is before or after the turning point and selects the cooldown curve with the calculated cooldown parameters if it is before the turning point. IF not it uses the heat-up function and the computed parameters. Figure 3.17, Figure 3.18 and Figure 3.19 show the results of the prediction in general and in detail.

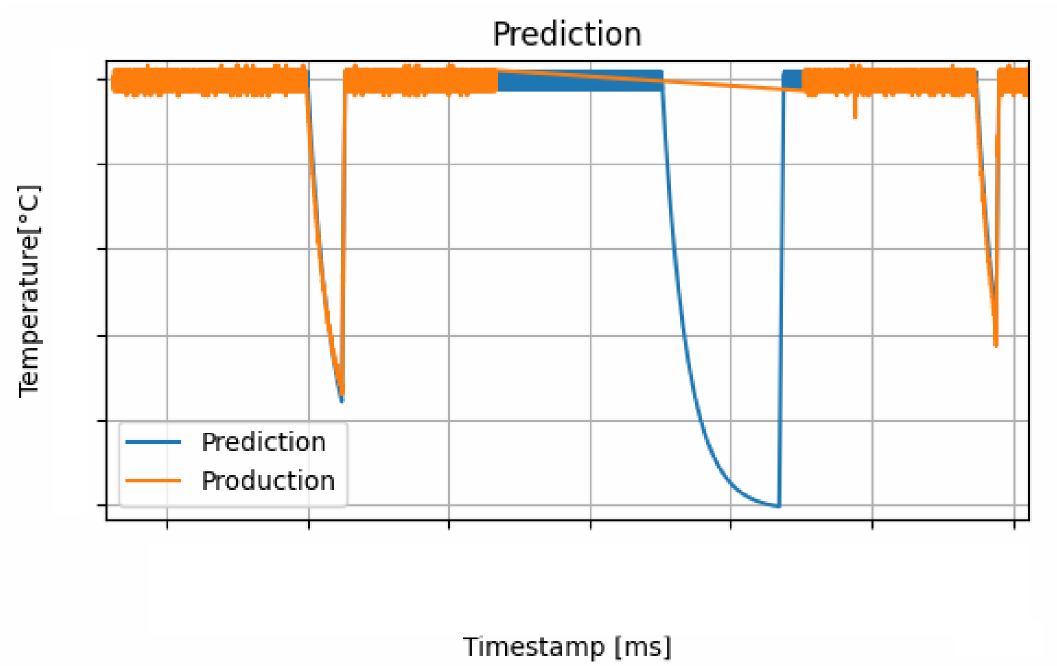

Figure 3.17.: Real data vs. prediction data
The orange curve shows the real data, and the blue curve shows the predicted data. The predicted data follows the real data quite well. There is a gap in the real data from a recording error in the middle of the graph, but the prediction does still work because it does not depend on the real data. For more details, see Figure 3.18 and Figure 3.19.

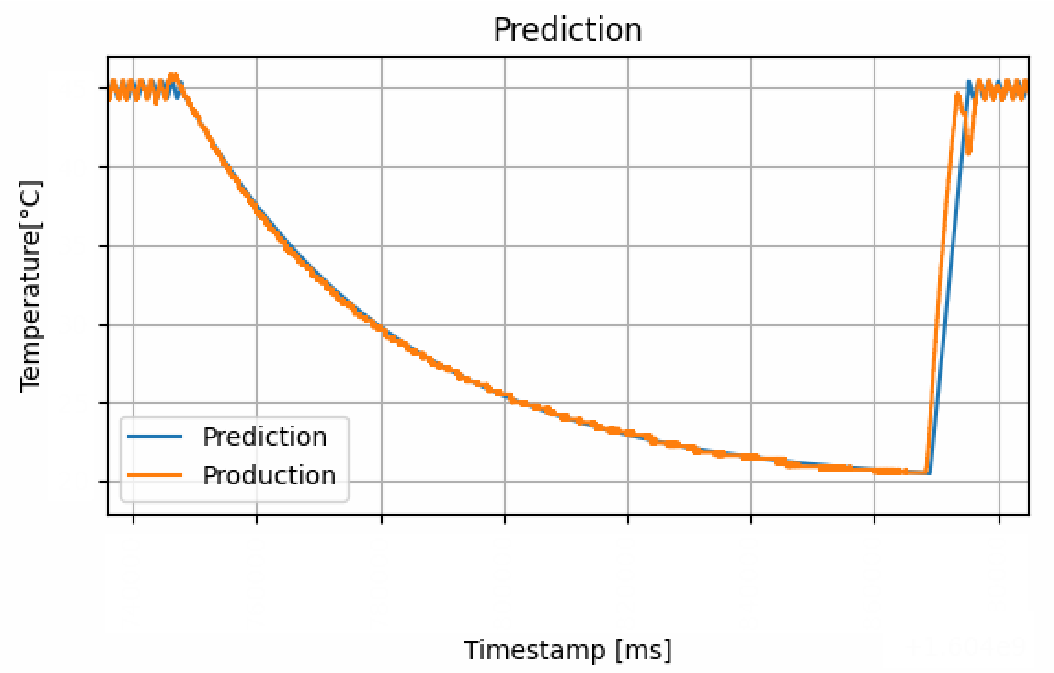

Figure 3.18.: Real data vs. prediction data: Off-time phase
The orange curve shows the real data, and the blue curve shows the predicted data. This graph is a more detailed view of the off-time phase. The prediction is pretty accurate. Only in the heat-up phase, there is a small drop in the real data, which cannot be considered in the forecast.

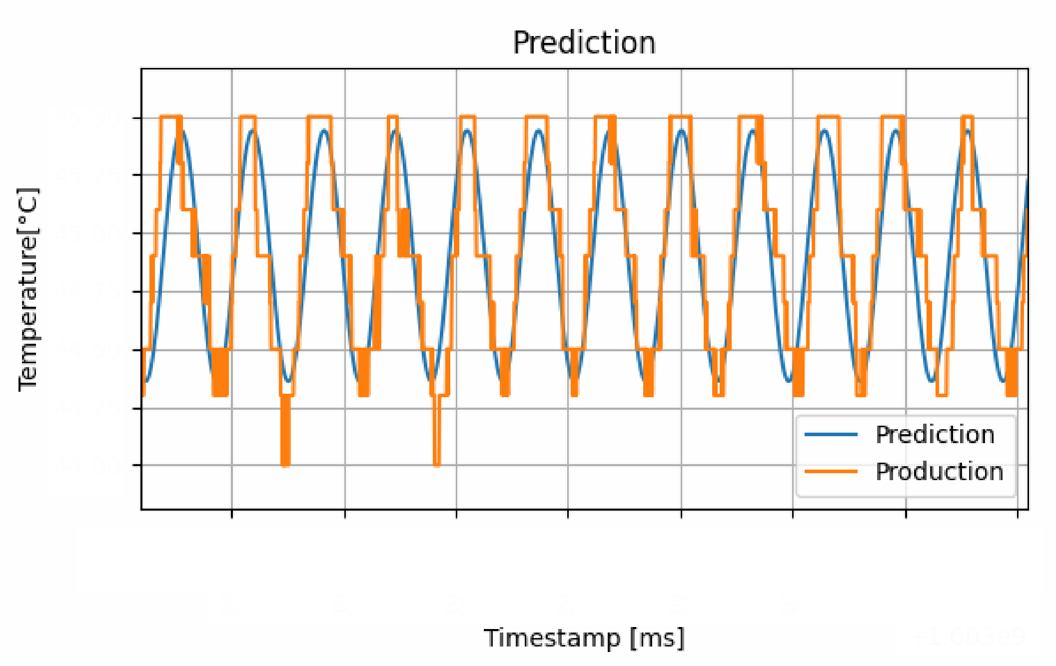

Figure 3.19.: Real data vs. prediction data: Production phase
The orange curve shows the real data, and the blue curve shows the predicted data. This graph is a more detailed view of the production phase. It shows the real data and the approximated sine function. The approximations fit the real data well. In some cases, the prediction is shifted, and the real data and the prediction data are inversed. It is not an actual fault because it can even happen in actual production that the data shift, caused by ambient conditions or shortstops in production.

4. Discussion

The key feature of the DET model is the imitation of the real plant. It is the main feature for the digital model's energy calculation and makes the twin more comparable with its real antagonist. The thesis's main parts are the DT model, the data models for the electroplating as preparatory study for the DT model, and sensor data approximation. All aspects brought good results. The DT model handles various control mechanisms that are essential for the operation of the plant and the correctness of the model. The data model for the electroplating works well. They show accurate results and fit the actual data well. Since the plant uses quite the same plating method, a transfer from the lab-scale model to the real-world model is likely and can be done in follow-up work. The current solution for the sensor data approximations works well for liquid tanks, which have cool-down and heat-up phases. Adopting other scenarios is possible, but it is an effort to find proper functions and optimize them to fit the data. The DET project is ongoing; thus the methods and tools developed in this thesis are a vital part of the project.

4.1. Digital Energy Twin Model

The development of the DET model is an ongoing process, and many parts of the model are still in development or haven't even started. The primary air consumers, the drilling machines, were not modeled yet. Due to these circumstances, it is impossible to test the control models developed in the thesis with real data inputs; thus, it is impossible to show the control logic under real conditions. The results show the control module structure and experiments with test data to see if the implementation works as expected. Also, the water consumers and water return devices are not implemented in the DET model by now. This affects the tank logic and the overflow logic. All control signals generated by these two modules depend on the water level in the tanks. So the evaluation of the model also took place with test data instead of real data. When the other parts will be finished, another test with real data should evaluate the actual scenario's control models' functionality. With new insights and further developement of the other parts it can happen that the created models need to be adapted, but the underlaying concept stays the same.

4.2. Electroplating and Predictions

Overall, the data models work well (see Chapter 4.2.1 and Chapter 4.2.2), but there are also limitations by the mathematical foundation of the models. The training set heavily limits the decision tree regression and the random forest regression. Both regressions cannot predict outside of the limits of the training set parameters. For them, it is not possible to see patterns in the data. A pattern would be a direct proportion between the duration time and the coating thickness in the electroplating data set. The longer the coating takes, the thicker the layer becomes. Also, polynomial regression is not aware of such outlying data. The ML cannot consider physical constraints, which are not covered by the training set. A perfect example would be the whole consumption of the anode. If there is no anode left, the reaction cannot occur anymore, and then the duration time can be infinite long without depositing any copper. But it is not possible to take all these effects into account. The data models represent a working, non-malicious environment. In future work, it would be interesting to integrate physical knowledge in ML algorithms. Rueden et al., 2019 show approaches for this.

4.2.1. Coating thickness prediction

The R^2 value is a relevant measurement and a good indicator of the quality of data models. Chapter 3.2.2 shows this information for the used data models. Table 4.1 shows the best results for each of the data models on the test set.

Table 4.1.: Best results for the data models

Data model	R^2 on test set	R^2 on training set
Polynomial regression (degree = 2)	0.982	0.974
Decision tree regression (depth = 7)	0.940	0.997
Random forest regression	0.949	0.994
Neural networks	0.946	0.991

Linear regression and polynomial regression are combined into one line in the table because the linear regression is a polynomial regression of the degree at most one. Polynomial regression performs well for this data model, and even a small polynomial degree has excellent results on the test set and the training set. The other methods also perform well on the data and are very close to the polynomial regression results. Decision tree regression and random forest regression are very similar because they are based on the same background. Separating the data into a test set and a training set is crucial to detect and reduce overfitting. Most data models overfit when they get too confident on the training data. This especially happens to higher degrees for the polynomial regression.

4.2.2. Electric potential energy prediction

The R^2 value is a relevant measurement and a good indicator of the quality of the method. Chapter 3.2.3 shows this information for the used data models. Table 4.2 shows the best results for each of the data models on the test set.

Table 4.2.: Best results for the data models

Data model	R^2 on test set	R^2 on training set
Polynomial regression (degree = 4)	1.000	1.000
Decision tree regression (depth = 9)	0.895	1.000
Random forest regression	0.887	0.987
Neural networks	0.939	0.990

For the electric potential energy, a polynomial regression has the best performance as well. The model is based on more parameters than the coating thickness model, so it is not surprising that also the polynomial regression needs a higher degree to have the best performance. The other data models also perform excellently on the training set, but they have weaknesses in finding the real context of the features, and so they do not perform so well on the test data set. Decision tree regression and Random forest regression have a lousier performance than neural networks and polynomial regression. Neural networks work the same for both data model scenes.

4.3. Function-based approximation of data

The method approximated the data well. The main point of good approximation is to know the off-times of the plant. For past data, it is a look at the data to see when production ends and when it starts again. Nevertheless, for future predictions, this is not possible since the data does not exist yet. A reference point is the plant's shift plan, which is planned for the future and gives information on when production is on and when not. It leads to a rough estimation that works, but it negatively influences future predictions based on the approximation; they get inaccurate. The further the prediction is in the future, the more inaccurate it gets. A compromise is a limitation of future predictions. For example, limit them to two weeks. Thus the prognosis does not get too imprecise.

> *A fool with a tool is still a fool!* – Parker and HP OpenView Business Unit, 2001

Function-based approximation of data is an excellent method to generate predictions. Like every other prediction method, it has some advantages and some drawbacks. The structure is apparent, and there are no hidden parts that are defined by a training algorithm. The underlying data determine every parameter, and the connections are visible. It is easy to see how a program calculates the result of the prediction. It makes function-based approaches easy to understand and, therefore, suitable, controllable and adaptable. But this also leads to drawbacks. To create such a function-based approximation, one needs to understand the system and the underlying data. This is an easier task on data with a physical background than on natural-based data like speech recognition. On natural-based data, function-based approximations come to their limits. In general, the user has to know how to use the tools and where the boundaries are.

5. Conclusion

This thesis contributed to the development of Digital Energy Twins for Industry 4.0. DETs are important to optimize systems for various parameters without affecting the real production system. This thesis addressed three research topics. The research aimed to calculate the electroplating process's energy consumption with ML methods, to optimize sensor data usage by function-based approximation, and further developed the DT model with Modelica.

Based on the lab experiment and the collected data, the energy consumption was calculated. With various ML techniques, it is possible to predict the energy consumption for an electroplating process. The ML methods' main features are the voltages, amperage, temperature, coating area, and the duration of the plating process. A data model fed with these features creates a prediction very close to the real energy consumption. The R^2 value of the polynomial regression with a degree of two is 1.000. It is an excellent value, and R^2 is the right measurement for the method's quality. The chosen method provides a good estimate of the energy consumption. The accuracy is sufficient for the whole electroplating plant's energy calculation since all components scatter around their real values.

The function-based approximation of sensor data is a crucial method for the development of digital energy twins. It has some main advantages. First of all, it allows creating an interface for the DT model and gather the data in a computationally effective way. Further, the approximation also allows predicting data in the future. It only needs information about the weekends' shutdown or machine maintenance. It is possible to generate this information with the shift plan, the maintenance plan, and the plant's utilization schedule. Since these plans only contain rough estimations when the events happen, and unplanned events entail maintenance, predictions in the far future are inaccurate. The created program for function-based approximation can make these predictions, but it is not recommended

to predict too far into the future. Up to two weeks should be reasonable because it normally contains four events (two times weekends and two times maintenance), and then the expected behavior does not differ too much from the real one. Thus further calculations on the predictions, like energy calculations for the tempering, are possible without the risk of heavy miscalculation.
The DT model is a work in progress. The research in this thesis is a integral part of the whole model, impacting the DT model's work. The control models allow a precise control of the individual machines. Since each device has its own control model, it is easy to maintain and test. The delays in the control strategies cover the start-up time for the real machines. The start-up and run-on time of the the real machine are the most significant differences between the model and the real-world object, because Modelica libraries do not take such effects into account.

Here are some recommendations for the project and the handling of the tool created within this thesis.
The basis for the function-based approximations tool is the sensor data. The collection of the data started in October 2020. The tool needs the data to calculate the parameters for the functions. Even if there is already enough data for the tool to work, it is still recommended to collect further data for at least a year or even more. The current measurements were taken in autumn and winter, so the temperature was low, and the humidity was high. These or other seasonal effects may affect the measurements and lead to fluctuations in the data. It could then affect the tool's calculations because real data changes, but the function-based approximation parameters stay the same.
The prediction of the function-based approximations tool is based on production plans. The plans cannot take unexpected failures into account. The further the prediction reaches into the future, the higher the chance that an unexpected failure happens. It leads to the recommendation that the prediction should not be longer than two weeks into the future. This recommendation is not based on expert assessment within the project.
The energy models from the lab experiment are a standalone tool. The validation of this tool was done with the lab data. When the model was developed, the plant's data was not available, so it was impossible to cross-validate. As described in Chapter 3.2 the electroplating process is similar,

but the lab process still differs from the plant process. Before using the electroplating data models created, it is recommended to validate the model's results with the plant's energy consumption.

It is still a long way for the project to cross the finish line. The presented thesis supports the success of the project in various ways. The modeling part allows the model to generate more accurate results. With more complex control sequences, the model gets closer to the real system and allows a better and more precise energy calculation. The data models for the electroplating process are an alternative for the real process in the plant. They allow the simplification of a complex process without losing accuracy. Since not the process but the process's energy consumption is the project's primary goal, it is a suitable simplification that saves a lot of modeling work to represent the process. The function-based approximation predicts data for the future. Having information for the future also allows calculating future energy consumptions and simulating future events with the DET model, and this is one of the main goals of a DET. All this drives the project towards its goal of creating a Digital Energy Twin.

Bibliography

Aggarwal, Charu C. (2020). *Linear Algebra and Optimization for Machine Learning*. 1st ed. 20. Springer (cit. on p. 18).

Bendel, Oliver (2019). *Industrie 4.0*. URL: https://wirtschaftslexikon.gabler.de/definition/industrie-40-54032/version-368841 (Accessed on 10/22/2020) (cit. on p. 2).

Black, Newton Henry and Harvey Nathaniel Davis (1922). *Practical Physics: Fundamental Principles and Applications to Daily Life*. Macmillan (cit. on pp. 14, 15).

El Zein, Ahmad L and Nour A Chehayeb (2015). "The effect of greenhouse gases on earth's temperature." In: *International Journal of Environmental Monitoring and Analysis* 3 (cit. on p. 1).

ENERTEC Naftz & Partner GmbH & Co KG (2020). *Übersicht Werk Hinterberg* (cit. on p. 27).

Flauger, Jürgen et al. (2020). *Steigender Energiebedarf: Deutschland droht die Ökostrom-Lücke*. URL: https://www.handelsblatt.com/unternehmen/energie/energie-steigender-energiebedarf-deutschland-droht-die-oekostrom-luecke/25385468.html (Accessed on 10/24/2020) (cit. on p. 2).

Fritzson, P and B Thiele (2016). "Introduction to Object-Oriented Modeling, Simulation, Debugging and Dynamic Optimization with Modelica using OpenModelica." In: *Simulation* (cit. on p. 10).

Fritzson, Peter (2011). *Introduction to modeling and simulation of technical and physical systems with Modelica*. John Wiley & Sons (cit. on p. 10).

Gaul, Bernhard (2018). *Österreichs Klimaplan für 2030: Milliardenstrafe aus Brüssel droht*. URL: https://kurier.at/politik/inland/oesterreichs-klimaplan-fuer-2030-milliardenstrafe-aus-bruessel-droht/400346833 (Accessed on 11/02/2020) (cit. on p. 5).

Glaessgen, Edward and David Stargel (2012). "The digital twin paradigm for future NASA and US Air Force vehicles." In: *53rd Structures, Structural Dynamics, and Materials Conference*, p. 1818 (cit. on p. 5).

Grieves, Michael (2002). "Conceptual ideal for PLM." In: *Presentation for the Product Lifecycle Management (PLM) center, University of Michigan* (cit. on p. 5).

Grömer, Michael (2021). "Development, validation and simplification of component models for DigitalEnergyTwin" (cit. on pp. 44–46, 95).

Hasegawa, Tomoko et al. (2018). "Risk of increased food insecurity under stringent global climate change mitigation policy." In: *Nature Climate Change* 8, pp. 699–703 (cit. on p. 1).

International Energy Agency (2019). *Stromerzeugung weltweit nach Energieträger im Jahresvergleich 1998 und 2017 (in Terawattstunden)*. URL: https://de.statista.com/statistik/daten/studie/190298/umfrage/stromerzeugung-weltweit-nach-energietraegern-seit-1998/ (Accessed on 11/26/2020) (cit. on p. 2).

IPCC (Intergov. Panel Clim. Change) (2018). *Global Warming of 1.5° C. An IPCC Special Report on the Impacts of Global Warming of 1.5° C Above Pre-Industrial Levels and Related Global Greenhouse Gas Emission Pathways, in the Context of Strengthening the Global Response to the Threat of Climate Change* (cit. on p. 1).

Jelinek, T. W. (2013). *Praktische Galvanotechnik : ein Lehr- und Handbuch. 96 Tabellen im Text, einem speziellen Tabellen-Anhang und einer Übersicht "Chemikalien für die Galvanotechnik"*. 7., aktual. Leuze Verlag (cit. on pp. 12, 46).

Kanani, Nasser (2009). *Galvanotechnik : Grundlagen, Verfahren und Praxis einer Schlüsseltechnologie*. Carl Hanser Verlag GmbH Co KG (cit. on p. 12).

Kritzinger, Werner et al. (2018). "Digital Twin in manufacturing: A categorical literature review and classification." In: *IFAC-PapersOnLine* 51.11, pp. 1016–1022 (cit. on pp. 6, 7).

Lasi, Heiner et al. (2014). "Industry 4.0." In: *Business & information systems engineering* 6.4, pp. 239–242 (cit. on p. 2).

Li, Lorraine (2019). "Classification and Regression Analysis with Decision Trees." In: *Towards Data Science*. URL: https://towardsdatascience.com/https-medium-com-lorrli-classification-and-regression-analysis-with-decision-trees-c43cdbc58054 (Accessed on 12/30/2020) (cit. on p. 22).

Masson-Delmotte, Valérie et al. (2018). "Global warming of 1.5 C." In: *An IPCC Special Report on the impacts of global warming of 1.5 C* 1, pp. 1–9 (cit. on p. 2).

Modelica Association (2020). *The Modelica Association*. URL: https://www.modelica.org/ (Accessed on 11/19/2020) (cit. on p. 9).

Nocedal, Jorge (2006). *Numerical optimization*. 2. ed. Springer series in operations research and financial engineering (cit. on p. 21).

Owusu, Phebe Asantewaa and Samuel Asumadu-Sarkodie (2016). "A review of renewable energy sources, sustainability issues and climate change mitigation." In: *Cogent Engineering* 3.1 (cit. on p. 1).

Parker, Lindsay and HP OpenView Business Unit (2001). "A fool with a tool is still a fool." In: *HP Open View* (cit. on p. 72).

Patel, Meghna Babubhai, Jagruti N Patel, and Upasana M Bhilota (2020). "Latest Technology and Future Trends." In: *Applications of Artificial Neural Networks for Nonlinear Data*. IGI Global, pp. 270–273 (cit. on p. 18).

Pedregosa, Fabian et al. (2011). "Scikit-learn: Machine learning in Python." In: *The Journal of machine Learning research* 12, pp. 2825–2830 (cit. on p. 20).

Plamann, Wilfried and Detlef Schulz (2016). *Handbuch Elektrotechnik: Grundlagenund Anwendungen für Elektrotechniker*. Springer (cit. on p. 54).

Ramírez, Hermes et al. (2017). "Modelica Language Specification." In: *Data in Brief* 25 (cit. on p. 9).

Rashid, Tariq (2017). *Neuronale Netze selbst programmieren: Ein verständlicher Einstieg mit Python*. O'Reilly (cit. on p. 20).

Reay, Dave et al. (2007). "Climate change 2007: spring-time for sinks." In: *Nature* 446, pp. 727–8 (cit. on pp. 1, 2).

Rinne, Horst and Günter Ickler (1986). *Grundstudium Statistik*. 2. Aufl., Verlag für Wirtschaftsskripten (cit. on p. 52).

Rohith, Gandhi (2018). "Introduction to Machine Learning Algorithms: Linear Regression." In: *Towards Data Science*. URL: https://towardsdatascience.com/introduction-to-machine-learning-algorithms-linear-regression-14c4e325882a (Accessed on 12/28/2020) (cit. on p. 20).

Rojas, Raul (1996). *Theorie der neuronalen Netze: Eine systematische Einführung*. 1. Aufl. Springer (cit. on p. 20).

Rueden, Laura von et al. (2019). "Informed Machine Learning–A Taxonomy and Survey of Integrating Knowledge into Learning Systems." In: *arXiv preprint arXiv:1903.12394* (cit. on p. 70).

Sai Ajay, Muktha (2020). "Introduction to Artificial Neural Networks." In: *Towards Data Science*. URL: https://towardsdatascience.com/introduction-to-artificial-neural-networks-ac338f4154e5 (Accessed on 01/08/2021) (cit. on p. 20).

Tao, Fei et al. (2018). "Digital twin-driven product design, manufacturing and service with big data." In: *The International Journal of Advanced Manufacturing Technology* 94.9, pp. 3563–3576 (cit. on p. 5).

Uhlemann, Thomas H-J, Christian Lehmann, and Rolf Steinhilper (2017). "The digital twin: Realizing the cyber-physical production system for industry 4.0." In: *Procedia Cirp* 61, pp. 335–340 (cit. on p. 3).

Unruh, Jürgen (2016). *Lehrbuch der Galvanotechnik*. Leuze Verlag (cit. on pp. 12, 13, 15, 17, 52).

Virtanen, Pauli et al. (2020). "SciPy 1.0: fundamental algorithms for scientific computing in Python." In: *Nature methods* 17.3, pp. 261–272 (cit. on p. 63).

Watts, C et al. (2016). "A brewing storm: the climate change risks to coffee." In: *A brewing storm: the climate change risks to coffee.* (cit. on p. 1).

Wetter, Michael et al. (2014). "Modelica buildings library." In: *Journal of Building Performance Simulation* 7.4, pp. 253–270 (cit. on p. 9).

WKO Austria (2020). *Bruttoinlandsprodukt (BIP)*. URL: https://www.wko.at/service/zahlen-daten-fakten/BIP.html (Accessed on 10/24/2020) (cit. on p. 2).

Wuebbles, Donald J et al. (2017). *Climate science special report: Fourth national climate assessment (NCA4), Volume I* (cit. on p. 1).

Yiu, Tony (2019a). "Understanding Neural Networks." In: *Towards Data Science*. URL: https://towardsdatascience.com/understanding-neural-networks-19020b758230 (Accessed on 01/08/2021) (cit. on p. 20).

Yiu, Tony (2019b). "Understanding Random Forest." In: *Towards Data Science*. URL: https://towardsdatascience.com/understanding-random-forest-58381e0602d2 (Accessed on 12/30/2020) (cit. on p. 23).

List of Figures

List of Tables

List of Reactions

List of Equations

Appendix

Appendix A.

Overview energy flow

ENERTEC Naftz & Partner GmbH & Co KG created the overview on the next page. It is the basis for the DET model. It shows the structure of the plant and how the energy flows of the machines are connected. The overview has small modifications caused by regulations. The modifications hide the name of the company and the location of the plant. All modifications are marked with three red crosses.

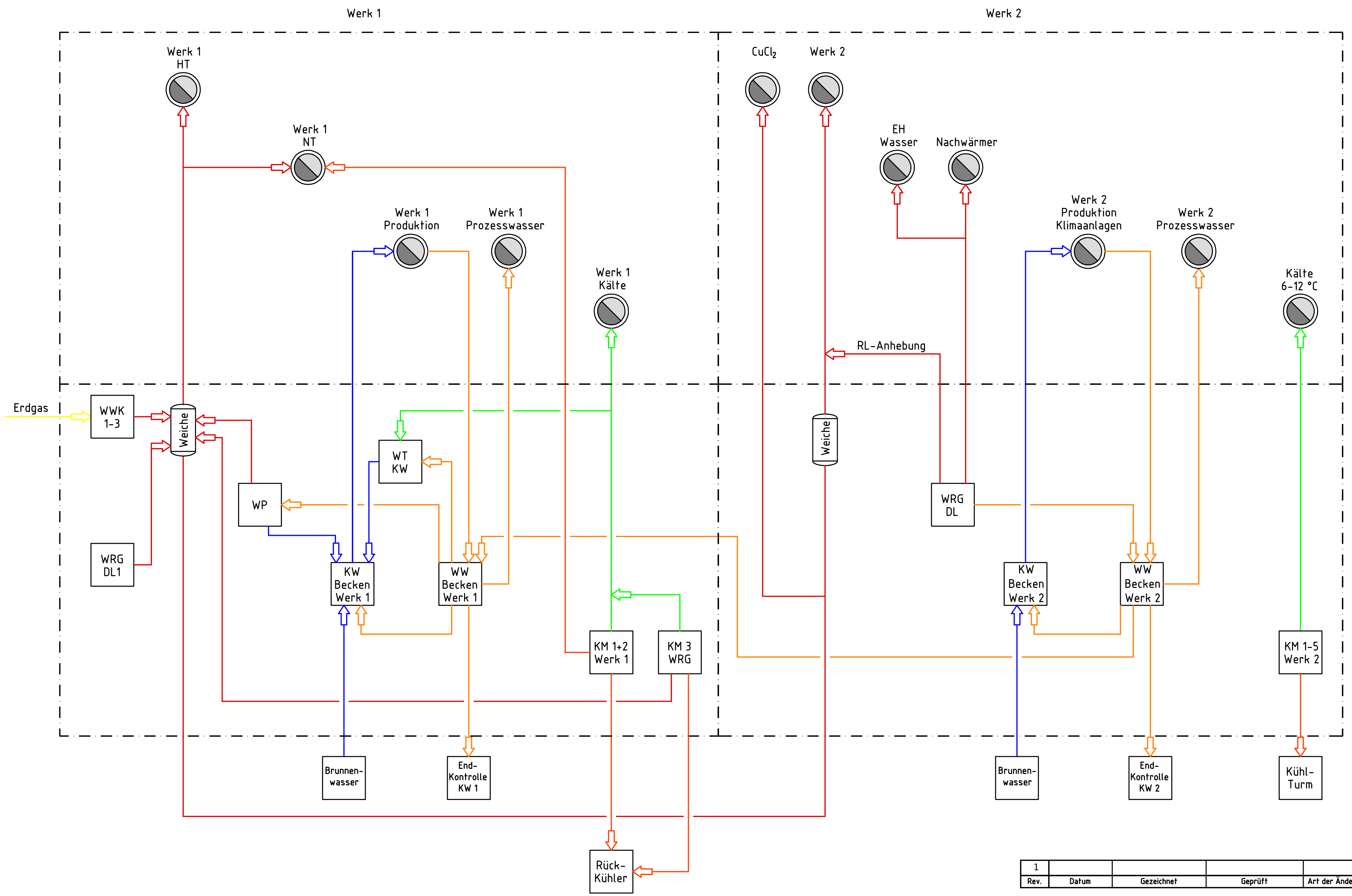

1				
Rev.	Datum	Gezeichnet	Geprüft	Art der Änderung / Revision

ENTWURF

ENERTEC Naftz & Partner GmbH & Co KG
Asperngasse 2-4, 8020 Graz, Austria
Tel.: +43 / 316 / 42 64 35 - 0 Fax: DW - 99
E-mail: office@enertec.at
Web: www.enertec.at

Diese Zeichnung ist unser geistiges Eigentum. Ohne unsere ausdrückliche Genehmigung darf sie weder kopiert noch an Dritte weitergegeben werden. Verstöße werden nach dem Urheberrechtsgesetz geahndet. Alle Angaben sind vom Bauausführenden zu überprüfen. Aussparungen sind vom Ausführenden zu prüfen bzw. anzugeben. Naturmaße nehmen. Der Inhalt dieser Zeichnung gilt als verbindlich, wenn nicht innerhalb von 3 Werktagen dagegen Einspruch erhoben wird.

Auftraggeber: XXX

Planinhalt: Übersicht Werk XXX
Stand Herbst 2020

Gezeichnet	Geprüft	Freigegeben
THPE	SWAN	
Gezeichnet Datum	Geprüft Datum	Freigegeben Datum
28.09.2020		

Projektnummer: EBG9-HTBW.050	Maßstab: o.M.
Zeichn. Nr.: EBG9-SWAN-S001-000	Revision: 0

Plotdatum: 04.11.2020

S:\BA0-BZ9\BG9-HTBW.050\S\EBG9-SWAN-S001-000-(Übersicht Wärmeversorgung XXX).dwg

Appendix B.

Lab values table

The following table holds the values of the lab experiment. The table only shows the cleaned values. For original data, see Appendix C. The data set was created in cooperation with Michael Grömer (Grömer, 2021).

$No.$ = Experiment number
m_{C,t_1} = Mass of the cathode before the experiment
m_{A1,t_1} = Mass of anode 1 before the experiment
m_{A2,t_1} = Mass of anode 2 before the experiment
m_{C,t_2} = Mass of the cathode after the experiment
m_{A1,t_2} = Mass of anode 1 after the experiment
m_{A2,t_2} = Mass of anode 2 after the experiment
d = duration time
U = Voltage
T = Temperature
I = Amperage

No.	m_{C,t_1} [g]	m_{A1,t_1} [g]	m_{A2,t_1} [g]	m_{C,t_2} [g]	m_{A1,t_2} [g]	m_{A2,t_2} [g]	d [min]	U [V]	T [°C]	I [A]
1	17.42	15.70	15.88	17.81	15.50	15.70	30.05	0.700	39.0	0.6480
2	17.80	15.51	15.70	18.71	15.05	15.28	45	1.200	39.0	0.9833
4	18.69	15.04	15.26	19.40	14.74	14.91	50	0.600	60.0	0.6567
5	20.10	14.35	14.54	20.77	14.01	14.21	25	1.500	39.0	1.3253
6	14.73	15.04	15.32	15.30	14.77	15.04	35.5	0.700	25.5	0.8023
7	16.61	15.87	15.67	17.11	15.63	15.40	52	0.600	39.0	0.4850
8	15.15	14.78	15.04	15.53	14.58	14.87	55	0.250	60.2	0.3303
9	20.73	14.01	14.20	21.67	13.54	13.73	68	1.100	22.0	0.6867
10	15.52	14.58	14.85	16.01	14.33	14.62	38	0.600	59.0	0.6187
12	17.30	15.52	15.30	17.72	15.31	15.10	25	1.100	23.5	0.7933
13	17.08	16.65	16.82	17.84	16.23	16.39	22	1.800	39.0	1.7113
14	15.99	14.32	14.61	16.46	14.09	14.38	16.5	1.200	59.0	1.3893
15	18.17	12.74	13.09	18.47	12.60	12.95	25	0.800	21.7	0.5870
16	18.49	14.63	15.49	19.72	14.04	14.82	35	0.300	39.1	1.7187
17	18.46	15.02	16.63	18.94	14.79	16.39	61	0.300	60.2	0.3770
18	18.24	14.38	16.23	18.49	14.24	16.10	65	0.350	24.3	0.1953
19	15.76	14.09	16.40	16.71	13.61	15.88	45	1.100	39.5	1.0467
20	15.80	14.55	14.73	16.14	14.38	14.53	35	0.300	58.3	0.4937
21	17.06	19.03	17.85	18.57	18.20	17.16	75	1.300	25.0	0.9837
22	15.37	18.39	12.94	15.95	18.08	12.67	45	0.600	38.8	0.6470
23	15.61	12.59	14.02	16.16	12.31	13.77	40	0.500	59.7	0.6480
24	15.95	18.07	12.67	16.19	17.96	12.56	24	0.400	39.2	0.4130
25	16.12	14.37	14.53	16.28	14.32	14.48	42	0.100	58.7	0.1493
26	18.49	14.25	16.09	19.50	13.74	15.60	41	1.800	25.1	1.1917

No.	m_{C,t_1} [g]	m_{A1,t_1} [g]	m_{A2,t_1} [g]	m_{C,t_2} [g]	m_{A1,t_2} [g]	m_{A2,t_2} [g]	d [min]	U [V]	T [°C]	I [A]
27	16.17	17.96	12.56	16.64	17.73	12.32	20	1.100	38.5	1.1217
28	16.68	15.53	17.90	17.07	15.37	17.71	36	0.419	59.5	0.4990
29	15.96	17.52	17.43	16.25	17.39	17.28	33	0.318	39.2	0.4150
30	16.95	15.44	16.67	17.08	15.37	16.61	51	0.207	24.1	0.1215
31	16.03	14.93	15.01	16.22	14.83	14.92	39	0.234	59.2	0.2570
32	16.71	13.62	15.89	16.92	13.51	15.79	33	0.368	39.0	0.3030
33	16.24	14.30	14.47	16.38	14.23	14.40	17	0.670	24.8	0.4325
34	16.24	17.38	17.28	17.00	17.02	16.89	41	1.014	39.4	0.8930
35	16.38	14.24	14.40	16.62	14.10	14.27	32	0.582	26.1	0.3763
36	16.60	17.72	16.02	17.19	17.42	15.73	18	2.171	26.4	1.5290
37	16.53	14.96	17.14	17.67	14.35	16.56	40	1.398	28.2	1.3987
38	21.85	16.77	13.44	22.32	16.51	13.27	40	0.352	38.0	0.2853
39	15.92	15.35	17.40	16.35	15.15	17.17	45	0.420	58.4	0.4293
40	18.13	16.19	13.70	18.56	15.95	13.52	45	0.383	44.8	0.4390
41	17.42	14.82	13.51	18.06	14.51	13.18	25	1.411	39.7	1.2420
42	17.94	14.25	14.08	18.34	14.07	13.85	45	0.388	59.0	0.4497
43	17.76	16.54	15.58	18.71	16.07	15.09	35	1.800	28.0	1.3093
44	18.63	17.78	17.15	18.79	17.69	17.08	15	0.445	44.8	0.4767
45	18.17	14.33	15.01	18.44	14.19	14.88	45	0.254	60.3	0.3013
46	17.05	17.25	16.09	17.23	17.16	15.99	50	0.180	45.7	0.1657
47	17.68	14.35	15.71	19.03	13.65	15.06	50	1.026	60.6	1.1573
48	17.41	15.15	12.91	17.72	15.00	12.77	50	0.360	38.2	0.3227
49	16.27	13.74	18.71	18.00	12.94	17.80	80	0.717	44.4	1.3497
50	14.36	15.32	18.19	14.96	15.03	17.89	35	0.833	38.8	0.8153

No.	m_{C,t_1} [g]	m_{A1,t_1} [g]	m_{A2,t_1} [g]	m_{C,t_2} [g]	m_{A1,t_2} [g]	m_{A2,t_2} [g]	d [min]	U [V]	T [°C]	I [A]
51	15.70	13.25	13.84	15.84	13.18	13.75	50	0.213	25.2	0.1577
52	17.12	14.06	17.14	17.26	13.98	17.06	50	0.174	38.7	0.1460
53	16.59	14.51	15.99	16.78	14.40	15.89	50	0.153	48.3	0.1610
54	16.97	13.51	13.18	17.14	13.42	13.09	50	0.154	58.9	0.1867
55	18.05	19.10	19.54	18.50	17.85	19.34	50	0.630	24.9	0.4470
56	19.10	19.83	18.77	19.55	19.60	18.55	50	0.533	37.0	0.4460
57	19.00	18.62	18.72	19.28	18.48	18.59	50	0.380	48.3	0.4507
58	19.11	18.04	16.36	19.58	17.82	16.11	50	0.325	58.1	0.4447
59	19.47	17.68	13.63	20.27	17.32	13.19	50	1.020	26.6	0.7710
60	19.24	12.75	17.06	20.03	12.40	16.65	50	0.835	38.8	0.7543
61	18.59	14.85	14.17	19.35	14.46	13.77	50	0.582	61.1	0.7343
62	19.13	15.04	14.99	19.94	14.62	14.59	50	0.656	49.8	0.7767
63	18.91	17.04	16.10	20.06	16.49	15.49	50	1.322	27.8	1.1007
64	19.75	17.81	13.96	20.85	17.30	13.36	50	1.170	38.4	1.0740
65	20.08	18.54	18.56	21.20	17.95	18.02	50	0.817	60.3	1.0583
66	19.10	17.83	15.87	20.21	17.30	15.26	50	0.839	49.5	1.0523
67	15.81	17.27	16.46	15.91	17.22	16.40	30	0.261	26.4	0.1560
68	18.45	15.23	14.45	18.65	15.13	14.36	30	0.410	38.6	0.3027
69	18.28	13.76	13.33	18.56	13.61	13.19	30	0.464	39.4	0.4540
70	17.56	16.63	17.30	17.93	16.43	17.11	30	0.705	49.2	0.5990
71	18.06	13.18	18.06	18.36	13.03	17.86	30	0.755	26.3	0.5060
72	21.18	17.34	19.67	21.47	17.19	19.52	30	0.667	38.5	0.4923
73	19.57	13.16	14.40	19.87	13.00	14.23	30	0.549	59.4	0.4977
74	20.85	12.37	17.70	21.15	12.20	17.55	30	0.666	49.3	0.4957

No.	m_{C,t_1} [g]	m_{A1,t_1} [g]	m_{A2,t_1} [g]	m_{C,t_2} [g]	m_{A1,t_2} [g]	m_{A2,t_2} [g]	d [min]	U [V]	T [°C]	I [A]
75	18.78	16.39	17.21	19.25	16.15	16.97	30	1.172	25.8	0.7857
76	19.34	13.74	14.57	19.82	13.50	14.32	30	0.913	38.5	0.8010
77	20.01	19.05	18.17	20.50	18.81	17.92	30	0.740	59.4	0.7700
78	19.55	13.40	13.17	20.04	13.14	12.94	30	0.813	49.3	0.7980
79	19.88	19.46	13.58	20.61	19.04	13.26	30	1.494	27.3	1.1893
80	15.91	14.34	15.11	16.63	13.94	14.77	30	1.541	38.6	1.1859
81	21.49	18.14	17.08	22.23	17.81	16.69	30	1.065	58.5	1.1913
82	21.15	17.62	18.66	21.86	17.25	18.30	30	0.118	33.4	1.1155
83	18.41	21.56	13.04	19.36	21.10	12.54	30	1.259	49.2	1.0410
84	20.04	19.51	17.86	20.96	19.04	17.41	30	1.934	29.6	1.4883
85	18.53	17.18	17.55	19.47	16.73	17.05	30	1.637	38.8	1.4977
86	17.12	12.20	13.00	18.02	11.73	12.51	30	1.457	58.5	1.4833
87	16.17	14.59	14.65	16.23	14.56	14.61	30	0.174	28.9	0.1057
88	16.75	15.38	14.20	16.81	15.35	14.16	30	0.148	38.3	0.1083
89	18.50	14.17	14.23	18.56	14.14	14.19	30	0.125	59.5	0.1243
90	17.71	16.40	13.08	17.78	16.37	13.05	30	0.131	48.9	0.1087
91	18.37	19.02	13.90	18.48	18.95	13.84	30	0.365	23.7	0.2010
92	17.22	13.03	16.35	17.35	12.97	16.29	30	0.291	38.6	0.2100
93	15.86	18.28	14.73	15.99	18.20	14.66	30	0.240	59.7	0.2063
94	17.27	13.24	17.24	17.38	13.18	17.18	29.5	0.236	50.0	0.2043
95	17.77	17.91	16.71	18.20	17.68	16.48	30	1.048	24.2	0.7013
96	20.04	16.94	17.80	20.46	16.73	17.58	30	0.833	38.5	0.6973
97	18.56	17.03	16.66	18.98	16.83	16.42	30	0.710	59.4	0.7000
98	20.49	17.40	21.08	20.91	17.16	20.86	30	0.742	49.4	0.7047

No.	m_{C,t_1} [g]	m_{A1,t_1} [g]	m_{A2,t_1} [g]	m_{C,t_2} [g]	m_{A1,t_2} [g]	m_{A2,t_2} [g]	d [min]	U [V]	T [°C]	I [A]
99	16.81	18.96	14.66	17.14	18.80	14.50	20	1.165	25.7	0.8190
100	21.85	13.13	12.52	22.17	12.97	12.35	20	0.877	38.5	0.7910
101	20.94	18.20	17.18	21.25	18.04	17.00	20	0.713	58.2	0.7917
102	16.23	12.93	13.84	16.56	12.76	13.67	20	0.822	50.1	0.8160
103	15.98	12.97	12.50	16.14	12.88	12.42	20	0.632	25.6	0.2947
104	17.34	14.55	14.61	17.51	14.47	14.52	20	0.493	37.4	0.3987
105	18.48	14.11	15.33	18.65	14.03	15.25	20	0.360	59.5	0.4063
106	17.38	14.16	14.18	17.55	14.07	14.09	20	0.434	50.0	0.4040
107	16.57	16.72	18.01	16.77	16.61	17.90	40	0.436	25.7	0.2537
108	22.17	17.14	16.45	22.37	17.05	16.34	40	0.342	37.8	0.2517
109	21.25	14.47	16.81	21.44	14.35	16.71	40	0.235	59.6	0.2547
110	17.13	16.38	12.93	17.33	16.29	12.84	40	0.282	49.9	0.2510
111	16.61	16.27	11.69	17.12	16.03	11.46	45	0.903	23.4	0.5507
112	19.26	17.66	17.55	19.76	17.43	17.30	45	0.651	38.0	0.5473
113	19.82	20.84	15.23	20.33	20.57	14.99	45	0.477	59.6	0.5500
114	19.45	16.97	18.97	19.98	16.71	18.71	45	0.597	49.9	0.5543
115	16.66	17.03	14.33	16.94	16.88	14.20	15	1.437	23.8	0.9830
116	16.66	16.08	14.50	16.96	15.93	14.35	16	0.897	38.0	0.9725
117	16.96	18.77	17.89	17.25	18.60	17.75	14.5	1.103	60.4	0.9915
118	17.05	18.55	12.82	17.36	18.38	12.67	15	0.940	47.8	0.9955
119	21.45	14.01	12.40	21.86	13.81	12.18	60	0.555	24.6	0.3520
120	22.37	12.35	13.17	22.78	12.14	12.94	59	0.472	39.1	0.3493
121	16.77	14.08	12.72	17.17	13.88	12.51	58	0.337	59.1	0.3473
122	17.33	14.45	12.86	17.74	14.25	12.65	57	0.379	49.2	0.3533

No.	m_{C,t_1} [g]	m_{A1,t_1} [g]	m_{A2,t_1} [g]	m_{C,t_2} [g]	m_{A1,t_2} [g]	m_{A2,t_2} [g]	d [min]	U [V]	T [°C]	I [A]
123	21.86	20.12	17.36	22.14	19.98	17.24	25	0.818	24.7	0.5557
124	22.78	17.81	19.80	23.05	17.65	19.69	25	0.635	37.8	0.5497
125	17.16	18.41	17.72	17.44	18.26	17.57	25	0.477	58.5	0.5510
126	17.73	16.89	19.57	18.01	16.74	19.42	25	0.573	49.5	0.5557
127	16.79	14.06	13.64	16.87	14.01	13.59	21	0.289	37.7	0.2063
128	16.97	15.45	17.01	17.06	15.41	16.96	22	0.355	25.7	0.2040
129	16.77	21.71	17.29	16.84	21.66	17.25	18.5	0.187	64.9	0.2060
130	15.83	17.05	17.41	15.94	16.98	17.36	24.5	0.250	49.2	0.2063
131	19.74	14.97	12.64	20.35	14.67	12.33	25.5	1.524	26.5	1.1530
132	17.11	14.23	12.66	17.70	13.94	12.35	26	1.375	38.5	1.1390
133	16.94	18.69	18.58	17.54	18.36	18.29	25.5	0.987	58.0	1.1563
134	16.94	16.70	18.37	17.54	16.42	18.02	25	1.165	48.6	1.1520
135	17.05	18.27	12.33	17.45	18.06	12.16	70	0.375	26.5	0.2433
136	16.83	13.92	14.65	17.23	13.72	14.46	70	0.368	34.7	0.2470
137	16.87	16.92	18.35	17.28	16.70	18.14	70	0.260	53.6	0.2553
138	15.90	18.01	19.68	16.34	17.77	19.49	70	0.294	44.0	0.3307
139	17.24	12.32	16.86	17.82	12.02	16.58	20	1.872	27.7	1.4290
140	17.53	17.24	16.73	18.19	16.90	16.41	20	1.844	34.4	1.5800
141	17.53	17.34	17.57	18.32	16.97	17.14	20	1.264	54.4	1.7603
142	17.43	19.97	21.63	18.03	19.61	21.35	20	1.315	44.6	1.3694
143	18.77	15.39	17.63	19.59	14.99	17.22	60	0.904	27.5	0.6843
144	20.33	17.22	19.39	21.16	16.80	18.97	60	0.890	34.0	0.6897
145	17.34	13.58	18.63	18.20	13.16	18.17	60	0.595	55.2	0.6957
146	18.01	14.00	16.94	18.86	13.61	16.49	60	0.655	45.1	0.6923

No.	m_{C,t_1} [g]	m_{A1,t_1} [g]	m_{A2,t_1} [g]	m_{C,t_2} [g]	m_{A1,t_2} [g]	m_{A2,t_2} [g]	d [min]	U [V]	T [°C]	I [A]
147	18.62	16.40	19.42	18.82	16.30	19.33	90	0.204	25.0	0.1053
148	15.34	16.79	18.97	15.53	16.69	18.88	90	0.169	24.1	0.1040
150	22.97	13.16	21.62	23.15	13.06	21.51	90	0.154	46.0	0.1043
151	17.22	13.71	12.01	17.58	13.52	11.84	15	1.560	27.2	1.1950
152	17.44	16.67	19.48	17.80	16.50	19.29	15	1.548	31.9	1.1817
153	17.27	16.40	16.57	17.64	16.22	16.37	15	0.953	55.5	1.1867
154	16.33	17.75	18.13	16.69	17.55	17.95	15	1.073	46.2	1.1827
155	18.80	12.92	13.43	19.92	12.36	12.87	80	0.951	27.2	0.6950
156	23.15	14.24	15.90	24.25	13.62	15.41	80	0.801	34.0	0.6880
157	17.80	12.17	13.78	18.94	11.55	13.26	80	0.601	54.7	0.6897
158	18.19	12.12	20.51	19.34	11.48	19.99	80	0.595	43.2	0.6977
159	18.17	14.45	21.34	18.66	14.18	21.09	15	1.965	27.7	1.5860
160	15.52	19.59	12.15	16.00	19.34	11.90	15	1.737	35.2	1.5687
161	17.70	16.87	17.12	18.21	16.58	16.88	15	1.216	54.8	1.5870
162	19.94	18.04	16.94	20.43	17.78	16.68	15	1.317	44.6	1.5870
163	19.74	11.81	16.48	19.95	11.72	16.38	10	1.200	27.3	0.9835
164	17.09	19.32	17.92	17.28	19.22	17.80	10	1.240	34.3	0.9875
165	18.30	17.52	20.34	18.51	17.41	20.24	10	0.820	54.8	0.9855
166	17.13	17.56	17.91	17.34	17.45	17.81	10	0.900	45.1	0.9920
167	19.59	14.15	13.05	21.18	13.42	12.17	80	1.300	27.1	0.9880
168	17.88	14.32	11.42	19.45	13.53	10.64	80	1.100	33.1	0.9823
169	17.65	15.99	21.50	19.32	15.18	20.56	80	0.791	54.7	0.9900
170	18.84	13.85	12.47	20.48	13.03	11.64	80	0.867	43.2	0.9927
171	21.56	16.21	13.48	21.84	16.07	13.34	70	0.320	26.8	0.2020

No.	m_{C,t_1} [g]	m_{A1,t_1} [g]	m_{A2,t_1} [g]	m_{C,t_2} [g]	m_{A1,t_2} [g]	m_{A2,t_2} [g]	d [min]	U [V]	T [°C]	I [A]
172	24.24	16.68	13.51	25.28	16.19	12.97	70	0.828	33.9	0.7273
173	15.98	12.80	12.35	16.25	12.70	12.21	70	0.195	55.0	0.2037
174	18.92	13.61	15.39	19.20	13.46	15.25	70	0.232	44.2	0.2043
175	25.26	15.24	13.33	26.33	14.69	12.81	65	1.090	25.8	0.8140
176	16.25	16.18	12.21	17.42	15.60	11.60	65	0.890	34.6	0.8693
177	19.20	12.69	13.44	20.37	12.13	12.82	65	0.628	53.4	0.8450
178	21.84	12.95	16.06	22.93	12.47	15.44	65	0.771	44.6	0.8230
179	17.80	16.36	13.25	18.27	16.11	13.02	45	0.750	27.0	0.5260
180	19.84	11.55	16.86	20.30	11.30	16.63	45	0.622	34.0	0.5193
181	16.70	19.31	19.97	17.18	19.07	19.70	45	0.396	55.3	0.5157
182	18.50	18.87	11.46	18.99	18.62	11.20	45	0.560	43.7	0.5310
183	17.59	18.24	14.17	18.91	17.54	13.52	45	2.013	28.6	1.4600
184	19.42	19.82	17.83	20.67	19.24	17.09	45	1.421	34.5	1.3730
185	19.93	16.29	11.90	21.26	15.67	11.20	45	1.051	54.9	1.5065
186	17.28	16.26	18.86	18.65	15.63	18.11	45	1.260	44.5	1.3460
187	19.75	11.58	12.11	20.14	11.42	11.89	10	1.590	30.5	1.2690
188	17.34	15.43	12.46	17.72	15.24	12.25	10	1.581	34.8	1.2775
189	17.42	16.67	12.79	17.82	14.47	12.59	10	0.960	55.0	1.2625
190	22.93	12.80	15.59	23.33	12.61	15.39	10	1.080	42.5	1.2630
191	18.98	11.18	12.59	19.35	11.01	12.40	85	0.380	25.9	0.2257
192	20.13	19.68	11.19	20.49	19.49	11.01	84	0.356	33.2	0.2513
193	17.73	14.45	12.58	18.10	14.26	12.40	83	0.200	54.4	0.2237
194	17.17	12.24	15.23	17.54	12.06	15.03	82	0.244	44.8	0.2283
195	19.25	15.17	11.71	19.89	14.83	11.41	55	0.840	27.9	0.5775

No.	m_{C,t_1} [g]	m_{A1,t_1} [g]	m_{A2,t_1} [g]	m_{C,t_2} [g]	m_{A1,t_2} [g]	m_{A2,t_2} [g]	d [min]	U [V]	T [°C]	I [A]
196	19.78	18.07	17.43	20.42	17.75	17.09	55	0.694	34.0	0.5615
197	17.65	20.63	15.38	18.31	20.28	15.05	55	0.464	55.0	0.5695
198	19.75	10.62	15.61	20.41	10.28	15.30	55	0.537	44.5	0.5805
199	21.14	11.28	13.39	21.58	11.11	13.16	15	1.780	28.9	1.4375
200	16.29	12.17	20.27	16.71	11.99	19.95	15	1.657	24.8	1.3765
201	18.41	11.62	13.51	18.84	11.43	13.28	15	1.105	54.9	1.3825
202	17.39	13.01	17.79	17.86	12.76	17.57	15	1.200	43.9	1.4170

Table B.1.: Documented lab values

The following table holds the calculated values for each experiment based on the original values from Table B.1.

$No.$	=	Experiment number
$\vec{j}$	=	Current density
A	=	Platting area
Δm_C	=	Cathode mass difference before and after the experiment
Δm_{A1}	=	Anode 1 mass difference before and after the experiment
Δm_{A2}	=	Anode 2 mass difference before and after the experiment
t_e	=	expected layer thickness
t_r	=	real layer thickness
Δt	=	Deviation of expected to real layer thickness
P	=	Electric power
W	=	Electric potential energy

No.	$\vec{j}$ [A cm^{-2}]	A [cm^2]	Δm_C [g]	Δm_{A1} [g]	Δm_{A2} [g]	t_e [µm]	t_r [µm]	Δt [%]	P [W]	W [W h]
1	2.012	32.20	0.39	-0.20	-0.18	12.9844	13.5176	4.1065	0.4536	0.2272
2	3.054	32.20	0.91	-0.46	-0.42	29.5064	31.5411	6.8958	1.1800	0.8850
4	2.549	25.76	0.71	-0.30	-0.35	27.3671	30.7613	12.4025	0.3940	0.3283
5	4.116	32.20	0.67	-0.34	-0.33	22.0937	23.2226	5.1096	1.9880	0.8283
6	2.492	32.20	0.57	-0.27	-0.28	18.9927	19.7565	4.0218	0.5616	0.3323
7	1.883	25.76	0.50	-0.24	-0.27	21.0213	21.6629	3.0522	0.2910	0.2522
8	1.026	32.20	0.38	-0.20	-0.17	12.1149	13.1710	8.7179	0.0826	0.0757
9	2.133	32.20	0.94	-0.47	-0.47	31.1357	32.5810	4.6419	0.7553	0.8560
10	1.921	32.20	0.49	-0.25	-0.23	15.6763	16.9837	8.3399	0.3712	0.2351

No.	$\vec{j}$ [A cm^{-2}]	A [cm^2]	Δm_C [g]	Δm_{A1} [g]	Δm_{A2} [g]	t_e [µm]	t_r [µm]	Δt [%]	P [W]	W [W h]
12	3.080	25.76	0.42	-0.21	-0.20	16.5314	18.1968	10.0744	0.8727	0.3636
13	5.315	32.20	0.76	-0.42	-0.43	25.1050	26.3421	4.9274	3.0804	1.1295
14	4.315	32.20	0.47	-0.23	-0.23	15.2860	16.2905	6.5712	1.6672	0.4585
15	1.877	31.28	0.30	-0.14	-0.14	10.0733	10.7040	6.2614	0.4696	0.1957
16	5.189	33.12	1.23	-0.59	-0.67	38.9968	41.4483	6.2865	0.5156	0.3008
17	1.301	28.98	0.48	-0.23	-0.24	17.0385	18.4857	8.4932	0.1131	0.1150
18	0.700	27.90	0.25	-0.14	-0.13	9.7711	10.0006	2.3488	0.0684	0.0741
19	3.291	31.81	0.95	-0.48	-0.52	31.7959	33.3355	4.8420	1.1513	0.8635
20	1.477	33.43	0.34	-0.17	-0.20	11.0962	11.3497	2.2845	0.1481	0.0864
21	3.308	29.73	1.51	-0.83	-0.69	53.2731	56.6772	6.3899	1.2788	1.5985
22	2.099	30.82	0.58	-0.31	-0.27	20.2835	21.0033	3.5485	0.3882	0.2912
23	2.058	31.48	0.55	-0.28	-0.25	17.6768	19.4969	10.2961	0.3240	0.2160
24	1.317	31.35	0.24	-0.11	-0.11	6.7891	8.5446	25.8585	0.1652	0.0661
25	0.452	33.05	0.16	-0.05	-0.05	4.0745	5.4029	32.6009	0.0149	0.0105
26	4.201	28.37	1.01	-0.51	-0.49	36.9841	39.7402	7.4522	2.1450	1.4658
27	3.578	31.35	0.47	-0.23	-0.24	15.3654	16.7332	8.9022	1.2338	0.4113
28	1.736	28.74	0.39	-0.16	-0.19	13.4193	15.1434	12.8481	0.2091	0.1254
29	1.382	30.03	0.29	-0.13	-0.15	9.7919	10.7779	10.0699	0.0000	0.0000
30	0.389	31.25	0.13	-0.07	-0.06	4.2578	4.6432	9.0509	0.0252	0.0214
31	0.791	32.48	0.19	-0.10	-0.09	6.6258	6.5287	1.4655	0.0601	0.0391
32	0.938	32.31	0.21	-0.11	-0.10	6.6458	7.2551	9.1680	0.1115	0.0613
33	1.469	29.44	0.14	-0.07	-0.07	5.3631	5.3081	1.0250	0.2898	0.0821
34	2.974	30.03	0.76	-0.36	-0.39	26.1782	28.2456	7.8974	0.9055	0.6188
35	1.278	29.44	0.24	-0.14	-0.13	8.7842	9.0996	3.5908	0.2190	0.1168

No.	$\vec{j}$ [A cm^{-2}]	A [cm^2]	Δm_C [g]	Δm_{A1} [g]	Δm_{A2} [g]	t_e [µm]	t_r [µm]	Δt [%]	P [W]	W [W h]
36	4.622	33.08	0.59	-0.30	-0.29	17.8650	19.9071	11.4306	3.3195	0.9958
37	4.319	32.38	1.14	-0.61	-0.58	37.0940	39.2886	5.9164	1.9553	1.3036
38	0.866	32.96	0.47	-0.26	-0.17	7.4353	15.9155	114.0513	0.1004	0.0670
39	1.419	30.26	0.43	-0.20	-0.23	13.7105	15.8616	15.6895	0.1803	0.1352
40	1.313	33.44	0.43	-0.24	-0.18	12.6855	14.3526	13.1420	0.1681	0.1261
41	4.072	30.50	0.64	-0.31	-0.33	21.8572	23.4177	7.1398	1.7525	0.7302
42	1.515	29.68	0.40	-0.18	-0.23	14.6403	15.0432	2.7518	0.1745	0.1309
43	4.350	30.10	0.95	-0.47	-0.49	32.6897	35.2248	7.7551	2.3568	1.3748
44	1.494	31.90	0.16	-0.09	-0.07	4.8124	5.5976	16.3179	0.2121	0.0530
45	0.901	33.43	0.27	-0.14	-0.13	8.7097	9.0144	3.4991	0.0765	0.0574
46	0.547	30.28	0.18	-0.09	-0.10	5.8730	6.6338	12.9536	0.0298	0.0249
47	3.562	32.49	1.35	-0.70	-0.65	38.2457	46.3789	21.2657	1.1874	0.9895
48	1.040	31.03	0.31	-0.15	-0.14	11.1628	11.1492	0.1219	0.1162	0.0968
49	4.249	31.76	1.73	-0.80	-0.91	72.9890	60.7882	16.7159	0.9677	1.2903
50	2.642	30.87	0.60	-0.29	-0.30	19.8510	21.6952	9.2900	0.6792	0.3962
51	0.522	30.22	0.14	-0.07	-0.09	5.6017	5.1710	7.6896	0.0336	0.0280
52	0.496	29.43	0.14	-0.08	-0.08	5.3260	5.3093	0.3132	0.0254	0.0212
53	0.505	31.91	0.19	-0.11	-0.10	5.4173	6.6462	22.6847	0.0246	0.0205
54	0.565	33.06	0.17	-0.09	-0.09	6.0617	5.7390	5.3230	0.0287	0.0240
55	1.465	30.50	0.45	-1.25	-0.20	15.7329	16.4656	4.6568	0.2816	0.2347
56	1.472	30.31	0.45	-0.23	-0.22	15.7986	16.5714	4.8915	0.2377	0.1981
57	1.461	30.84	0.28	-0.14	-0.13	15.6891	10.1336	35.4100	0.1713	0.1427
58	1.462	30.42	0.47	-0.22	-0.25	15.6950	17.2459	9.8818	0.1445	0.1204
59	2.473	31.18	0.80	-0.36	-0.44	26.5508	28.6402	7.8694	0.7864	0.6554

No.	$\vec{j}$ [$A\,cm^{-2}$]	A [cm^2]	Δm_C [g]	Δm_{A1} [g]	Δm_{A2} [g]	t_e [µm]	t_r [µm]	Δt [%]	P [W]	W [W h]
60	2.439	30.93	0.79	-0.35	-0.41	26.1818	28.5054	8.8745	0.6299	0.5249
61	2.428	30.25	0.76	-0.39	-0.40	26.0648	28.0438	7.5927	0.4274	0.3562
62	2.476	31.36	0.81	-0.42	-0.40	26.5849	28.8236	8.4209	0.5095	0.4246
63	3.493	31.51	1.15	-0.55	-0.61	37.4974	40.7292	8.6187	1.4551	1.2126
64	3.358	31.98	1.10	-0.51	-0.60	36.0530	38.3878	6.4758	1.2566	1.0472
65	3.472	30.48	1.12	-0.59	-0.54	37.2757	41.0095	10.0166	0.8647	0.7205
66	3.499	30.07	1.11	-0.53	-0.61	37.5671	41.1945	9.6560	0.8829	0.7358
67	0.531	29.39	0.10	-0.05	-0.06	3.4195	3.7980	11.0674	0.0407	0.0204
68	1.032	29.33	0.20	-0.10	-0.09	6.6482	7.6117	14.4924	0.1241	0.0620
69	1.571	28.90	0.28	-0.15	-0.14	10.1190	10.8131	6.8596	0.2107	0.1053
70	2.057	29.12	0.37	-0.20	-0.19	13.2509	14.1818	7.0252	0.4223	0.2111
71	1.616	31.30	0.30	-0.15	-0.20	10.4119	10.6958	2.7264	0.3820	0.1910
72	1.572	31.33	0.29	-0.15	-0.15	10.1233	10.3317	2.0587	0.3284	0.1642
73	1.633	30.47	0.30	-0.16	-0.17	10.5202	10.9879	4.4465	0.2732	0.1366
74	1.594	31.09	0.30	-0.17	-0.15	10.2697	10.7696	4.8680	0.3301	0.1651
75	2.392	32.84	0.47	-0.24	-0.24	15.4111	15.9736	3.6504	0.9208	0.4604
76	2.623	30.53	0.48	-0.24	-0.25	16.8986	17.7285	4.9109	0.7313	0.3657
77	2.562	30.06	0.49	-0.24	-0.25	16.5016	18.1946	10.2597	0.5698	0.2849
78	2.673	29.86	0.49	-0.26	-0.23	17.2154	18.3156	6.3909	0.6488	0.3244
79	3.889	30.59	0.73	-0.42	-0.32	25.0477	26.6378	6.3483	1.7769	0.8884
80	4.007	29.60	0.72	-0.40	-0.34	25.8078	27.1485	5.1952	1.8275	0.9137
81	3.813	31.25	0.74	-0.33	-0.39	24.5579	26.4303	7.6241	1.2688	0.6344
82	3.544	31.47	0.71	-0.37	-0.36	22.8310	25.1782	10.2808	0.1316	0.0658
83	3.093	33.66	0.95	-0.46	-0.50	19.9204	31.4979	58.1185	1.3106	0.6553

No.	$\vec{j}$ [A cm^{-2}]	A [cm^2]	Δm_C [g]	Δm_{A1} [g]	Δm_{A2} [g]	t_e [µm]	t_r [µm]	Δt [%]	P [W]	W [W h]
84	4.703	31.65	0.92	-0.47	-0.45	30.2949	32.4465	7.1023	2.8784	1.4392
85	4.523	33.12	0.94	-0.45	-0.50	29.1321	31.6807	8.7487	2.4517	1.2258
86	4.459	33.26	0.90	-0.47	-0.49	28.7240	30.1967	5.1272	2.1612	1.0806
87	0.327	32.29	0.06	-0.03	-0.04	2.1076	2.0736	1.6160	0.0184	0.0092
88	0.334	32.41	0.06	-0.03	-0.04	2.1530	2.0661	4.0377	0.0160	0.0080
89	0.398	31.26	0.06	-0.03	-0.04	2.5618	2.1420	16.3868	0.0155	0.0078
90	0.346	31.39	0.07	-0.03	-0.03	2.2297	2.4887	11.6125	0.0142	0.0071
91	0.630	31.89	0.11	-0.07	-0.06	4.0595	3.8492	5.1783	0.0734	0.0367
92	0.690	30.44	0.13	-0.06	-0.06	4.4432	4.7658	7.2594	0.0611	0.0306
93	0.667	30.93	0.13	-0.08	-0.07	4.2974	4.6913	9.1655	0.0495	0.0248
94	0.676	30.22	0.11	-0.06	-0.06	4.2832	4.0629	5.1442	0.0482	0.0237
95	2.285	30.69	0.43	-0.23	-0.23	14.7214	15.6388	6.2320	0.7350	0.3675
96	2.321	30.05	0.42	-0.21	-0.22	14.9500	15.6013	4.3567	0.5809	0.2904
97	2.304	30.39	0.42	-0.20	-0.24	14.8380	15.4255	3.9591	0.4970	0.2485
98	2.303	30.60	0.42	-0.24	-0.22	14.8330	15.3181	3.2706	0.5229	0.2614
99	2.647	30.94	0.33	-0.16	-0.16	11.3672	11.9038	4.7207	0.9541	0.3180
100	2.549	31.03	0.32	-0.16	-0.17	10.9460	11.5089	5.1420	0.6937	0.2312
101	2.552	31.02	0.31	-0.16	-0.18	10.9603	11.1544	1.7705	0.5645	0.1882
102	2.552	31.97	0.33	-0.17	-0.17	10.9605	11.5201	5.1057	0.6708	0.2236
103	0.963	30.59	0.16	-0.09	-0.08	4.1370	5.8382	41.1210	0.1862	0.0621
104	1.306	30.51	0.17	-0.08	-0.09	5.6103	6.2177	10.8260	0.1965	0.0655
105	1.309	31.03	0.17	-0.08	-0.08	5.6229	6.1141	8.7349	0.1463	0.0488
106	1.368	29.53	0.17	-0.09	-0.09	5.8746	6.4246	9.3629	0.1753	0.0584
107	0.789	32.16	0.20	-0.11	-0.11	6.7753	6.9418	2.4564	0.1106	0.0737

No.	$\vec{j}$ [A cm^{-2}]	A [cm^2]	Δm_C [g]	Δm_{A1} [g]	Δm_{A2} [g]	t_e [µm]	t_r [µm]	Δt [%]	P [W]	W [W h]
108	0.804	31.32	0.20	-0.09	-0.11	6.9012	7.1269	3.2706	0.0861	0.0574
109	0.815	31.25	0.19	-0.12	-0.10	6.9995	6.7861	3.0486	0.0598	0.0399
110	0.802	31.28	0.20	-0.09	-0.09	6.8917	7.1360	3.5449	0.0708	0.0472
111	1.833	30.05	0.51	-0.24	-0.23	17.7084	18.9444	6.9797	0.4973	0.3729
112	1.694	32.31	0.50	-0.23	-0.25	16.3702	17.2740	5.5208	0.3563	0.2672
113	1.810	30.39	0.51	-0.27	-0.24	17.4877	18.7310	7.1094	0.2624	0.1968
114	1.704	32.52	0.53	-0.26	-0.26	16.4675	18.1867	10.4396	0.3309	0.2482
115	3.323	29.58	0.28	-0.15	-0.13	10.7030	10.5646	1.2935	1.4126	0.3531
116	2.978	32.66	0.30	-0.15	-0.15	10.2295	10.2517	0.2177	0.8723	0.2326
117	3.372	29.40	0.29	-0.17	-0.14	10.4996	11.0089	4.8503	1.0936	0.2643
118	3.355	29.67	0.31	-0.17	-0.15	10.8062	11.6610	7.9100	0.9358	0.2339
119	1.045	33.67	0.41	-0.20	-0.22	13.4682	13.5904	0.9073	0.1954	0.1954
120	1.113	31.39	0.41	-0.21	-0.23	14.0981	14.5775	3.4009	0.1649	0.1621
121	1.083	32.09	0.40	-0.20	-0.21	13.4813	13.9139	3.2091	0.1171	0.1131
122	1.125	31.40	0.41	-0.20	-0.21	13.7739	14.5752	5.8174	0.1339	0.1272
123	1.607	34.58	0.28	-0.14	-0.12	8.6256	9.0370	4.7698	0.4545	0.1894
124	1.775	30.96	0.27	-0.16	-0.11	9.5301	9.7332	2.1308	0.3490	0.1454
125	1.699	32.43	0.28	-0.15	-0.15	9.1202	9.6361	5.6572	0.2628	0.1095
126	1.628	34.13	0.28	-0.15	-0.15	8.7406	9.1575	4.7698	0.3184	0.1327
127	0.694	29.75	0.08	-0.05	-0.05	3.1272	3.0012	4.0304	0.0596	0.0209
128	0.668	30.53	0.09	-0.04	-0.05	3.1564	3.2901	4.2371	0.0724	0.0266
129	0.684	30.10	0.07	-0.05	-0.04	2.7185	2.5955	4.5246	0.0385	0.0119
130	0.695	29.67	0.11	-0.07	-0.05	3.6583	4.1378	13.1071	0.0516	0.0211
131	3.492	33.02	0.61	-0.30	-0.31	19.1213	20.6210	7.8432	1.7572	0.7468

No.	$\vec{j}$ [A cm^{-2}]	A [cm^2]	Δm_C [g]	Δm_{A1} [g]	Δm_{A2} [g]	t_e [µm]	t_r [µm]	Δt [%]	P [W]	W [W h]
132	3.679	30.96	0.59	-0.29	-0.31	20.5379	21.2688	3.5589	1.5661	0.6787
133	3.788	30.53	0.60	-0.33	-0.29	20.7375	21.9339	5.7695	1.1413	0.4851
134	3.527	32.66	0.60	-0.28	-0.35	18.9337	20.5035	8.2907	1.3421	0.5592
135	0.795	30.61	0.40	-0.21	-0.17	11.9486	14.5851	22.0655	0.0913	0.1065
136	0.821	30.08	0.40	-0.20	-0.19	12.3402	14.8395	20.2535	0.0909	0.1060
137	0.930	27.44	0.41	-0.22	-0.21	13.9853	16.6757	19.2369	0.0664	0.0775
138	1.118	29.57	0.44	-0.24	-0.19	16.8092	16.6090	1.1909	0.0972	0.1134
139	4.816	29.67	0.58	-0.30	-0.28	20.6808	21.8155	5.4869	2.6751	0.8917
140	4.830	32.71	0.66	-0.34	-0.32	20.7430	22.5196	8.5649	2.9135	0.9712
141	5.799	30.36	0.79	-0.37	-0.43	24.9023	29.0452	16.6366	2.2251	0.7417
142	4.180	32.76	0.60	-0.36	-0.28	17.9500	20.4409	13.8765	1.8007	0.6002
143	2.250	30.41	0.82	-0.40	-0.41	28.9914	30.0952	3.8072	0.6186	0.6186
144	2.128	32.41	0.83	-0.42	-0.42	27.4135	28.5815	4.2606	0.6138	0.6138
145	2.311	30.10	0.86	-0.42	-0.46	29.7726	31.8856	7.0973	0.4139	0.4139
146	2.170	31.90	0.85	-0.39	-0.45	27.9594	29.7381	6.3616	0.4535	0.4535
147	0.348	30.31	0.20	-0.10	-0.09	6.7157	7.3645	9.6615	0.0215	0.0322
148	0.344	30.20	0.19	-0.10	-0.09	6.6555	7.0225	5.5141	0.0176	0.0264
150	0.347	30.10	0.18	-0.10	-0.11	6.6974	6.6734	0.3587	0.0161	0.0241
151	3.934	30.38	0.36	-0.19	-0.17	12.6687	13.2253	4.3941	1.8642	0.4661
152	3.817	30.96	0.36	-0.17	-0.19	12.2918	12.9767	5.5720	1.8292	0.4573
153	4.311	27.52	0.37	-0.18	-0.20	13.8859	15.0034	8.0474	1.1309	0.2827
154	3.944	29.99	0.36	-0.20	-0.18	12.7012	13.3976	5.4827	1.2690	0.3173
155	2.282	30.46	1.12	-0.56	-0.56	39.1939	41.0388	4.7070	0.6609	0.8813
156	2.293	30.01	1.10	-0.62	-0.49	39.3790	40.9083	3.8836	0.5511	0.7348

No.	$\vec{j}$ [A cm^{-2}]	A [cm^2]	Δm_C [g]	Δm_{A1} [g]	Δm_{A2} [g]	t_e [µm]	t_r [µm]	Δt [%]	P [W]	W [W h]
157	2.315	29.79	1.14	-0.62	-0.52	39.7632	42.7061	7.4010	0.4145	0.5527
158	2.111	33.05	1.15	-0.64	-0.52	36.2593	38.8340	7.1007	0.4151	0.5535
159	5.209	30.45	0.49	-0.27	-0.25	16.7752	17.9598	7.0617	3.1165	0.7791
160	4.993	31.42	0.48	-0.25	-0.25	16.0821	17.0527	6.0356	2.7248	0.6812
161	5.231	30.34	0.51	-0.29	-0.24	16.8485	18.7627	11.3614	1.9298	0.4824
162	4.729	33.56	0.49	-0.26	-0.26	15.2322	16.2976	6.9943	2.0901	0.5225
163	3.282	29.97	0.21	-0.09	-0.10	7.0472	7.8215	10.9884	1.1802	0.1967
164	3.182	31.03	0.19	-0.10	-0.12	6.8328	6.8336	0.0113	1.2245	0.2041
165	3.347	29.45	0.21	-0.11	-0.10	7.1859	7.9594	10.7631	0.8081	0.1347
166	3.151	31.49	0.21	-0.11	-0.10	6.7646	7.4435	10.0374	0.8928	0.1488
167	3.224	30.64	1.59	-0.73	-0.88	55.3796	57.9072	4.5641	1.2844	1.7125
168	3.238	30.34	1.57	-0.79	-0.78	55.6191	57.7574	3.8445	1.0806	1.4408
169	3.588	27.59	1.67	-0.81	-0.94	61.6268	67.5451	9.6034	0.7831	1.0441
170	3.049	32.56	1.64	-0.82	-0.83	52.3683	56.2149	7.3453	0.8606	1.1475
171	0.667	30.28	0.28	-0.14	-0.14	10.0261	10.3198	2.9298	0.0646	0.0754
172	2.394	30.39	1.04	-0.49	-0.54	35.9770	38.1996	6.1780	0.6022	0.7026
173	0.670	30.40	0.27	-0.10	-0.14	10.0686	9.9117	1.5585	0.0397	0.0463
174	0.680	30.05	0.28	-0.15	-0.14	10.2215	10.4009	1.7544	0.0474	0.0553
175	2.649	30.73	1.07	-0.55	-0.52	36.9654	38.8575	5.1184	0.8873	0.9612
176	2.842	30.59	1.17	-0.58	-0.61	39.6654	42.6905	7.6264	0.7737	0.8382
177	2.790	30.29	1.17	-0.56	-0.62	38.9375	43.1138	10.7257	0.5307	0.5749
178	2.686	30.64	1.09	-0.48	-0.62	37.4900	39.7065	5.9122	0.6345	0.6874
179	1.709	30.78	0.47	-0.25	-0.23	16.5124	17.0429	3.2125	0.3945	0.2959
180	1.695	30.63	0.46	-0.25	-0.23	16.3818	16.7608	2.3132	0.3230	0.2423

No.	$\vec{j}$ [A cm^{-2}]	A [cm^2]	Δm_C [g]	Δm_{A1} [g]	Δm_{A2} [g]	t_e [µm]	t_r [µm]	Δt [%]	P [W]	W [W h]
181	1.721	29.96	0.48	-0.24	-0.27	16.6283	17.8788	7.5207	0.2042	0.1532
182	1.791	29.64	0.49	-0.25	-0.26	17.3074	18.4481	6.5913	0.2974	0.2230
183	4.820	30.29	1.32	-0.70	-0.65	46.5671	48.6318	4.4338	2.9390	2.2042
184	4.444	30.89	1.25	-0.58	-0.74	42.9421	45.1588	5.1622	1.9510	1.4633
185	5.040	29.89	1.33	-0.62	-0.70	48.6985	49.6613	1.9771	1.5833	1.1875
186	4.465	30.15	1.37	-0.63	-0.75	43.1404	50.7201	17.5697	1.6960	1.2720
187	4.226	30.03	0.39	-0.16	-0.22	9.0746	14.4966	59.7480	2.0177	0.3363
188	4.186	30.52	0.38	-0.19	-0.21	8.9889	13.8983	54.6163	2.0197	0.3366
189	4.066	31.05	0.40	-2.20	-0.20	8.7293	14.3761	64.6877	1.2120	0.2020
190	4.135	30.54	0.40	-0.19	-0.20	8.8782	14.6155	64.6225	1.3640	0.2273
191	0.759	29.71	0.37	-0.17	-0.19	13.8612	13.8978	0.2647	0.0858	0.1215
192	0.829	30.32	0.36	-0.19	-0.18	14.9531	13.2537	11.3649	0.0895	0.1253
193	0.722	30.99	0.37	-0.19	-0.18	12.8634	13.3264	3.5988	0.0447	0.0619
194	0.762	29.98	0.37	-0.18	-0.20	13.4092	13.7738	2.7191	0.0557	0.0761
195	1.911	30.22	0.64	-0.34	-0.30	22.5640	23.6328	4.7365	0.4851	0.4447
196	1.901	29.53	0.64	-0.32	-0.34	22.4532	24.1868	7.7209	0.3897	0.3572
197	1.916	29.72	0.66	-0.35	-0.33	22.6297	24.7856	9.5267	0.2642	0.2422
198	1.751	33.15	0.66	-0.34	-0.31	20.6790	22.2199	7.4513	0.3117	0.2858
199	4.728	30.40	0.44	-0.17	-0.23	15.2290	16.1531	6.0684	2.5588	0.6397
200	4.605	29.89	0.42	-0.18	-0.32	14.8320	15.6825	5.7339	2.2809	0.5702
201	4.637	29.81	0.43	-0.19	-0.23	14.9345	16.0966	7.7816	1.5277	0.3819
202	4.360	32.50	0.47	-0.25	-0.22	14.0435	16.1415	14.9395	1.7004	0.4251

Table B.2.: Calculated lab values

Appendix C.

Lab values

The following pages contain the original documentation of the lab experiment.

Versuch #1

- Fläche 0,234 dm²
- Stromst. : 0,25 A
- Dauer

Temp = 23 °C

Kontrolle Strom	Metallteil 1/A	Referenz /A	Uhrzeit
~~0 min~~	~~0,25~~	~~0,272~~	~~9:00~~
5 min	0,25	0,268	9:05
10 min	0,25	0,272	9:10
15			
20	0,25	0,272	9:20
25	0,25	0,272	9:30
30			
35		0,272	10:10
40		0,275	
45			
50			
55			
60			

Messung # 2

Versuchstück # 1

Fläche: 2 × 4,6 × 3,5

t_0 { Anode 1 : 15,70 g
Anode 2 : 15,88 g
Kathode : 17,42 g

t_1 { A1 : 15,50
A2 : 15,70
K : 17,81

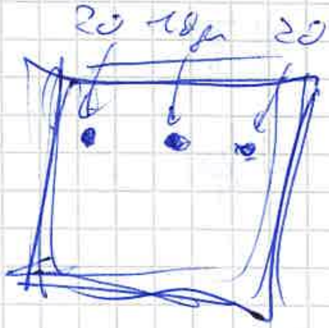

Messung #3

Versuchstück # 1

I

t_0 { A1 : ~~[illegible]~~ 15,51
A2 15,70
K 17,80

$I = 0{,}990\,A$ $I_2 = 0{,}98$

$U = 1{,}2\,V$

$t = 15\ min$

t_1 { A1 : 15,05 g
A2 : 15,28 g
K1 : 18,71 g

Messung #4

Kathode 2

Anode 3 + 4

$T = 25{,}5\,°C$

Fläche:

t_0:
- K2 : 15,96 g
- A3 : 16,55 g
- A4 : 16,38 g

t_1:
- 4 : 17,05
- A

$I_1 = 1{,}01\,A$

$I_2 = 0{,}997$

$V = 2{,}7\,V$

Time = 20 min

Versuch # 5

Kathode 1, Anode 1+2

t_0 {
- K : 18,67
- A1 : 15,04
- A2 : 15,26

t_1 {
- K : 19,40
- A1 : 14,74
- A2 : 14,97

$I_1 = 0{,}66\,A$ I_2 I_3

Temp = 59,8

U = 0,6 V

Dauer : 40 min

Versuch #6

U1, A1, A2

t_0	U	~~18,38~~	20,10
	A1	~~14,74~~	14,35
	A2	~~14,97~~	14,54

t_1	U :	20,77
	A1 :	14,01
	A2 :	14,21

I_1 = 1,326

I_2 = ~~1,345~~ A 1.320 A

I_3 = ~~1,322~~ A

Temp = ~~40°C~~ 38°C

U = 1,5V

11:17

Time = 25 min

Versuch #7

N3, A5, A6

Fläche 7,5 × 4,6

I_0	N :	14,73
	~~A6~~ A5 :	15,04
	A6 :	15,32

I_2	N	~~15,20~~ 15,30
	A5	14,77
	A6	15,04

I_1 = ~~0,966 A~~ 0,805 A

I_2

I_3

Temp = 25°

U ~~R~~

Time = 35,5 min

W. Versuch # 8 NT: 2

K: 2 A~~?~~: 3 A: 4

K2: 16,61	K2: 17,11
A3: 15,87	A3: 15,68
A4: 15,67	A4: 15,40

I_1 = 0,505 A
I_2 = 0,501
I_3 = 0,449

Temp: 40,2 T_2 = 32°C
U = 9,6 V
Time = 10:45 : 52 min

Versuch #9 N3 NT:1

t_0 {
N3 : 15,15
A5 : 14,78
A6 : 15,04
}

t_1 {
N3 : 15,53
A5 : 14,58
A6 : 14,87
}

I_1 : 0,375
I_2
I_3 = 0,326
U = 0,2 - 0,3 V
Temp : 60,2 , T_2 = 59
Time : 10:41
: 50 min

Versuch #90

Netzteil: 3

K1, A1, A2

K	20,73
A1	14,01
A2	14,20

K	: 21,67
A1	: 13.54
A2	: 13.70

$I_1 = 0,695$

I_2

I_3 0,689 $I_3 = 0,676$

Temp = 22 °C

U = 1,1V

Time : 11:00

67min

#11

U3 A5 A6

t_0	U3	15,52		U3	16,01
	A5	14,58		A5	14,33
	A6	14,85		A6	14,62

$I_1 = 0{,}630$

$I_2 = 0{,}613$

$I_3 = 0{,}613$ ✓

$T_1 = 58{,}1\ °C$

$T_2 = 60{,}6$

T_3

$U = 0{,}6$

Start = 12:22 - 13:00 38 min

883

A 12

K2 A3 A4

K2	17,17
A3	15,63
A4	15,39

K2
A3
A4

Temp₁ = 23,4 °C

F_1 = 0,257

F_2 = 0,255

U = 0,65 V

Start: 12:20
14

~~35 min 15 sek~~
~~36 min~~ 37 min

#13

K4 A7 ~~A8~~

Fläche: 3,5 × 4,6 × 2

K4	17,04	K4	17,08
A7	16,65	A7	16,63
A8	16,82	A8	16,79

Temp 1 = 39,5 °C
T_2 = 38
I_1 = 0,107 A
I_2 = 0,108
I_3 = 0,05

U = 0,1 V

Time = 12:01
13:12

30 min

14

NT:3

K2	17,30	K2 17,72
A3	15,52	A3 15,31
A4	15,30	A4 15,10

Temp = 23,5

I_1 = 0,805 A   0,570

I_2 = ~~0,800 A~~

I_3 = 0,765

Time: 13:25 → ~~[illegible]~~ 25:00

U = 1,1V

15 NT: 2

W4	17,08		W4	17,84
A7	16,65		A7	16,23
A8	16,82		A8	16,34

Temp 1 = 39,6
T_2 = 38,6

I_1 = 1,803 I_1 = 1,544
I_2 = 1,787
Start: 13:14

22 min

U = 1,8 V

16

K3	15,99
A5	14,32
A6	14,61

K3	16,46	KT: 1
A5	14,09	
A6	14,38	

T = 59,5 °C

I_1 = 1,405 A
I_2 = 1,387 A
I_3 = 1,380 A

U = 1,2 V

13:35 → 16:30 min

WS 15 Soll 25 min 20°C 1,9 $\frac{A}{dm^2}$

	Anfang	Ende	Fläche Ui
Kathode	18,17	18,47	
Anode 1	12,74	12,60	4,6 x
Anode 2	13,09	12,95	3,4

Temp: 21,7
I_1: 0,597 I_2: 0,582 I_3: 0,582
V: 0,8
Start: 10:23 Stop: 10:28 (25 min)

WS 16 Soll 35 min 40°C 4,9 $\frac{A}{dm^2}$

	Anfang	Ende	Fläche Ui
K	18,49	19,72	4,6 x
A 1	14,63	14,04	
A 2	15,49	14,82	3,6

Temp: 39,1
I_1: 1,622 I_2: 1,770 I_3: 1,764
V: 0,3
Start: 10:01 Ende: 10:36 35 min

WS 17 Soll 60 min 60 °C 1,3 $\frac{A}{dm^2}$

	Start	Ende	Fläche K_1
K_1	18,46	18,44	4,6 x 3,15
A_1	15,015	14,74	
A_2	16,63	16,39	

Temp: 60,1

I_1: 0,377 I_2: 0,377 I_3: 0,372

V 0,3

Start: 9:51 Ende: 10 52 (61 min)

WS20 Soll 35 min 60 °C 1,5 $\frac{A}{dm^2}$

	Start	Ende	Fläche K_1
K_1	15,80	16,14	4,58 x 3,65
A1	14,55	14,38	
A2	14,73	14,53	

Temp 58,3

I_1 0,501 I_2 0,497 I_3 0,483

V 0,3

Start: 11:30 Ende: 12:05

Soll 65 min 20° C 0,7 $\frac{A}{dm^2}$ WS 18

	Start	End	Fläche 4
V1	18,24	18,49	4,65 × 3
A1	14,38	14,24	
A2	16,23	16,10	

Temp: 24,3

I_1: 0,195 I_2 0,196 I_3 0,195

V: 0,35

Startzeit 11:08 Endzeit 12:13

WS 19

Soll 45 min 40° C 3,3 $\frac{A}{dm^2}$

	Start	End	Fläche 4
V1	15,76	16,71	4,65 × 3,45
A1	14,09	13,61	
A2	16,40	15,88	

Temp: 39,5

I_1: 1,050 I_2 1,028 I_3 1,062

V: 1,1

Startzeit 11:13 Endzeit 11:58 45 min

Soll 75 min 20° 3,3 A/dm² WS 21

	Start	Ende	Fläche K
K	17,06	18,57	4,61 × 3,225
A1	19,03	18,20	(=0,481 A)
A2	17,85	17,16	

Temp 25,0
V: 1,3
I_1: 0,980 I_2 0,981 I_3 0,982
Start ~~[illegible]~~ Ende

Soll 45 min 40°C 2,1 A/dm² WS 22

	Start	Ende	Fläche K
K	15,37	15,45	4,60 × 3,35
A1	18,39	18,08	(=0,64722 A)
A2	12,94	12,67	

Temp 38,8
V 0,6
I_1 0,647 I_2 0,647 I_3 0,647
Start 12:58 Ende 13:43

VJ 23 Soll 40 min 60°C 2,1 A/dm²

	Start	Ende	Fläche
K	15,61	16,16	4,63 × 3,4
A 1	12,59	12,31	(=0,6611 A)
A 2	14,02	13,77	

Temp 59,7

U: 0,5

I_1 0,661 I_2 0,642 I_3 0,641

Start 12:55 Ende 13:35

NTC

#24

t_0 { U22 : 15,95 ; A22-1 : 18,07 ; A22-2 : 12,67 }

t_1 { U22 : 16,19 ; A22-1 : 17,96 ; A22-2 : 12,56 }

I_1 : 0,452 A

I_2 : 0,437

I_3 : 0,35

T_1 : 39,°C

T_2 : 39,2°C

T_3 :

U = 0,4V

Startzeit : 14:41 : 24 min

A = 3,4 · 4,61 · 2

25

N 41

H20	: 16,12	H20	: 16,28
A20-1	: 14,37	A20-1	: 14,32
A20-2	: 14,53	A20-2	: 14,48

$A = 4{,}57 \cdot 3{,}64 \cdot 2$

I_1 : 0,150
I_2 : 0,15
I_3 : 0,148
: 0,150 A

T_{ap1} = 58,4°C

T_{ap2} = 56,5
T_3 = 60,7

Time : 15:03 : 45 → 42 min

U = 0,1V

26

NT3

U18 : 18,49

A 18-1 : 14,25

A 18-2 : 16,09

U 18 : 19,50

A 18-1 : 13,74

A 18-2 : 15,60

T_1 = 24,1
T_2 = 25,0
T_3 = 26,2

I_1 : 1,209 A 1,139
I_2 : 1,185 A
I_3 : 1,187

U = 1,8 V

Start : 15:29 } ~~15:59~~ → 70 Min

16:10 } 41 min

A = 4,65 · 3,05 × 2

N T 1

A 2 2

	L_0	F_1
U 22	16,17	16,64
A22/1	17,96	17,73
A22/2	12,56	12,32

F_1 = 1,152   1,107
F_2 = 1,105
F_3 = 1,108

T_1 = 32,8
T_2 = 38,6
T_3 = 39,1

U = 1,1V

T = 16:00   16:20

20 min

VersuchNr.	31					
SOLL	40	min.	60	°C		A/dm^2
					0,25	A

	Nummer	Masse Start [g]	Masse Ende [g]	Fläche Kathode [cm^2]
Kathode	426	16,03	16,22	4,64×3,5
Anode 1	426-1	14,93	14,83	
Anode 2	426-2	15,07	14,92	

Temp_1 [°C]	58,5	Temp_2[°C]	60,1	Temp_3 [°C]	59,0
I_1 [A]	0,258	I_2 [A]	0,256	I_3 [A]	–
U [V]	0,234				
Startzeit	[illegible]:44	Endzeit			
		Dauer [min-]	39		
Netzteil	1				

VersuchNr.	32					
SOLL	45	min.	40	°C		A/dm^2
					0,3	A

	Nummer	Masse Start [g]	Masse Ende [g]	Fläche Kathode [cm^2]
Kathode	19	16,71	16,92	~~4,46×3,3~~
Anode 1	19-1	13,62	13,51	
Anode 2	19-2	15,89	15,79	

Temp_1 [°C]	38,8	Temp_2[°C]	38,6	Temp_3 [°C]	39,5	
I_1 [A]	0,308	I_2 [A]	0,301	I_3 [A]	0,303	0,244
U [V]	0,368					
Startzeit	09:59	Endzeit				
		Dauer [min-]	33			
Netzteil	2					

VersuchNr.	33					
SOLL		min.	25	°C		A/dm^2
					0,43	A

	Nummer	Masse Start [g]	Masse Ende [g]	Fläche Kathode [cm^2]
Kathode	20	16,74	16,38	4,46×3,3
Anode 1	20-1	14,30	14,23	
Anode 2	20-2	14,47	14,40	

Temp_1 [°C]	24,7	Temp_2[°C]	24,8	Temp_3 [°C]	
I_1 [A]	0,430	I_2 [A]	0,436	I_3 [A]	–
U [V]	0,67				
Startzeit		Endzeit			
		Dauer [min-]	17		
Netzteil	3				

VersuchNr.	34					
SOLL	~~30~~ 35	min.	40	°C		A/dm^2
					0,4	A

	Nummer	Masse Start [g]	Masse Ende [g]	Fläche Kathode [cm^2]
Kathode	6	16,24	17,00	
Anode 1	6-1	17,38	17,02	
Anode 2	6-2	17,28	16,89	

Temp_1 [°C]	38,8	Temp_2[°C]	39,5	Temp_3 [°C]	38,8
I_1 [A]	0,409	I_2 [A]	0,892	I_3 [A]	0,876
U [V]	1,014				
Startzeit			Endzeit		
			Dauer [min-]	41	
Netzteil					

VersuchNr.	35					
SOLL	30	min.	60	°C		A/dm^2
					0,75	A

	Nummer	Masse Start [g]	Masse Ende [g]	Fläche Kathode [cm^2]
Kathode	45	17,06		
Anode 1	5-1	15,34		
Anode 2	5-2	17,69		

Temp_1 [°C]	58,2	Temp_2[°C]		Temp_3 [°C]	
I_1 [A]	0,754	I_2 [A]	0,75	I_3 [A]	
U [V]	0,664				
Startzeit			Endzeit		
			Dauer [min-]		
Netzteil					

Netzteil #1 ausgefallen

VersuchNr.	36					
SOLL	35	min.	25	°C		A/dm^2
					0,37	A

	Nummer	Masse Start [g]	Masse Ende [g]	Fläche Kathode [cm^2]
Kathode	420	16,38	16,62	
Anode 1	A20-1	14,24	14,10	
Anode 2	A20-2	14,40	14,27	

Temp_1 [°C]	26,0	Temp_2[°C]	26,1	Temp_3 [°C]	
I_1 [A]	0,374	I_2 [A]	0,376	I_3 [A]	0,379
U [V]	0,582				
Startzeit			Endzeit		
			Dauer [min-]	32	
Netzteil					

VersuchNr.	37					
SOLL	40	min.	20	°C	4,3	A/dm^2
					1,29	A

	Nummer	Masse Start [g]	Masse Ende [g]	Fläche Kathode [cm^2]
Kathode	A 19-2	16,53	17,67	4,60 x 3,52
Anode 1	A 26-2	14,46	14,35	
Anode 2	A 21,2	17,14	16,56	

Temp_1 [°C]	28,0	Temp_2[°C]	28,2	Temp_3 [°C]	28,5
I_1 [A]	1,348	I_2 [A]	1,348	I_3 [A]	1,400
U [V]	1,800				
Startzeit	/	Endzeit		/	
		Dauer [min-]		40	
Netzteil	3				

✓

VersuchNr.	38					
SOLL	80	min.	40	°C	0,9	A/dm^2
					0,2966	A

	Nummer	Masse Start [g]	Masse Ende [g]	Fläche Kathode [cm^2]
Kathode	1	21,85	22,32	4,675 x 3,525
Anode 1	45	16,77	16,51	
Anode 2	15	13,49	13,27	

Temp_1 [°C]	38	Temp_2[°C]	38,0	Temp_3 [°C]	38,0
I_1 [A]	0,298	I_2 [A]	0,292	I_3 [A]	0,266
U [V]	0,352				
Startzeit	/	Endzeit		/	
		Dauer [min-]		80	
Netzteil	2				

✓

VersuchNr.	39					
SOLL	45	min.	60	°C	1,5	A/dm^2
					0,4538	A

	Nummer	Masse Start [g]	Masse Ende [g]	Fläche Kathode [cm^2]
Kathode	U5-1	15,42	16,35	3,51 x 8,310
Anode 1	A 27-1	15,35	15,15	
Anode 2	U2	17,40	17,17	

Temp_1 [°C]	58,3	Temp_2[°C]	58,5	Temp_3 [°C]	58,5
I_1 [A]	0,455	I_2 [A]	0,413	I_3 [A]	0,420
U [V]	0,420				
Startzeit	/	Endzeit		⌒	
		Dauer [min-]		45	
Netzteil	1				

✓

VersuchNr.	40		50			
SOLL	45 ~~70~~	min.	~~40~~	°C	1,5	A/dm^2
					0,5016	A

	Nummer	Masse Start [g]	Masse Ende [g]	Fläche Kathode [cm^2]
Kathode	A5-2	18,13	18,56	4,67 x 3,58
Anode 1	V14	16,19	15,45	
Anode 2	A2	13,70	13,52	

Temp_1 [°C]	44,8	Temp_2[°C]	44,8	Temp_3 [°C]	44,8
I_1 [A]	0,444	I_2 [A]	0,438	I_3 [A]	0,435
U [V]	0,383				
Startzeit	/	Endzeit	/		
		Dauer [min-]	45		
Netzteil	4				

✓

VersuchNr.	41					
SOLL	25	min.	40	°C	4,1	A/dm^2
					1,2506	A

	Nummer	Masse Start [g]	Masse Ende [g]	Fläche Kathode [cm^2]
Kathode	A7-2	17,42	18,06	4,24 x 3,555
Anode 1	A26-1	14,82	14,51	
Anode 2	A1	13,51	13,18	

Temp_1 [°C]	39,7	Temp_2[°C]	39,7	Temp_3 [°C]	39,8 ~~1,238~~
I_1 [A]	1,256	I_2 [A]	1,240	I_3 [A]	1,230
U [V]	1,411				
Startzeit	/	Endzeit	/		
		Dauer [min-]	25		
Netzteil	2				

✓

VersuchNr.	42		60			
SOLL	45	min.	~~50~~	°C	1,5	A/dm^2
					0,4452	A

	Nummer	Masse Start [g]	Masse Ende [g]	Fläche Kathode [cm^2]
Kathode	A6-1	17,44	18,34	4,27 x 3,475
Anode 1	A20-2	14,25	14,07	
Anode 2	A20-1	14,08	13,85	

Temp_1 [°C]	58,5 ~~44,8~~	Temp_2[°C]	59,0	Temp_3 [°C]	59,4
I_1 [A]	0,430 ~~0,449~~	I_2 [A]	0,451	I_3 [A]	0,468
U [V]	0,388 ~~0,383~~				
Startzeit	/	Endzeit	/		
		Dauer [min-]	45 min		
Netzteil	1				

✓

VersuchNr.	43						
SOLL	35	min.	20	°C	4,5	A/dm^2	
					1,3546	A	

	Nummer	Masse Start [g]	Masse Ende [g]	Fläche Kathode [cm^2]
Kathode	A6-2	17,76	18,71	4,30 x 3,50
Anode 1	A21-2	16,54	16,07	
Anode 2	A5-1	15,58	15,09	

Temp_1 [°C]	26,8	Temp_2[°C]	28,5	Temp_3 [°C]	28,7
I_1 [A]	1,333	I_2 [A]	1,310	I_3 [A]	1,285
U [V]	1,800				
Startzeit	/	Endzeit	/		
		Dauer [min-]	35		
Netzteil	3				

VersuchNr.	44						
SOLL	15	min.	50	°C	1,5	A/dm^2	
					0,4785	A	

	Nummer	Masse Start [g]	Masse Ende [g]	Fläche Kathode [cm^2]
Kathode	A21-1	18,63	18,79	4,61 x 3,46
Anode 1	418	17,78	17,69	
Anode 2	4 2	17,15	17,08	

Temp_1 [°C]	44,8	Temp_2[°C]	44,8	Temp_3 [°C]	44,8
I_1 [A]	0,482	I_2 [A]	0,477	I_3 [A]	0,471
U [V]	0,445				
Startzeit	/	Endzeit	/		
		Dauer [min-]	15min		
Netzteil	4				

VersuchNr.	45						
SOLL	45	min.	60	°C	0,9	A/dm^2	
					0,3009	A	

	Nummer	Masse Start [g]	Masse Ende [g]	Fläche Kathode [cm^2]
Kathode	A22-11	18,17	18,44	4,63 x 3,61
Anode 1	A26-2	14,33	14,19	
Anode 2	4 23	15,07	14,88	

Temp_1 [°C]	59,4	Temp_2[°C]	60,6	Temp_3 [°C]	60,9
I_1 [A]	0,302	I_2 [A]	0,300	I_3 [A]	0302
U [V]	0,254				
Startzeit	/	Endzeit	/		
		Dauer [min-]	45		
Netzteil	1				

VersuchNr.	46					
SOLL	50	min.	50	°C	0,5	A/dm^2
					0,1514	A

	Nummer	Masse Start [g]	Masse Ende [g]	Fläche Kathode [cm^2]
Kathode	K6	17,05	17,23	4,32 x 3,505
Anode 1	A18-2	17,25	17,16	
Anode 2	K20	16,07	15,99	

Temp_1 [°C]	45,7	Temp_2[°C]	45,7	Temp_3 [°C]	45,7
I_1 [A]	0,170	I_2 [A]	0,159	I_3 [A]	0,168
U [V].	0,180				
Startzeit	/	Endzeit	[illegible]		
		Dauer [min-]	50		
Netzteil	4				

VersuchNr.	47					
SOLL	50	min.	60	°C	3,9	A/dm^2
					1,2669	A

	Nummer	Masse Start [g]	Masse Ende [g]	Fläche Kathode [cm^2]
Kathode	A19-2	17,68	19,03	4,545 x 3,535
Anode 1	A23-2	14,35	13,65	
Anode 2	K22	15,71	15,06	

Temp_1 [°C]	59,1	Temp_2[°C]	61,2	Temp_3 [°C]	61,4
I_1 [A]	1,263	I_2 [A]	0,972	I_3 [A]	1,232
U [V]	1,026				
Startzeit	/	Endzeit	-		
		Dauer [min-]	50		
Netzteil	1				

VersuchNr.	48					
SOLL	50	min.	40	°C	1,1	A/dm^2
					0,34135	A

	Nummer	Masse Start [g]	Masse Ende [g]	Fläche Kathode [cm^2]
Kathode	K7	17,41	17,72	4,31 x 3,60
Anode 1	A7-1	15,15	15,00	
Anode 2	A18-1	12,41	12,77	

Temp_1 [°C]	38,6	Temp_2[°C]	38,0	Temp_3 [°C]	38,0
I_1 [A]	0,341	I_2 [A]	0,331	I_3 [A]	0,296
U [V]	0,360				
Startzeit	/	Endzeit	/		
		Dauer [min-]	50		
Netzteil	2				

49

VersuchNr.	~~54~~ 46					
SOLL	80	min.	50	°C	3,87	A/dm^2
					1,1752	A

	Nummer	Masse Start [g]	Masse Ende [g]	Fläche Kathode [cm^2]
Kathode	A18-2	16,27	18,00	4,59 x 3,46
Anode 1	A18-1	13,74	12,94	
Anode 2	U 18	18,71	17,80	

Temp_1 [°C]	44,4	Temp_2[°C]	44,6	Temp_3 [°C]	44,2
I_1 [A]	1,760	I_2 [A]	1,145	I_3 [A]	1,144
U [V]	0,717				
Startzeit	13:33			Endzeit	/
				Dauer [min-]	80 min
Netzteil	4				

VersuchNr.	~~5~~ ~~47~~ 50					
SOLL	35	min.	40	°C	2,7	A/dm^2
					0,8334	A

	Nummer	Masse Start [g]	Masse Ende [g]	Fläche Kathode [cm^2]
Kathode	A23-2	14,36	14,96	4,60 x 3,355
Anode 1	U23	15,32	15,03	
Anode 2	A21-1	18,19	17,89	

Temp_1 [°C]	39,0	Temp_2[°C]	38,6	Temp_3 [°C]	38,7
I_1 [A]	0,833	I_2 [A]	0,803	I_3 [A]	0,810
U [V]	0,924				
Startzeit	/			Endzeit	/
				Dauer [min-]	35 min
Netzteil	2				

VersuchNr.	26					
SOLL	15	min.	20	°C	4,7	A/dm^2
					1,5547	A

	Nummer	Masse Start [g]	Masse Ende [g]	Fläche Kathode [cm^2]
Kathode	TEST	16,60	17,19	4,525 x 3,655
Anode 1	A22-1	17,72	17,42	
Anode 2	U 22	16,02	15,73	

Temp_1 [°C]	25,2	Temp_2[°C]	26,6	Temp_3 [°C]	27,3
I_1 [A]	1,550	I_2 [A]	1,524	I_3 [A]	1,516
U [V]	2,121				
Startzeit	/			Endzeit	/
				Dauer [min-]	18 min
Netzteil	3				

VersuchNr.	51						
SOLL	50	min.	20	°C	0,5	A/dm^2
					0,15108	A

	Nummer	Masse Start [g]	Masse Ende [g]	Fläche Kathode [cm^2]
Kathode	A5-1	15,70	15,86	4,28 x 3,53
Anode 1	15	13,25	13,18	
Anode 2	A 20-1	13,84	13,75	

Temp_1 [°C]	25,3	Temp_2[°C]	25,0	Temp_3 [°C]	25,2
I_1 [A]	0,156	I_2 [A]	0,158	I_3 [A]	0,159
U [V]	0,213				
Startzeit	✓	Endzeit	–		
		Dauer [min-]	50		
Netzteil	3				

VersuchNr.	52					
SOLL	50	min.	40	°C	0,5	A/dm^2
					0,147147	A

	Nummer	Masse Start [g]	Masse Ende [g]	Fläche Kathode [cm^2]
Kathode	K5	17,12	17,26	4,29 x 3,43
Anode 1	A 20-2	14,06	13,98	
Anode 2	A 18-2	17,14	17,06	

Temp_1 [°C]	37,2	Temp_2[°C]	38,4	Temp_3 [°C]	38,6
I_1 [A]	0,147	I_2 [A]	0,146	I_3 [A]	0,145
U [V]	0,174				
Startzeit	✓	Endzeit	✓		
		Dauer [min-]	50		
Netzteil	2				

VersuchNr.	53					
SOLL	50	min.	50	°C	0,5	A/dm^2
					0,15953	A

	Nummer	Masse Start [g]	Masse Ende [g]	Fläche Kathode [cm^2]
Kathode	K 19	16,59	16,78	4,545 x 3,51
Anode 1	A 26-1	14,51	14,40	
Anode 2	K 20	15,99	15,89	

Temp_1 [°C]	44,7	Temp_2[°C]	50,1	Temp_3 [°C]	50,2
I_1 [A]	0,159	I_2 [A]	0,162	I_3 [A]	0,161
U [V]	0,153				
Startzeit	✓	Endzeit	–		
		Dauer [min-]	50		
Netzteil	4				

VersuchNr.	54					
SOLL	50	min.	60	°C	0,5	A/dm^2
					0,1653	A

	Nummer	Masse Start [g]	Masse Ende [g]	Fläche Kathode [cm^2]
Kathode	A21-2	16,97	17,14	4.56 x 3,625
Anode 1	A2	13,51	13,42	
Anode 2	A1	13,18	13,09	

Temp_1 [°C]	56,0	Temp_2[°C]	60,4	Temp_3 [°C]	60,4
I_1 [A]	0,165	I_2 [A]	0,168	I_3 [A]	0,223
U [V]	0,154				
Startzeit	✓		Endzeit	✓	
			Dauer [min-]	50	
Netzteil	1				

✓

VersuchNr.	55					
SOLL	50	min.	20	°C	1,5	A/dm^2
					0,45689	A

	Nummer	Masse Start [g]	Masse Ende [g]	Fläche Kathode [cm^2]
Kathode	501	18,05	18,50	4,290 x 3,555
Anode 1	505	18,10	17,85	
Anode 2	506	19,54	19,34	

Temp_1 [°C]	22,3	Temp_2[°C]	26,0	Temp_3 [°C]	26,4
I_1 [A]	0,453	I_2 [A]	0,445	I_3 [A]	0,443
U [V]	0,630				
Startzeit	✓		Endzeit	✓	
			Dauer [min-]	50	
Netzteil	3				

✓

VersuchNr.	56					
SOLL	50	min.	40	°C	1,5	A/dm^2
					0,45461	A

	Nummer	Masse Start [g]	Masse Ende [g]	Fläche Kathode [cm^2]
Kathode	502	19,10	19,55	4,305 x 3,520
Anode 1	507	19,83	19,60	
Anode 2	508	18,77	18,55	

Temp_1 [°C]	35,2	Temp_2[°C]	37,5	Temp_3 [°C]	38,3
I_1 [A]	0,456	I_2 [A]	0,441	I_3 [A]	0,441
U [V]	0,533				
Startzeit	✓		Endzeit	✓	
			Dauer [min-]	50	
Netzteil	2				

✓

VersuchNr.	57						
SOLL	50 ~~[illegible]~~	min.	50	°C		1,5	A/dm^2
						0,46257	A

	Nummer	Masse Start [g]	Masse Ende [g]	Fläche Kathode [cm^2]
Kathode	503	~~[illegible]~~ 19,00	19,28	4,295 x 3,590
Anode 1	509	18,62	18,48	
Anode 2	510	18,72	18,59	

Temp_1 [°C]	46,1	Temp_2[°C]	49,7	Temp_3 [°C]	49,1
I_1 [A]	0,457	I_2 [A]	0,448	I_3 [A]	0,447
U [V]	0,380				
Startzeit	✓		Endzeit	~~56~~	
			Dauer [min-]	50	
Netzteil	4				

✓

VersuchNr.	58						
SOLL	50	min.	60	°C		1,5	A/dm^2
						0,45598	A

	Nummer	Masse Start [g]	Masse Ende [g]	Fläche Kathode [cm^2]
Kathode	504	19,41	19,58	4,290 x 3,543
Anode 1	511	18,04	17,82	
Anode 2	512	16,36	16,11	

Temp_1 [°C]	55,8	Temp_2[°C]	58,3	Temp_3 [°C]	60,1
I_1 [A]	0,455	I_2 [A]	0,440	I_3 [A]	0,439
U [V]	0,325				
Startzeit	✓		Endzeit	~~50~~	
			Dauer [min-]	50	
Netzteil	1				

✓

VersuchNr.	59						
SOLL	50	min.	20	°C		2,5	A/dm^2
						0,7725	A

	Nummer	Masse Start [g]	Masse Ende [g]	Fläche Kathode [cm^2]
Kathode	520	19,47	20,27	4,30 x 3,625
Anode 1	H18	17,68	17,32	
Anode 2	A23-2	13,63	13,19	

Temp_1 [°C]	26,4	Temp_2[°C]	26,7	Temp_3 [°C]	26,8
I_1 [A]	0,781	I_2 [A]	0,767	I_3 [A]	0,765
U [V]	1,020				
Startzeit	✓		Endzeit	✓	
			Dauer [min-]	50	
Netzteil	3				

✓

VersuchNr.	60						
SOLL	50	min.	40	°C		2,5	A/dm^2
						0,7733	A

	Nummer	Masse Start [g]	Masse Ende [g]	Fläche Kathode [cm^2]
Kathode	521	19,24	20,03	4,24 x 3,605
Anode 1	A18-1	12,75	12,40	
Anode 2	42	17,06	16,65	

Temp_1 [°C]	39,3	Temp_2[°C]	38,5	Temp_3 [°C]	38,5
I_1 [A]	0,773	I_2 [A]	0,748	I_3 [A]	0,742
U [V]	0,835				
Startzeit	/		Endzeit	–	
			Dauer [min-]	50	
Netzteil	2				

✓

VersuchNr.	61						
SOLL	50	min.	60	°C		2,5	A/dm^2
						0,756615	A

	Nummer	Masse Start [g]	Masse Ende [g]	Fläche Kathode [cm^2]
Kathode	522	18,59	~~18,59~~ 17,35	4,26 x 3,55
Anode 1	423	14,85	14,46	
Anode 2	A26-2	14,17	13,77	

Temp_1 [°C]	60,8	Temp_2[°C]	60,5	Temp_3 [°C]	62,1
I_1 [A]	0,757	I_2 [A]	0,726	I_3 [A]	0,720
U [V]	0,562				
Startzeit	/		Endzeit	/	
			Dauer [min-]	50	
Netzteil	1				

✓

VersuchNr.	62						
SOLL	50	min.	50	°C		2,5	A/dm^2
						0,7841	A

	Nummer	Masse Start [g]	Masse Ende [g]	Fläche Kathode [cm^2]
Kathode	523	19,13	19,94	4,273 x 3,67
Anode 1	422	15,04	14,62	
Anode 2	A7-1	14,99	14,59	

Temp_1 [°C]	~~[illegible]~~ 50,2	Temp_2[°C]	49,5	Temp_3 [°C]	49,6
I_1 [A]	0,787	I_2 [A]	0,770	I_3 [A]	0,773
U [V]	0,656				
Startzeit	/		Endzeit	–	
			Dauer [min-]	50	
Netzteil	4				

✓

VersuchNr.	63						
SOLL	50	min.	20	°C		3,5	A/dm^2
						1,1029	A

	Nummer	Masse Start [g]	Masse Ende [g]	Fläche Kathode [cm^2]
Kathode	509	18,91	20,06	4,305 x 3,66
Anode 1	543	17,04	16,4[illegible]9	
Anode 2	512	16,10	15,49	

Temp_1 [°C]	27,2	Temp_2[°C]	28,3	Temp_3 [°C]	28
I_1 [A]	1,109	I_2 [A]	1,099	I_3 [A]	1,044
U [V]	1,322				
Startzeit	/		Endzeit	/	
			Dauer [min-]	50	
Netzteil	3				

✓

VersuchNr.	64						
SOLL	50	min.	40	°C		3,5	A/dm^2
						1,0853	A

	Nummer	Masse Start [g]	Masse Ende [g]	Fläche Kathode [cm^2]
Kathode	506	14,75	20,85	4,245 x 3,61
Anode 1	511	17,81	17,30	
Anode 2	544	13,96	13,36	

Temp_1 [°C]	38,0	Temp_2[°C]	38,6	Temp_3 [°C]	38,7
I_1 [A]	1,085	I_2 [A]	1,068	I_3 [A]	1,069
U [V]	1,170				
Startzeit	/		Endzeit	/	
			Dauer [min-]	50	
Netzteil	2				

✓

VersuchNr.	65						
SOLL	50	min.	60	°C		3,5	A/dm^2
						1,0668	A

	Nummer	Masse Start [g]	Masse Ende [g]	Fläche Kathode [cm^2]
Kathode	507	20,08	21,20	4,275 x 3,565
Anode 1	508	18,54	17,45	
Anode 2	542	18,56	18,02	

Temp_1 [°C]	54,0	Temp_2[°C]	61,1	Temp_3 [°C]	54,8
I_1 [A]	1,068	I_2 [A]	1,055	I_3 [A]	1,052
U [V]	0,817				
Startzeit	/		Endzeit	/	
			Dauer [min-]	50	
Netzteil	1				

✓

VersuchNr.	66					
SOLL	50	min.	50	°C	3,5	A/dm^2
					1,0526	A

	Nummer	Masse Start [g]	Masse Ende [g]	Fläche Kathode [cm^2]
Kathode	540	19,10	20,21	29 4,5~~8~~ x 3,505
Anode 1	505	17,83	17,30	
Anode 2	541	15,87	15,26	

Temp_1 [°C]	50,1	Temp_2[°C]	49,5	Temp_3 [°C]	48,7
I_1 [A]	1,053	I_2 [A]	1,051	I_3 [A]	1,053
U [V]	0,839				
Startzeit	/	Endzeit	/		
		Dauer [min-]	50		
Netzteil	4				

✓

VersuchNr.	67					
SOLL	30	min.	25	°C		A/dm^2
					0,15	A

	Nummer	Masse Start [g]	Masse Ende [g]	Fläche Kathode [cm^2]
Kathode	41	15,81	15,91	4,21 x 3,49
Anode 1	1-1	17,27	17,22	
Anode 2	1-2	16,46	16,40	

Temp_1 [°C]	26,4	Temp_2[°C]	26,5	Temp_3 [°C]	26,4
I_1 [A]	0,156	I_2 [A]	0,157	I_3 [A]	0,155
U [V]	0,261				
Startzeit	/	Endzeit	/		
		Dauer [min-]	30		
Netzteil	3				

✓

VersuchNr.	68					
SOLL	30	min.	40	°C		A/dm^2
					0,3	A

	Nummer	Masse Start [g]	Masse Ende [g]	Fläche Kathode [cm^2]
Kathode	42	18,45	18,65	~~4,2425 x~~ 3,
Anode 1	2-1	15,23	15,13	
Anode 2	2-2	14,45	14,36	

4,25 x 3,45

Temp_1 [°C]	38,7	Temp_2[°C]	38,6	Temp_3 [°C]	38,4
I_1 [A]	0,308	I_2 [A]	0,299	I_3 [A]	0,301
U [V]	0,410				
Startzeit	/	Endzeit	/		
		Dauer [min-]	30		
Netzteil	2				

✓

VersuchNr.	67					
SOLL	30	min.	60	°C		A/dm^2
					0,45	A

	Nummer	Masse Start [g]	Masse Ende [g]	Fläche Kathode [cm^2]
Kathode	43	18,28	18,56	4,25 × 7,4
Anode 1	3-1	13,76	13,61	
Anode 2	3-2	13,33	13,19	

Temp_1 [°C]	57,6	Temp_2[°C]	60,2	Temp_3 [°C]	60,5
I_1 [A]	0,454	I_2 [A]	0,451	I_3 [A]	0,457
U [V]	0,464				
Startzeit	/		Endzeit	/	
			Dauer [min-]	36	
Netzteil	1				

VersuchNr.	70					
SOLL	30	min.	80	°C		A/dm^2
					0,6	A

	Nummer	Masse Start [g]	Masse Ende [g]	Fläche Kathode [cm^2]
Kathode	44	17,56	17,93	4,22 × 7,45
Anode 1	4-1	16,63	16,43	
Anode 2	4-2	17,30	17,11	

Temp_1 [°C]	49,3	Temp_2[°C]	48,7	Temp_3 [°C]	48,5
I_1 [A]	0,606	I_2 [A]	0,597	I_3 [A]	0,594
U [V]	0,705				
Startzeit	/		Endzeit	/	
			Dauer [min-]	30	
Netzteil	4				

VersuchNr.	31					
SOLL	30	min.	25	°C		A/dm^2
					0,5	A

	Nummer	Masse Start [g]	Masse Ende [g]	Fläche Kathode [cm^2]
Kathode	A7-2	18,06	18,36	4,30 × 3,64
Anode 1	666	13,18	13,03	
Anode 2	106	18,06	17,86	

Temp_1 [°C]	26,2	Temp_2[°C]	26,4	Temp_3 [°C]	26,4
I_1 [A]	0,514	I_2 [A]	0,502	I_3 [A]	0,509
U [V]	0,755				
Startzeit	/		Endzeit	/	
			Dauer [min-]	30	
Netzteil	3				

VersuchNr.	72						
SOLL	30	min.	40	°C		A/dm^2	
					0,5	A	

	Nummer	Masse Start [g]	Masse Ende [g]	Fläche Kathode [cm^2]
Kathode	507	21,18	21,47	4,315 x 3,63
Anode 1	105	17,34	17,19	
Anode 2	104	19,67	19,52	

Temp_1 [°C]	38,8	Temp_2[°C]	38,5	Temp_3 [°C]	38,4
I_1 [A]	0,501	I_2 [A]	0,488	I_3 [A]	0,488
U [V]	0,667				
Startzeit		Endzeit			
		Dauer [min-]	30		
Netzteil	2				

VersuchNr.	73						
SOLL	30	min.	60	°C		A/dm^2	
					0,5	A	

	Nummer	Masse Start [g]	Masse Ende [g]	Fläche Kathode [cm^2]
Kathode	504	19,57	19,87	4,31 x 3,535
Anode 1	103	13,16	13,00	
Anode 2	101	14,40	14,23	

Temp_1 [°C]	60,2	Temp_2[°C]	59,0	Temp_3 [°C]	57,0
I_1 [A]	0,500	I_2 [A]	0,494	I_3 [A]	0,494
U [V]	0,549				
Startzeit	/	Endzeit	/		
		Dauer [min-]	30		
Netzteil	1				

VersuchNr.	74						
SOLL	30	min.	50	°C		A/dm^2	
					0,5	A	

	Nummer	Masse Start [g]	Masse Ende [g]	Fläche Kathode [cm^2]
Kathode	506	20,85	21,15	4,33 x 3,59
Anode 1	102	12,37	12,20	
Anode 2	100	17,70	17,55	

Temp_1 [°C]	49,6	Temp_2[°C]	49,0	Temp_3 [°C]	49,2
I_1 [A]	0,498	I_2 [A]	0,494	I_3 [A]	0,495
U [V]	0,666				
Startzeit	/	Endzeit	/		
		Dauer [min-]	30		
Netzteil	4				

VersuchNr.	75						
SOLL	30	min.	25	°C			A/dm^2
						0,8	A
	Nummer	Masse Start [g]	Masse Ende [g]	Fläche Kathode [cm^2]			
Kathode	A21-1	18,78	19,25	4,725 x 3,475			
Anode 1	113	16,39	16,15				
Anode 2	A11	17,21	16,97				
Temp_1 [°C]	25,6	Temp_2[°C]	25,9	Temp_3 [°C]	26,1		
I_1 [A]	0,805	I_2 [A]	0,777	I_3 [A]	0,775		
U [V]	1,172						
Startzeit	13:16		Endzeit				
			Dauer [min-]	30			
Netzteil	3						

VersuchNr.	76						
SOLL	30	min.	40	°C			A/dm^2
						0,8	A
	Nummer	Masse Start [g]	Masse Ende [g]	Fläche Kathode [cm^2]			
Kathode	522	14,335	14,82	4,3125 x 3,54			
Anode 1	112	13,74	13,50				
Anode 2	111	14,57	14,32				
Temp_1 [°C]	37,7	Temp_2[°C]	38,4	Temp_3 [°C]			
I_1 [A]	0,803	I_2 [A]	0,800	I_3 [A]	–		
U [V]	0,413						
Startzeit	17:19		Endzeit				
			Dauer [min-]	30			
Netzteil	2						

VersuchNr.	77						
SOLL	30	min.	60	°C			A/dm^2
						0,8	A
	Nummer	Masse Start [g]	Masse Ende [g]	Fläche Kathode [cm^2]			
Kathode	521	20,01	20,50	4,30 x 3,445			
Anode 1	523	19,05	18,81				
Anode 2	K2	18,17	17,92				
Temp_1 [°C]	59,2	Temp_2[°C]	59,5	Temp_3 [°C]			
I_1 [A]	0,802	I_2 [A]	0,784	I_3 [A]	0,786		
U [V]	0,740						
Startzeit	13:23		Endzeit	13:53			
			Dauer [min-]	30			
Netzteil	1						

VersuchNr.	78					
SOLL	30	min.	50	°C		A/dm^2
					0,8	A
	Nummer	Masse Start [g]	Masse Ende [g]	Fläche Kathode [cm^2]		
Kathode	502	14,55	20,04	4,29 x 3,48		
Anode 1	110	13,40	13,14			
Anode 2	A3-2	13,17	12,94			
Temp_1 [°C]	48,9	Temp_2[°C]	49,2	Temp_3 [°C]		
I_1 [A]	0,804	I_2 [A]	0,797	I_3 [A]	0,793	
U [V]	0,873					
Startzeit	15:24		Endzeit			
			Dauer [min-]	30		
Netzteil	4					

VersuchNr.	79					
SOLL	30	min.	25	°C		A/dm^2
					1,2	A
	Nummer	Masse Start [g]	Masse Ende [g]	Fläche Kathode [cm^2]		
Kathode	504	14,88	20,61	4,32 x 3,540		
Anode 1	122	14,46	14,04			
Anode 2	127	13,59	13,26			
Temp_1 [°C]	26,5	Temp_2[°C]	28,1	Temp_3 [°C]		
I_1 [A]	1,203	I_2 [A]	1,185	I_3 [A]	~~0,180~~	1,180
U [V]	1,494					
Startzeit			Endzeit			
			Dauer [min-]	30		
Netzteil	3					

VersuchNr.	80					
SOLL	30	min.	40	°C		A/dm^2
					1,2	A
	Nummer	Masse Start [g]	Masse Ende [g]	Fläche Kathode [cm^2]		
Kathode	K1	~~16~~, 15,40	16,63	4,265 x 3,47		
Anode 1	120	14,34	13,94			
Anode 2	A2-1	15,11	14,77			
Temp_1 [°C]	38,0	Temp_2[°C]	39,1	Temp_3 [°C]		
I_1 [A]	1,206	I_2 [A]	1,174	I_3 [A]	~~0,177~~	1,177
U [V]	1,541					
Startzeit	13:54		Endzeit			
			Dauer [min-]	30		
Netzteil	2					

VersuchNr.	81						
SOLL	30	min.	60	°C		A/dm^2	
					1,2	A	

	Nummer	Masse Start [g]	Masse Ende [g]	Fläche Kathode [cm^2]
Kathode	507	21,49	22,23	4,34 x 3,60
Anode 1	K3	18,17	17,81	
Anode 2	A4-2	17,08	16,69	

Temp_1 [°C]	58,8	Temp_2[°C]	58,1	Temp_3 [°C]		
I_1 [A]	1,208	I_2 [A]	1,183	I_3 [A]	~~1,183~~	1,183
U [V]	1,066					
Startzeit			Endzeit			
			Dauer [min-]	30		
Netzteil	2					

✓

VersuchNr.	82					
SOLL	30	min.	50	°C		A/dm^2
					1,2	A

	Nummer	Masse Start [g]	Masse Ende [g]	Fläche Kathode [cm^2]
Kathode	506	21,15	21,86	4,335 x 3,63
Anode 1	K4	17,62	17,25	
Anode 2	503	18,66	18,30	

Temp_1 [°C]	49,1	Temp_2[°C]	49,8	Temp_3 [°C]		
I_1 [A]	~~1,208~~	I_2 [A]	1,206	I_3 [A]	1,116	~~0,115~~ 1,115
U [V]	1,118					
Startzeit			Endzeit			
			Dauer [min-]	30		
Netzteil	4					

✓

VersuchNr.	83					
SOLL		min.		°C		A/dm^2
						A

	Nummer	Masse Start [g]	Masse Ende [g]	Fläche Kathode [cm^2]
Kathode				
Anode 1				
Anode 2				

Temp_1 [°C]		Temp_2[°C]		Temp_3 [°C]	
I_1 [A]		I_2 [A]		I_3 [A]	
U [V]					
Startzeit			Endzeit		
			Dauer [min-]		
Netzteil					

VersuchNr.	83					
SOLL	30	min.	50	°C		A/dm^2
					1,5	A

	Nummer	Masse Start [g]	Masse Ende [g]	Fläche Kathode [cm^2]
Kathode	122-11	18,41	19,36	4,6175 x 3,645
Anode 1	130	21,56	21,10	
Anode 2	131	13,04	12,54	

Temp_1 [°C]	48,5	Temp_2[°C]	49,9	Temp_3 [°C]	
I_1 [A]	1,503	I_2 [A]	1,501	I_3 [A]	1,516
U [V]	1,159				
Startzeit			Endzeit		
			Dauer [min-]	30	
Netzteil	4				

✓

VersuchNr.						
SOLL		min.		°C		A/dm^2
						A

	Nummer	Masse Start [g]	Masse Ende [g]	Fläche Kathode [cm^2]
Kathode				
Anode 1				
Anode 2				

Temp_1 [°C]		Temp_2[°C]		Temp_3 [°C]	
I_1 [A]		I_2 [A]		I_3 [A]	
U [V]					
Startzeit			Endzeit		
			Dauer [min-]		
Netzteil					

VersuchNr.						
SOLL		min.		°C		A/dm^2
						A

	Nummer	Masse Start [g]	Masse Ende [g]	Fläche Kathode [cm^2]
Kathode				
Anode 1				
Anode 2				

Temp_1 [°C]		Temp_2[°C]		Temp_3 [°C]	
I_1 [A]		I_2 [A]		I_3 [A]	
U [V]					
Startzeit			Endzeit		
			Dauer [min-]		
Netzteil					

VersuchNr.	84					
SOLL	30	min.	25	°C		A/dm^2
					1,5	A

	Nummer	Masse Start [g]	Masse Ende [g]	Fläche Kathode [cm^2]
Kathode	509	20,04	20,96	4,335 x 3,65
Anode 1	132	14,51	14,04	
Anode 2	106	17,86	17,41	

Temp_1 [°C]	28,7	Temp_2[°C]	30,5	Temp_3 [°C]	
I_1 [A]	1,517	I_2 [A]	1,473	I_3 [A]	1,475
U [V]	~~2,053~~ 1,934				
Startzeit			Endzeit		
			Dauer [min-]	30	
Netzteil	3				

VersuchNr.	85					
SOLL	30	min.	40	°C		A/dm^2
					1,5	A

	Nummer	Masse Start [g]	Masse Ende [g]	Fläche Kathode [cm^2]
Kathode	A5-2	18,53	19,47	4,625 x 3,58
Anode 1	105	17,18	16,73	
Anode 2	100	17,55	17,05	

Temp_1 [°C]	38,7	Temp_2[°C]	38,9	Temp_3 [°C]	
I_1 [A]	1,509	I_2 [A]	1,492	I_3 [A]	1,492
U [V]	1,637				
Startzeit			Endzeit		
			Dauer [min-]	30	
Netzteil	2				

VersuchNr.	86					
SOLL	30	min.	60	°C		A/dm^2
					1,5	A

	Nummer	Masse Start [g]	Masse Ende [g]	Fläche Kathode [cm^2]
Kathode	A21-2	17,12	18,02	4,62 x 3,60
Anode 1	102	12,20	11,73	
Anode 2	103	13,00	12,51	

Temp_1 [°C]	58,5	Temp_2[°C]		Temp_3 [°C]	
I_1 [A]	1,507	I_2 [A]	1,475	I_3 [A]	1,472
U [V]	1,457				
Startzeit			Endzeit		
			Dauer [min-]	30	
Netzteil	1				

VersuchNr.	87					
SOLL	30	min.	25	°C		A/dm^2
					0,10	A

	Nummer	Masse Start [g]	Masse Ende [g]	Fläche Kathode [cm^2]
Kathode	426	16,17	16,23	4,64 x 3,48
Anode 1	144	14,57	14,56	
Anode 2	147	14,65	14,69	

Temp_1 [°C]	28,9	Temp_2[°C]	28,8	Temp_3 [°C]	—
I_1 [A]	0,107	I_2 [A]	0,109	I_3 [A]	0,101
U [V]	0,174				
Startzeit	—	Endzeit	—		
		Dauer [min-]	30		
Netzteil	3				

VersuchNr.	88					
SOLL	30	min.	40	°C		A/dm^2
					0,10	A

	Nummer	Masse Start [g]	Masse Ende [g]	Fläche Kathode [cm^2]
Kathode	419	16,75	~~[illegible]~~ 16,81	4,565 x 3,55
Anode 1	143	15,38	15,35	
Anode 2	142	14,20	14,16	

Temp_1 [°C]	39,4	Temp_2[°C]	37,5	Temp_3 [°C]	37,9
I_1 [A]	0,108	I_2 [A]	0,108	I_3 [A]	~~0,101~~ 0,109
U [V]	0,148				
Startzeit	—	Endzeit	—		
		Dauer [min-]	30		
Netzteil	2				

VersuchNr.	89					
SOLL	30	min.	60	°C		A/dm^2
					0,1	A

	Nummer	Masse Start [g]	Masse Ende [g]	Fläche Kathode [cm^2]
Kathode	501	18,50	18,56	4,33 x 3,61
Anode 1	140	14,17	14,14	
Anode 2	101	14,23	14,19	

Temp_1 [°C]	58,9	Temp_2[°C]	57,2	Temp_3 [°C]	60,4
I_1 [A]	0,105	I_2 [A]	0,108	I_3 [A]	0,106
U [V]	0,125				
Startzeit		Endzeit			
		Dauer [min-]			
Netzteil	1				

VersuchNr.	90					
SOLL	30	min.	50	°C		A/dm^2
					0,10	A

	Nummer	Masse Start [g]	Masse Ende [g]	Fläche Kathode [cm^2]
Kathode	47	17,71	17,78	4,33 x 3,625
Anode 1	146	16,40	16,37	
Anode 2	145	13,08	13,05	

Temp_1 [°C]	49,0	Temp_2[°C]	48,9	Temp_3 [°C]	48,8
I_1 [A]	0,106	I_2 [A]	0,110	I_3 [A]	0,110
U [V]	0,131				
Startzeit			Endzeit		
			Dauer [min-]		
Netzteil	4				

VersuchNr.						
SOLL		min.		°C		A/dm^2
						A

	Nummer	Masse Start [g]	Masse Ende [g]	Fläche Kathode [cm^2]
Kathode				
Anode 1				
Anode 2				

Temp_1 [°C]		Temp_2[°C]		Temp_3 [°C]	
I_1 [A]		I_2 [A]		I_3 [A]	
U [V]					
Startzeit			Endzeit		
			Dauer [min-]		
Netzteil					

VersuchNr.						
SOLL		min.		°C		A/dm^2
						A

	Nummer	Masse Start [g]	Masse Ende [g]	Fläche Kathode [cm^2]
Kathode				
Anode 1				
Anode 2				

Temp_1 [°C]		Temp_2[°C]		Temp_3 [°C]	
I_1 [A]		I_2 [A]		I_3 [A]	
U [V]					
Startzeit			Endzeit		
			Dauer [min-]		
Netzteil					

VersuchNr.	91						
SOLL	30	min.	25	°C		A/dm^2	
					0,2	A	

	Nummer	Masse Start [g]	Masse Ende [g]	Fläche Kathode [cm^2]
Kathode	A7-2	18,37	18,48	4,37 × 3,7
Anode 1	A40-1	19,02	18,95	
Anode 2	A40-2	13,90	13,84	

Temp_1 [°C]	23,5	Temp_2[°C]	27,3	Temp_3 [°C]	24,4
I_1 [A]	0,201	I_2 [A]	0,201	I_3 [A]	0,201
U [V]	0,365				
Startzeit			Endzeit		
			Dauer [min-]	30	
Netzteil					

VersuchNr.	92						
SOLL	30	min.	40	°C		A/dm^2	
					0,2	A	

	Nummer	Masse Start [g]	Masse Ende [g]	Fläche Kathode [cm^2]
Kathode	46	17,22	17,35	3,54 × 4,3
Anode 1	A41-1	13,03	12,97	
Anode 2	A41-2	16,35	16,29	

Temp_1 [°C]	39,1	Temp_2[°C]	38,4	Temp_3 [°C]	38,4
I_1 [A]	0,210	I_2 [A]	0,210	I_3 [A]	0,210
U [V]	0,291				
Startzeit			Endzeit		
			Dauer [min-]	30	
Netzteil					

VersuchNr.	93						
SOLL	30	min.	60	°C		A/dm^2	
					0,2	A	

	Nummer	Masse Start [g]	Masse Ende [g]	Fläche Kathode [cm^2]
Kathode	45-1	15,86	15,99	3,63 × 4,26
Anode 1	A42-1	18,28	18,20	
Anode 2	A42-2	14,73	14,66	

Temp_1 [°C]	58,6	Temp_2[°C]	60,5	Temp_3 [°C]	59,9
I_1 [A]	0,208	I_2 [A]	0,206	I_3 [A]	0,205
U [V]	0,240				
Startzeit			Endzeit		
			Dauer [min-]	30	
Netzteil					

VersuchNr.	94					
SOLL	30	min.	50	°C		A/dm^2
					0,2	A

	Nummer	Masse Start [g]	Masse Ende [g]	Fläche Kathode [cm^2]
Kathode	45	17,27	17,38	3,53~4,28
Anode 1	A43-1	13,24	13,18	
Anode 2	A43-2	17,24	17,18	

Temp_1 [°C]	49,4	Temp_2[°C]	50,4	Temp_3 [°C]	50,1
I_1 [A]	0,205	I_2 [A]	0,203	I_3 [A]	0,205
U [V]	0,236				
Startzeit			Endzeit		
			Dauer [min-]	29,5	
Netzteil					

VersuchNr.						
SOLL		min.		°C		A/dm^2
						A

	Nummer	Masse Start [g]	Masse Ende [g]	Fläche Kathode [cm^2]
Kathode				
Anode 1				
Anode 2				

Temp_1 [°C]		Temp_2[°C]		Temp_3 [°C]	
I_1 [A]		I_2 [A]		I_3 [A]	
U [V]					
Startzeit			Endzeit		
			Dauer [min-]		
Netzteil					

VersuchNr.						
SOLL		min.		°C		A/dm^2
						A

	Nummer	Masse Start [g]	Masse Ende [g]	Fläche Kathode [cm^2]
Kathode				
Anode 1				
Anode 2				

Temp_1 [°C]		Temp_2[°C]		Temp_3 [°C]	
I_1 [A]		I_2 [A]		I_3 [A]	
U [V]					
Startzeit			Endzeit		
			Dauer [min-]		
Netzteil					

VersuchNr.	95					
SOLL	30	min.	25	°C		A/dm^2
					0,7	A

	Nummer	Masse Start [g]	Masse Ende [g]	Fläche Kathode [cm^2]
Kathode	47	17,77	18,20	4,31 × 3,56
Anode 1	47-1	17,91	17,68	
Anode 2	47-2	16,71	16,48	

Temp_1 [°C]	24,2	Temp_2[°C]	24,1	Temp_3 [°C]	
I_1 [A]	0,702	I_2 [A]	0,700	I_3 [A]	0,702
U [V]	1,048				
Startzeit			Endzeit		
			Dauer [min-]	30	
Netzteil					

VersuchNr.	96					
SOLL	30	min.	40	°C		A/dm^2
					0,7	A

	Nummer	Masse Start [g]	Masse Ende [g]	Fläche Kathode [cm^2]
Kathode	502	20,04	20,46	4,28 × 3,51
Anode 1	411	16,94	16,75	
Anode 2	412	17,80	17,58	

Temp_1 [°C]	38,4	Temp_2[°C]	38,6	Temp_3 [°C]	
I_1 [A]	0,699	I_2 [A]	0,697	I_3 [A]	0,696
U [V]	0,833				
Startzeit			Endzeit		
			Dauer [min-]	30	
Netzteil					

VersuchNr.	97					
SOLL	30	min.	60	°C		A/dm^2
					0,7	A

	Nummer	Masse Start [g]	Masse Ende [g]	Fläche Kathode [cm^2]
Kathode	501	18,56	18,98	3,55 × 4,28
Anode 1	4501-1	17,03	16,83	
Anode 2	4501-2	16,66	16,42	

Temp_1 [°C]	59,2	Temp_2[°C]	59,5	Temp_3 [°C]		
I_1 [A]	~~0,46~~	I_2 [A]	0,697	I_3 [A]	0,693	0,691
U [V]	0,710					
Startzeit			Endzeit			
			Dauer [min-]	30		
Netzteil						

VersuchNr.	98						
SOLL	30	min.	50	°C			A/dm^2
						0,7	A

	Nummer	Masse Start [g]	Masse Ende [g]	Fläche Kathode [cm^2]
Kathode	521	20,49	20,41	4,31 × 3,55
Anode 1	4521-1	17,40	17,16	
Anode 2	4521-2	~~21,88~~ 21,08	20,86	

Temp_1 [°C]	50,3	Temp_2[°C]	48,4	Temp_3 [°C]	
I_1 [A]	0,703	I_2 [A]	0,705	I_3 [A]	0,706
U [V]	0,742				
Startzeit			Endzeit		
			Dauer [min-]	30	
Netzteil					

VersuchNr.							
SOLL		min.		°C			A/dm^2
							A

	Nummer	Masse Start [g]	Masse Ende [g]	Fläche Kathode [cm^2]
Kathode				
Anode 1				
Anode 2				

Temp_1 [°C]		Temp_2[°C]		Temp_3 [°C]	
I_1 [A]		I_2 [A]		I_3 [A]	
U [V]					
Startzeit			Endzeit		
			Dauer [min-]		
Netzteil					

VersuchNr.							
SOLL		min.		°C			A/dm^2
							A

	Nummer	Masse Start [g]	Masse Ende [g]	Fläche Kathode [cm^2]
Kathode				
Anode 1				
Anode 2				

Temp_1 [°C]		Temp_2[°C]		Temp_3 [°C]	
I_1 [A]		I_2 [A]		I_3 [A]	
U [V]					
Startzeit			Endzeit		
			Dauer [min-]		
Netzteil					

VersuchNr.	99						
SOLL	20	min.	25	°C		A/dm^2	
					0,8	A	

	Nummer	Masse Start [g]	Masse Ende [g]	Fläche Kathode [cm^2]
Kathode	419	16,81	17,14	4,55 × 3,4
Anode 1	440-1	18,96	18,80	
Anode 2	442-2	14,66	14,50	

Temp_1 [°C]	26,0	Temp_2[°C]	25,3	Temp_3 [°C]	
I_1 [A]	0,815	I_2 [A]	0,823	I_3 [A]	0,819
U [V]	1,165				
Startzeit	–		Endzeit	–	
			Dauer [min-]	20	
Netzteil					

✓

VersuchNr.	100						
SOLL	20	min.	40	°C		A/dm^2	
					0,8	A	

	Nummer	Masse Start [g]	Masse Ende [g]	Fläche Kathode [cm^2]
Kathode	506	21,85	22,17	4,31 × 3,6
Anode 1	A1	~~1~~ 13,13	12,97	
Anode 2	A2	12,52	12,35	

Temp_1 [°C]	38,4	Temp_2[°C]	~~[illegible]~~ 38,5	Temp_3 [°C]	
I_1 [A]	0,792	I_2 [A]	0,792	I_3 [A]	0,789
U [V]	0,877				
Startzeit	–		Endzeit	–	
			Dauer [min-]	20	
Netzteil					

✓

VersuchNr.	101						
SOLL	20	min.	60	°C		A/dm^2	
					0,8	A	

	Nummer	Masse Start [g]	Masse Ende [g]	Fläche Kathode [cm^2]
Kathode	509	20,94	21,25	3,59 × 4,32
Anode 1	442-1	18,20	18,04	
Anode 2	443-2	17,18	~~16,9~~ 17,00	

Temp_1 [°C]	57,0	Temp_2[°C]	59,3	Temp_3 [°C]	
I_1 [A]	0,802	I_2 [A]	0,790	I_3 [A]	0,783
U [V]	0,713				
Startzeit	–		Endzeit	–	
			Dauer [min-]	20	
Netzteil	2				

✓

VersuchNr.	102						
SOLL	20	min.	50	°C		A/dm^2	
					0,8	A	

	Nummer	Masse Start [g]	Masse Ende [g]	Fläche Kathode [cm^2]
Kathode	426	16,23	16,56	3,46 × 4,62
Anode 1	A3-2	12,93	12,76	
Anode 2	A40-2	13,84	~~13,71~~ 13,67	

Temp_1 [°C]	50,0	Temp_2[°C]	50,1	Temp_3 [°C]	
I_1 [A]	0,811	I_2 [A]	0,818	I_3 [A]	0,819
U [V]	0,822				
Startzeit	–		Endzeit	–	
			Dauer [min-]	20	
Netzteil	4				

VersuchNr.	103						
SOLL	20	min.	25	°C		A/dm^2	
					0,4	A	

	Nummer	Masse Start [g]	Masse Ende [g]	Fläche Kathode [cm^2]
Kathode	A5-1	15,98	16,14	3,59 × 4,26
Anode 1	A41-1	12,97	12,88	
Anode 2	A41-2	12,50	12,42	

Temp_1 [°C]	25,6	Temp_2[°C]	25,6	Temp_3 [°C]	25,6
I_1 [A]	0,407	I_2 [A]	0,407	I_3 [A]	0,407
U [V]	0,632				
Startzeit			Endzeit		
			Dauer [min-]	20	
Netzteil	3				

VersuchNr.	104						
SOLL	20	min.	40	°C		A/dm^2	
					0,4	A	

	Nummer	Masse Start [g]	Masse Ende [g]	Fläche Kathode [cm^2]
Kathode	K6	17,34	17,51	3,54 × 4,31
Anode 1	A1	14,55	14,47	
Anode 2	A2	14,61	14,52	

Temp_1 [°C]	37,3	Temp_2[°C]	37,4	Temp_3 [°C]	
I_1 [A]	0,399	I_2 [A]	0,400	I_3 [A]	0,397
U [V]	0,493				
Startzeit			Endzeit		
			Dauer [min-]	20	
Netzteil	1				

VersuchNr.	105					
SOLL	20	min.	60	°C		A/dm^2
					0,4	A

	Nummer	Masse Start [g]	Masse Ende [g]	Fläche Kathode [cm^2]
Kathode	A 7-2	18,48	18,65	4,31 x 7,6
Anode 1	A 3	14,11	14,03	
Anode 2	A 4	15,33	15,25	

Temp_1 [°C]	59,4	Temp_2[°C]	59,6	Temp_3 [°C]	59,4
I_1 [A]	0,410	I_2 [A]	0,406	I_3 [A]	0,403
U [V]	0,360				
Startzeit			Endzeit		
			Dauer [min-]	20	
Netzteil	1				

✓

VersuchNr.	106					
SOLL	20	min.	50	°C		A/dm^2
						A

	Nummer	Masse Start [g]	Masse Ende [g]	Fläche Kathode [cm^2]
Kathode	K5	17,38	17,55	4,28 x 3,45
Anode 1	A5	14,16	14,07	
Anode 2	A6	14,18	14,08	

Temp_1 [°C]	50,0	Temp_2[°C]	50,7	Temp_3 [°C]	44,4
I_1 [A]	0,404	I_2 [A]	0,404	I_3 [A]	0,404
U [V]	0,434				
Startzeit			Endzeit		
			Dauer [min-]	20	
Netzteil	4				

✓

VersuchNr.						
SOLL		min.		°C		A/dm^2
						A

	Nummer	Masse Start [g]	Masse Ende [g]	Fläche Kathode [cm^2]
Kathode				
Anode 1				
Anode 2				

Temp_1 [°C]		Temp_2[°C]		Temp_3 [°C]	
I_1 [A]		I_2 [A]		I_3 [A]	
U [V]					
Startzeit			Endzeit		
			Dauer [min-]		
Netzteil					

VersuchNr.	107					
SOLL	40	min.	25	°C		A/dm^2
					0,25	A

	Nummer	Masse Start [g]	Masse Ende [g]	Fläche Kathode [cm^2]
Kathode	K26	16,57	16,77	3,48 × 4,62
Anode 1	A11	16,72	16,61	
Anode 2	A12	18,01	17,90	

Temp_1 [°C]	25,4	Temp_2[°C]	25,6	Temp_3 [°C]	26,0
I_1 [A]	0,253	I_2 [A]	0,253	I_3 [A]	0,255
U [V]	0,436				
Startzeit	–	Endzeit	–		
		Dauer [min-]	40		
Netzteil	3				

VersuchNr.	108					
SOLL	40	min.	40	°C		A/dm^2
					0,25	A

	Nummer	Masse Start [g]	Masse Ende [g]	Fläche Kathode [cm^2]
Kathode	506	22,17	22,37	4,35 × 3,6
Anode 1	A13	17,14	17,05	
Anode 2	A14	16,45	16,34	

Temp_1 [°C]	38,0	Temp_2[°C]	38,6	Temp_3 [°C]	36,9
I_1 [A]	0,253	I_2 [A]	0,251	I_3 [A]	0,257
U [V]	0,342				
Startzeit	–	Endzeit	–		
		Dauer [min-]	40		
Netzteil	2				

VersuchNr.	109					
SOLL	40	min.	60	°C		A/dm^2
					0,25	A

	Nummer	Masse Start [g]	Masse Ende [g]	Fläche Kathode [cm^2]
Kathode	509	21,25	21,44	3,6 × 4,34
Anode 1	A15	14,47	14,35	
Anode 2	A16	16,81	16,71	

Temp_1 [°C]	59,4	Temp_2[°C]	59,8	Temp_3 [°C]	59,2
I_1 [A]	0,253	I_2 [A]	0,256	I_3 [A]	0,255
U [V]	0,235				
Startzeit	–	Endzeit	–		
		Dauer [min-]	40		
Netzteil	1				

VersuchNr.	110					
SOLL	40	min.	50	°C		A/dm^2
					0,25	A

	Nummer	Masse Start [g]	Masse Ende [g]	Fläche Kathode [cm^2]
Kathode	419	17,13	17,33	~~[illegible]~~ 4,6 × 3,4
Anode 1	417	16,38	16,29	
Anode 2	418	12,93	12,84	

Temp_1 [°C]	50,5	Temp_2[°C]	49,6	Temp_3 [°C]	49,7
I_1 [A]	0,248	I_2 [A]	0,253	I_3 [A]	0,252
U [V]	0,282				
Startzeit	–		Endzeit	–	
			Dauer [min-]	40	
Netzteil	4				

VersuchNr.						
SOLL		min.		°C		A/dm^2
						A

	Nummer	Masse Start [g]	Masse Ende [g]	Fläche Kathode [cm^2]
Kathode				
Anode 1				
Anode 2				

Temp_1 [°C]		Temp_2[°C]		Temp_3 [°C]	
I_1 [A]		I_2 [A]		I_3 [A]	
U [V]					
Startzeit			Endzeit		
			Dauer [min-]		
Netzteil					

VersuchNr.						
SOLL		min.		°C		A/dm^2
						A

	Nummer	Masse Start [g]	Masse Ende [g]	Fläche Kathode [cm^2]
Kathode				
Anode 1				
Anode 2				

Temp_1 [°C]		Temp_2[°C]		Temp_3 [°C]	
I_1 [A]		I_2 [A]		I_3 [A]	
U [V]					
Startzeit			Endzeit		
			Dauer [min-]		
Netzteil					

VersuchNr.	111						
SOLL	~~40~~ 45	min.	20	°C		A/dm^2	
					0,55	A	

	Nummer	Masse Start [g]	Masse Ende [g]	Fläche Kathode [cm^2]
Kathode	41	16,61	17,12	7,51 × 4,28
Anode 1	A1	16,27	16,03	
Anode 2	A2	11,69	11,46	

Temp_1 [°C]	23,5	Temp_2[°C]	23,3	Temp_3 [°C]	23,3
I_1 [A]	0,557	I_2 [A]	0,559	I_3 [A]	0,536
U [V]	0,903				
Startzeit			Endzeit		
			Dauer [min-]	45	
Netzteil	3				

✓

VersuchNr.	112					
SOLL	45	min.	40	°C		A/dm^2
					0,55	A

	Nummer	Masse Start [g]	Masse Ende [g]	Fläche Kathode [cm^2]
Kathode	42	19,26	19,76	4,55 × 3,55
Anode 1	A3	17,66	17,43	
Anode 2	A4	17,55	17,30	

Temp_1 [°C]	37,5	Temp_2[°C]	38,4	Temp_3 [°C]	
I_1 [A]	0,553	I_2 [A]	0,547	I_3 [A]	0,542
U [V]	0,651				
Startzeit			Endzeit		
			Dauer [min-]	45	
Netzteil	2				

✓

VersuchNr.	113					
SOLL	45	min.	60	°C		A/dm^2
					0,55	A

	Nummer	Masse Start [g]	Masse Ende [g]	Fläche Kathode [cm^2]
Kathode	43	19,82	20,33	3,55 × 4,28
Anode 1	A5	20,84	20,57	
Anode 2	A6	15,23	14,99	

Temp_1 [°C]	56,7	Temp_2[°C]	61,6	Temp_3 [°C]	60,6
I_1 [A]	0,554	I_2 [A]	0,549	I_3 [A]	0,547
U [V]	0,477				
Startzeit			Endzeit		
			Dauer [min-]	45	
Netzteil	1				

✓

VersuchNr.	114					
SOLL	45	min.	50	°C		A/dm^2
					0,55	A

	Nummer	Masse Start [g]	Masse Ende [g]	Fläche Kathode [cm^2]
Kathode	A5-2	17,45	19,98	4,62 ×3,52
Anode 1	A7	16,97	16,71	
Anode 2	A8	18,97	18,71	

Temp_1 [°C]	50,9	Temp_2[°C]	49,9	Temp_3 [°C]	48,8
I_1 [A]	0,552	I_2 [A]	0,558	I_3 [A]	0,553
U [V]	0,597				
Startzeit			Endzeit		
			Dauer [min-]	45	
Netzteil	4				

VersuchNr.						
SOLL		min.		°C		A/dm^2
						A

	Nummer	Masse Start [g]	Masse Ende [g]	Fläche Kathode [cm^2]
Kathode				
Anode 1				
Anode 2				

Temp_1 [°C]		Temp_2[°C]		Temp_3 [°C]	
I_1 [A]		I_2 [A]		I_3 [A]	
U [V]					
Startzeit			Endzeit		
			Dauer [min-]		
Netzteil					

VersuchNr.						
SOLL		min.		°C		A/dm^2
						A

	Nummer	Masse Start [g]	Masse Ende [g]	Fläche Kathode [cm^2]
Kathode				
Anode 1				
Anode 2				

Temp_1 [°C]		Temp_2[°C]		Temp_3 [°C]	
I_1 [A]		I_2 [A]		I_3 [A]	
U [V]					
Startzeit			Endzeit		
			Dauer [min-]		
Netzteil					

VersuchNr.	115						
SOLL	15	min.	25	°C		A/dm^2	
					1,0	A	

	Nummer	Masse Start [g]	Masse Ende [g]	Fläche Kathode [cm^2]
Kathode	K5	16,66	16,94	3,48 × 4,25
Anode 1	5-1	17,03	16,88	
Anode 2	5-2	14,33	14,20	

Temp_1 [°C]	27,5	Temp_2[°C]	24,0	Temp_3 [°C]	
I_1 [A]	0,993	I_2 [A]	0,973	I_3 [A]	
U [V]	1,437				
Startzeit			Endzeit		
			Dauer [min-]	15	
Netzteil	3				

✓

VersuchNr.	116						
SOLL	15	min.	40	°C		A/dm^2	
					1,0	A	

	Nummer	Masse Start [g]	Masse Ende [g]	Fläche Kathode [cm^2]
Kathode	46	16,66	16,96	3,55 × 4,6
Anode 1	61	16,08	15,93	
Anode 2	62	14,50	14,35	

Temp_1 [°C]	37,5	Temp_2[°C]	38,5	Temp_3 [°C]	
I_1 [A]	1,000	I_2 [A]	0,945	I_3 [A]	
U [V]	0,897				
Startzeit			Endzeit		
			Dauer [min-]	16	
Netzteil	2				

✓

VersuchNr.	117						
SOLL	15	min.	60	°C		A/dm^2	
					1,0	A	

	Nummer	Masse Start [g]	Masse Ende [g]	Fläche Kathode [cm^2]
Kathode	47	16,96	17,25	3,5 × 4,2
Anode 1	71	18,77	18,60	
Anode 2	72	17,89	17,75	

Temp_1 [°C]	60,2	Temp_2[°C]	60,5	Temp_3 [°C]	58,0
I_1 [A]	0,996	I_2 [A]	0,987	I_3 [A]	
U [V]	1,103				
Startzeit			Endzeit		
			Dauer [min-]	14,5	
Netzteil	1				

✓

VersuchNr.	118						
SOLL	15	min.	50	°C		A/dm^2
					1,0	A

	Nummer	Masse Start [g]	Masse Ende [g]	Fläche Kathode [cm^2]
Kathode	48	17,05	17,36	3,45 × 4,3
Anode 1	81	18,55	18,38	
Anode 2	82	12,82	12,67	

Temp_1 [°C]	47,8	Temp_2[°C]		Temp_3 [°C]	
I_1 [A]	0,995	I_2 [A]	0,996	I_3 [A]	
U [V]	0,940				
Startzeit			Endzeit		
			Dauer [min-]	15	
Netzteil	4				

VersuchNr.						
SOLL		min.		°C		A/dm^2
						A

	Nummer	Masse Start [g]	Masse Ende [g]	Fläche Kathode [cm^2]
Kathode				
Anode 1				
Anode 2				

Temp_1 [°C]		Temp_2[°C]		Temp_3 [°C]	
I_1 [A]		I_2 [A]		I_3 [A]	
U [V]					
Startzeit			Endzeit		
			Dauer [min-]		
Netzteil					

VersuchNr.						
SOLL		min.		°C		A/dm^2
						A

	Nummer	Masse Start [g]	Masse Ende [g]	Fläche Kathode [cm^2]
Kathode				
Anode 1				
Anode 2				

Temp_1 [°C]		Temp_2[°C]		Temp_3 [°C]	
I_1 [A]		I_2 [A]		I_3 [A]	
U [V]					
Startzeit			Endzeit		
			Dauer [min-]		
Netzteil					

VersuchNr.	119					
SOLL	60	min.	25	°C		A/dm^2
					0,35	A

	Nummer	Masse Start [g]	Masse Ende [g]	Fläche Kathode [cm^2]
Kathode	509	21,45	21,86	4,55 × 3,7
Anode 1	A1	14,01	13,81	
Anode 2	A2	12,40	12,18	

Temp_1 [°C]	24,2	Temp_2[°C]	24,9	Temp_3 [°C]	
I_1 [A]	0,350	I_2 [A]	0,354	I_3 [A]	0,352
U [V]	0,555				
Startzeit			Endzeit		
			Dauer [min-]	60	
Netzteil	3				

✓

VersuchNr.	120					
SOLL	60	min.	40	°C		A/dm^2
					0,35	A

	Nummer	Masse Start [g]	Masse Ende [g]	Fläche Kathode [cm^2]
Kathode	506	22,37	22,78	3,65 × 4,3
Anode 1	A3	12,35	12,14	
Anode 2	A4	13,17	12,94	

Temp_1 [°C]	37,5	Temp_2[°C]	40,6	Temp_3 [°C]	
I_1 [A]	0,350	I_2 [A]	0,350	I_3 [A]	0,348
U [V]	0,472				
Startzeit			Endzeit		
			Dauer [min-]	57	
Netzteil	2				

✓

VersuchNr.	121					
SOLL	60	min.	60	°C		A/dm^2
					0,35	A

	Nummer	Masse Start [g]	Masse Ende [g]	Fläche Kathode [cm^2]
Kathode	426	16,77	17,17	3,45 × 4,65
Anode 1	A5	14,08	13,88	
Anode 2	A6	12,72	12,51	

Temp_1 [°C]	57,3	Temp_2[°C]	58,8	Temp_3 [°C]	
I_1 [A]	0,351	I_2 [A]	0,345	I_3 [A]	0,346
U [V]	0,337				
Startzeit			Endzeit		
			Dauer [min-]	58	
Netzteil	1				

✓

VersuchNr.	122					
SOLL	60	min.	50	°C		A/dm^2
					0,35	A

	Nummer	Masse Start [g]	Masse Ende [g]	Fläche Kathode [cm^2]
Kathode	K19	17,33	17,74	4,55 ~ 3,45
Anode 1	A7	14,45	14,25	
Anode 2	A8	12,86	12,65	

Temp_1 [°C]	49,8	Temp_2[°C]	48,6	Temp_3 [°C]	
I_1 [A]	0,352	I_2 [A]	0,357	I_3 [A]	0,351
U [V]	0,379				
Startzeit			Endzeit		
			Dauer [min-]	57	
Netzteil	4				

VersuchNr.						
SOLL		min.		°C		A/dm^2
						A

	Nummer	Masse Start [g]	Masse Ende [g]	Fläche Kathode [cm^2]
Kathode				
Anode 1				
Anode 2				

Temp_1 [°C]		Temp_2[°C]		Temp_3 [°C]	
I_1 [A]		I_2 [A]		I_3 [A]	
U [V]					
Startzeit			Endzeit		
			Dauer [min-]		
Netzteil					

VersuchNr.						
SOLL		min.		°C		A/dm^2
						A

	Nummer	Masse Start [g]	Masse Ende [g]	Fläche Kathode [cm^2]
Kathode				
Anode 1				
Anode 2				

Temp_1 [°C]		Temp_2[°C]		Temp_3 [°C]	
I_1 [A]		I_2 [A]		I_3 [A]	
U [V]					
Startzeit			Endzeit		
			Dauer [min-]		
Netzteil					

VersuchNr.	123					
SOLL	25	min.	25	°C		A/dm^2
					0,55	A

	Nummer	Masse Start [g]	Masse Ende [g]	Fläche Kathode [cm^2]
Kathode	509	21,86	22,14	4,55 × 3,8
Anode 1	A1	20,12	19,98	
Anode 2	A2	17,36	17,24	

Temp_1 [°C]	24,7	Temp_2[°C]	24,7	Temp_3 [°C]	
I_1 [A]	0,556	I_2 [A]	0,553	I_3 [A]	0,557
U [V]	0,818				
Startzeit			Endzeit		
			Dauer [min-]	25	
Netzteil	3				

VersuchNr.	124					
SOLL	25	min.	40	°C		A/dm^2
					0,55	A

	Nummer	Masse Start [g]	Masse Ende [g]	Fläche Kathode [cm^2]
Kathode	506	22,78	23,05	3,6 × 4,3
Anode 1	A3	17,21	17,65	
Anode 2	A4	19,30	19,69	

Temp_1 [°C]	37,8	Temp_2[°C]		Temp_3 [°C]	
I_1 [A]	0,548	I_2 [A]	0,551	I_3 [A]	0,550
U [V]	0,635				
Startzeit			Endzeit		
			Dauer [min-]	25	
Netzteil	2				

VersuchNr.	125					
SOLL	25	min.	60	°C		A/dm^2
					0,55	A

	Nummer	Masse Start [g]	Masse Ende [g]	Fläche Kathode [cm^2]
Kathode	426	17,16	17,44	3,45 × 4,7
Anode 1	A5	18,41	18,26	
Anode 2	A6	17,72	17,57	

Temp_1 [°C]	~~0,37~~ 37,8	Temp_2[°C]	56,6	Temp_3 [°C]	56,8	62,0
I_1 [A]	0,557	I_2 [A]	0,551	I_3 [A]	0,545	
U [V]	0,477					
Startzeit			Endzeit			
			Dauer [min-]	25		
Netzteil	1					

VersuchNr.	126					
SOLL	25	min.	~~60~~ 50	°C		A/dm^2
					0,55	A

	Nummer	Masse Start [g]	Masse Ende [g]	Fläche Kathode [cm^2]
Kathode	419	17,73	18,01	4,55×3,75
Anode 1	A7	16,87	16,74	
Anode 2	A8	19,57	19,42	

Temp_1 [°C]	50,3	Temp_2[°C]	48,7	Temp_3 [°C]	
I_1 [A]	0,553	I_2 [A]	0,556	I_3 [A]	0,558
U [V]	0,573				
Startzeit		Endzeit			
		Dauer [min-]	25		
Netzteil	14				

✓

VersuchNr.	127					
SOLL	20	min.	40	°C		A/dm^2
					0,2	A

	Nummer	Masse Start [g]	Masse Ende [g]	Fläche Kathode [cm^2]
Kathode	410	16,79	16,87	3,5 × 4,25
Anode 1	A11	14,06	14,01	
Anode 2	A12	13,64	13,59	

Temp_1 [°C]	37,8	Temp_2[°C]	37,8	Temp_3 [°C]	37,5
I_1 [A]	0,205	I_2 [A]	0,206	I_3 [A]	0,208
U [V]	0,289				
Startzeit		Endzeit			
		Dauer [min-]	21		
Netzteil	2				

✓

VersuchNr.	128					
SOLL	20	min.	25	°C		A/dm^2
					0,2	A

	Nummer	Masse Start [g]	Masse Ende [g]	Fläche Kathode [cm^2]
Kathode	411	16,98	17,06	3,55 × 4,3
Anode 1	A13	15,46	15,41	
Anode 2	A14	17,01	16,96	

Temp_1 [°C]	25,8	Temp_2[°C]	25,5	Temp_3 [°C]	
I_1 [A]	0,206	I_2 [A]	0,203	I_3 [A]	0,203
U [V]	0,355				
Startzeit		Endzeit			
		Dauer [min-]	22		
Netzteil	3				

✓

VersuchNr.	129						
SOLL	20	min.	60	°C		A/dm^2	
					0,2	A	

	Nummer	Masse Start [g]	Masse Ende [g]	Fläche Kathode [cm^2]
Kathode	K12	16,77	16,84	3,5 × 4,3
Anode 1	A15	21,71	21,66	
Anode 2	A16	17,29	17,25	

Temp_1 [°C]	64,7	Temp_2[°C]	65	Temp_3 [°C]	
I_1 [A]	0,206	I_2 [A]	0,206	I_3 [A]	0,206
U [V]	~~0,250~~	0,187V			
Startzeit			Endzeit		
			Dauer [min-]	18,5	
Netzteil	1				

✓

VersuchNr.	130						
SOLL	20	min.	50	°C		A/dm^2	
					0,2	A	

	Nummer	Masse Start [g]	Masse Ende [g]	Fläche Kathode [cm^2]
Kathode	K13	15,83	15,94	3,45 × 4,3
Anode 1	A17	17,05	16,98	
Anode 2	A18	17,41	17,36	

Temp_1 [°C]	49,2	Temp_2[°C]	50,1	Temp_3 [°C]	48,4
I_1 [A]	0,204	I_2 [A]	0,207	I_3 [A]	0,208
U [V]	0,250				
Startzeit			Endzeit		
			Dauer [min-]	24,5	
Netzteil	4				

✓

VersuchNr.	131						
SOLL	25	min.	25	°C		A/dm^2	
					1,15	A	

	Nummer	Masse Start [g]	Masse Ende [g]	Fläche Kathode [cm^2]
Kathode	K2	19,74	20,35	3,55 × 4,65
Anode 1	A20	14,97	14,67	
Anode 2	A21	12,64	~~12,58~~	12,38

Temp_1 [°C]	25,9	Temp_2[°C]	26,3	Temp_3 [°C]	27,4
I_1 [A]	1,155	I_2 [A]	1,155	I_3 [A]	1,149
U [V]	1,524				
Startzeit			Endzeit		
			Dauer [min-]	25,5	
Netzteil	3				

✓

VersuchNr.	132				
SOLL	25	min.	40	°C	A/dm^2
				1,15	A

	Nummer	Masse Start [g]	Masse Ende [g]	Fläche Kathode [cm^2]
Kathode	41	17,11	17,70	3,6 × 4,3
Anode 1	A22	14,23	13,94	
Anode 2	A23	12,66	12,35	

Temp_1 [°C]	38,4	Temp_2[°C]	38,3	Temp_3 [°C]	38,8
I_1 [A]	1,149	I_2 [A]	1,136	I_3 [A]	1,132
U [V]	1,375				
Startzeit		Endzeit			
		Dauer [min-]	26		
Netzteil	2				

VersuchNr.	133				
SOLL	25	min.	60	°C	A/dm^2
				1,15	A

	Nummer	Masse Start [g]	Masse Ende [g]	Fläche Kathode [cm^2]
Kathode	45	16,94	17,54	3,55 × 4,3
Anode 1	A24	18,69	18,36	
Anode 2	A25	18,58	18,29	

Temp_1 [°C]	59,2	Temp_2[°C]	58,1	Temp_3 [°C]	56,7
I_1 [A]	1,153	I_2 [A]	1,159	I_3 [A]	1,157
U [V]	0,987				
Startzeit		Endzeit			
		Dauer [min-]	25,5		
Netzteil	1				

VersuchNr.	134				
SOLL	25	min.	50	°C	A/dm^2
				1,15	A

	Nummer	Masse Start [g]	Masse Ende [g]	Fläche Kathode [cm^2]
Kathode	46	16,94	17,54	3,55 × 4,6
Anode 1	A26	16,70	16,42	
Anode 2	A27	18,37	18,02	

Temp_1 [°C]	47,5	Temp_2[°C]	48,5	Temp_3 [°C]	49,7
I_1 [A]	1,154	I_2 [A]	1,150	I_3 [A]	1,152
U [V]	1,165				
Startzeit		Endzeit			
		Dauer [min-]	25		
Netzteil	4				

VersuchNr.	135					
SOLL	70	min.	25	°C		A/dm^2
					0,25	A

	Nummer	Masse Start [g]	Masse Ende [g]	Fläche Kathode [cm^2]
Kathode	K11	17,05	17,45	4,305 x 3,555
Anode 1	A25	18,27	18,06	
Anode 2	A23	12,33	12,16	

Temp_1 [°C]	26,7	Temp_2[°C]	26,6	Temp_3 [°C]	26,3
I_1 [A]	0,247	I_2 [A]	0,241	I_3 [A]	0,242
U [V]	0,375				
Startzeit			Endzeit		
			Dauer [min-]	70	
Netzteil	3				

VersuchNr.	136					
SOLL	70	min.	35	°C		A/dm^2
					0,25	A

	Nummer	Masse Start [g]	Masse Ende [g]	Fläche Kathode [cm^2]
Kathode	K12	16,83	17,23	4,31 x 3,49
Anode 1	200	13,92	13,72	
Anode 2	A20	14,65	14,46	

Temp_1 [°C]	36,2	Temp_2[°C]	34,0	Temp_3 [°C]	33,8
I_1 [A]	0,250	I_2 [A]	0,246	I_3 [A]	0,245
U [V]	0,368				
Startzeit			Endzeit		
			Dauer [min-]	70	
Netzteil	1				

Abkühlungsphase des Wasserbads

VersuchNr.	137					
SOLL	70	min.	55	°C		A/dm^2
					0,25	A

	Nummer	Masse Start [g]	Masse Ende [g]	Fläche Kathode [cm^2]
Kathode	K10	16,87	17,28	4,335 x 3,165
Anode 1	A17	16,92	16,70	
Anode 2	A24	18,35	18,14	

Temp_1 [°C]	50,8	Temp_2[°C]	55	Temp_3 [°C]	55,1
I_1 [A]	0,250	I_2 [A]	0,258	I_3 [A]	0,258
U [V]	0,260				
Startzeit			Endzeit		
			Dauer [min-]	70	
Netzteil	2				

Aufheizphase

VersuchNr.	138						
SOLL	70	min.	45	°C		A/dm^2	
					0,25	A	

	Nummer	Masse Start [g]	Masse Ende [g]	Fläche Kathode [cm^2]
Kathode	V 13	[illegible]	16,34	4,285 x 3,45
Anode 1	A 27	18,09	17,77	
Anode 2	A 4	19,69	19,44	

Temp_1 [°C]	42,8	Temp_2[°C]	44,0	Temp_3 [°C]	45,1
I_1 [A]	0,249	I_2 [A]	0,247	I_3 [A]	0,248
U [V]	0,279				
Startzeit			Endzeit		
			Dauer [min-]	70	
Netzteil	4				

✓

VersuchNr.	139					
SOLL	20	min.	25	°C		A/dm^2
					1,5	A

	Nummer	Masse Start [g]	Masse Ende [g]	Fläche Kathode [cm^2]
Kathode	201	17,24	17,82	4,245 x 3,495
Anode 1	A21	12,32	12,02	
Anode 2	5-1	16,86	16,58	

Temp_1 [°C]	26,6	Temp_2[°C]	28,2	Temp_3 [°C]	28,2
I_1 [A]	1,497	I_2 [A]		I_3 [A]	1,395
U [V]	1,872				
Startzeit	/		Endzeit	/	
			Dauer [min-]	20	
Netzteil	1				

✓

VersuchNr.	140					
SOLL	20	min.	35	°C		A/dm^2
					1,5	A

	Nummer	Masse Start [g]	Masse Ende [g]	Fläche Kathode [cm^2]
Kathode	V 6	17,53	18,19	4,62 x 3,54
Anode 1	A 16	17,24	16,96	
Anode 2	A 7	16,73	16,41	

Temp_1 [°C]	33,8	Temp_2[°C]		Temp_3 [°C]	34,7
I_1 [A]	1,500	I_2 [A]		I_3 [A]	1,620
U [V]	1,844				
Startzeit			Endzeit	/	
			Dauer [min-]	20	
Netzteil	2				

✓

VersuchNr.	141					
SOLL	20	min.	55	°C		A/dm^2
					1,5	A

	Nummer	Masse Start [g]	Masse Ende [g]	Fläche Kathode [cm^2]
Kathode	K5	17,53	18,32	4,315 x 3,5175
Anode 1	A18	17,34	16,97	
Anode 2	A6	17,57	17,14	

Temp_1 [°C]	53,8	Temp_2[°C]	54,2	Temp_3 [°C]	55,1
I_1 [A]	1,500	I_2 [A]	1,890	I_3 [A]	1,891
U [V]	1,264				
Startzeit		Endzeit			
		Dauer [min-]	20		
Netzteil	1				

VersuchNr.	142					
SOLL	20	min.	45	°C		A/dm^2
					1,5	A

	Nummer	Masse Start [g]	Masse Ende [g]	Fläche Kathode [cm^2]
Kathode	K26	17,43	18,03	4,68 x 3,50
Anode 1	A1	14,97	14,61	
Anode 2	A15	21,63	21,35	

Temp_1 [°C]	45,1	Temp_2[°C]	44,8	Temp_3 [°C]	44,0
I_1 [A]	1,504	I_2 [A]	1,458	I_3 [A]	1,461
U [V]	1,315				
Startzeit	✓	Endzeit	✓		
		Dauer [min-]	20		
Netzteil	4				

VersuchNr.	143					
SOLL	60	min.	25	°C		A/dm^2
					0,7	A

	Nummer	Masse Start [g]	Masse Ende [g]	Fläche Kathode [cm^2]
Kathode	A5	18,77	19,59	4,265 x 3,565
Anode 1	A13	15,39	14,99	
Anode 2	A3	17,63	17,22	

Temp_1 [°C]	27,4	Temp_2[°C]	27,4	Temp_3 [°C]	27,3
I_1 [A]	0,708	I_2 [A]	0,673	I_3 [A]	0,672
U [V]	0,904				
Startzeit	✓	Endzeit	✓		
		Dauer [min-]	60		
Netzteil	3				

VersuchNr.	144						
SOLL	60	min.	35	°C		A/dm^2	
					0,7	A	

	Nummer	Masse Start [g]	Masse Ende [g]	Fläche Kathode [cm^2]
Kathode	202	20,33	21,16	4,65 x 3,485
Anode 1	2	17,22	16,80	
Anode 2	98	19,39	18,97	

Temp_1 [°C]	32,4	Temp_2[°C]	34,9	Temp_3 [°C]	34,8
I_1 [A]	0,699	I_2 [A]	0,685	I_3 [A]	0,685
U [V]	0,840				
Startzeit	/	Endzeit	/		
		Dauer [min-]	60		
Netzteil	1				

VersuchNr.	145						
SOLL	60	min.	55	°C		A/dm^2	
					0,7	A	

	Nummer	Masse Start [g]	Masse Ende [g]	Fläche Kathode [cm^2]
Kathode	203	17,34	18,20	4,325 x 3,48
Anode 1	208	13,58	13,16	
Anode 2	207	18,6[illegible]3	18,17	

Temp_1 [°C]	55,4	Temp_2[°C]	55,1	Temp_3 [°C]	55,5
I_1 [A]	0,704	I_2 [A]	0,692	I_3 [A]	0,691
U [V]	0,595				
Startzeit	/	Endzeit	/		
		Dauer [min-]	60		
Netzteil	2				

VersuchNr.	146						
SOLL	60	min.	45	°C		A/dm^2	
					0,7	A	

	Nummer	Masse Start [g]	Masse Ende [g]	Fläche Kathode [cm^2]
Kathode	4 19	18,01	18,86	4,59 x 3,475
Anode 1	206	14,00	13,61	
Anode 2	205	16,94	16,49	

Temp_1 [°C]	45,4	Temp_2[°C]	44,8	Temp_3 [°C]	45,2
I_1 [A]	0,697	I_2 [A]	0,690	I_3 [A]	0,640
U [V]	0,655				
Startzeit	/	Endzeit	/		
		Dauer [min-]	60		
Netzteil	4				

VersuchNr.	147						
SOLL	40	min.	25	°C			A/dm^2
						0,1	A

	Nummer	Masse Start [g]	Masse Ende [g]	Fläche Kathode [cm^2]
Kathode	207	18,62	18,82	4,245 x 3,57
Anode 1	A26	16,40	16,30	
Anode 2	211	19,42	19,33	

Temp_1 [°C]	24,3	Temp_2[°C]	25,1	Temp_3 [°C]	25,5
I_1 [A]	0,105	I_2 [A]	0,105	I_3 [A]	0,106
U [V]	0,204				
Startzeit	/	Endzeit	–		
		Dauer [min-]	40		
Netzteil	3				

VersuchNr.	148						
SOLL	40	min.	35	°C			A/dm^2
						0,1	A

	Nummer	Masse Start [g]	Masse Ende [g]	Fläche Kathode [cm^2]
Kathode	A13	15,34	15,53	4,265 x 3,54
Anode 1	A2	16,79	16,69	
Anode 2	A8	18,97	18,88	

Temp_1 [°C]	34,6	Temp_2[°C]	34,4	Temp_3 [°C]	34,2
I_1 [A]	0,101	I_2 [A]	0,103	I_3 [A]	0,108
U [V]	0,169				
Startzeit	/	Endzeit	–		
		Dauer [min-]	40		
Netzteil	2				

VersuchNr.	149						
SOLL	40	min.	55	°C			A/dm^2
						0,1	A

	Nummer	Masse Start [g]	Masse Ende [g]	Fläche Kathode [cm^2]
Kathode	A3	17,58	17,88	4,28 x 3,535
Anode 1	205	16,46	16,27	
Anode 2	206	13,62	13,4[illegible]	

Temp_1 [°C]	54,8	Temp_2[°C]	55,4	Temp_3 [°C]	55,1
I_1 [A]	0,100	I_2 [A]	0,172	I_3 [A]	0,171
U [V]	0,104				
Startzeit	–	Endzeit	/		
		Dauer [min-]	40		
Netzteil	7				

VersuchNr.	150						
SOLL	90	min.	45	°C			A/dm^2
						0,1	A

	Nummer	Masse Start [g]	Masse Ende [g]	Fläche Kathode [cm^2]
Kathode	210	22,97	23,15	4,27 x3,525
Anode 1	208	13,16	13,06	
Anode 2	509	21,62	21,51	

Temp_1 [°C]	46,8	Temp_2[°C]	45,3	Temp_3 [°C]	46
I_1 [A]	0,103	I_2 [A]	0,104	I_3 [A]	0,106
U [V]	0,154				
Startzeit		Endzeit			
		Dauer [min-]	40		
Netzteil	4				

VersuchNr.	151						
SOLL	15	min.	25	°C			A/dm^2
						1,2	A

	Nummer	Masse Start [g]	Masse Ende [g]	Fläche Kathode [cm^2]
Kathode	412	17,22	17,58	4,34x3,50
Anode 1	200	13,71	13,52	
Anode 2	A21	12,01	11,84	

Temp_1 [°C]	25,8	Temp_2[°C]	28,6	Temp_3 [°C]	27,1
I_1 [A]	1,204	I_2 [A]	1,192	I_3 [A]	1,184
U [V]	1,560				
Startzeit		Endzeit			
		Dauer [min-]	15		
Netzteil	3				

VersuchNr.	152						
SOLL	15	min.	35	°C			A/dm^2
						1,2	A

	Nummer	Masse Start [g]	Masse Ende [g]	Fläche Kathode [cm^2]
Kathode	411	17,44	17,80	4,3425 x 3,565
Anode 1	A17	16,67	16,50	
Anode 2	A4	19,48	19,29	

Temp_1 [°C]	35,2	Temp_2[°C]	34,9	Temp_3 [°C]	35,5
I_1 [A]	1,200	I_2 [A]	1,175	I_3 [A]	1,170
U [V]	1,548				
Startzeit		Endzeit			
		Dauer [min-]	15		
Netzteil	2				

VersuchNr.	153					
SOLL	15	min.	55	°C		A/dm^2
					1,2	A

	Nummer	Masse Start [g]	Masse Ende [g]	Fläche Kathode [cm^2]
Kathode	U10	17,27	17,64	4,355 x 3,16
Anode 1	A7	16,40	16,22	
Anode 2	5-1	16,57	16,37	

Temp_1 [°C]	55,8	Temp_2[°C]	55,2	Temp_3 [°C]	55,5
I_1 [A]	1,200	I_2 [A]	1,182	I_3 [A]	1,170
U [V]	0,953				
Startzeit		Endzeit			
		Dauer [min-]	15		
Netzteil	1				

VersuchNr.	154					
SOLL	15	min.	45	°C		A/dm^2
					1,2	A

	Nummer	Masse Start [g]	Masse Ende [g]	Fläche Kathode [cm^2]
Kathode	U13	16,33	16,69	4,38 x 3,455
Anode 1	A27	17,75	17,55	
Anode 2	A24	18,13	17,95	

Temp_1 [°C]	47,8	Temp_2[°C]	45,9	Temp_3 [°C]	44,8
I_1 [A]	1,130	I_2 [A]	1,176	I_3 [A]	1,179
U [V]	1,073				
Startzeit		Endzeit			
		Dauer [min-]	15		
Netzteil	4				

VersuchNr.	155					
SOLL	80	min.	25	°C		A/dm^2
					0,7	A

	Nummer	Masse Start [g]	Masse Ende [g]	Fläche Kathode [cm^2]
Kathode	207	18,80	19,92	4,26 x 3,575
Anode 1	222	12,92	12,36	
Anode 2	221	13,43	12,87	

Temp_1 [°C]	26,6	Temp_2[°C]	27	Temp_3 [°C]	27,4
I_1 [A]	0,700	I_2 [A]	0,694	I_3 [A]	0,691
U [V]	0,951				
Startzeit	-	Endzeit	-		
		Dauer [min-]	80		
Netzteil	3				

VersuchNr.	15 6						
SOLL	80	min.	35	°C		A/dm^2	
					0,7	A	
	Nummer	Masse Start [g]	Masse Ende [g]	Fläche Kathode [cm^2]			
Kathode	210	23,15	24,25	4,275 x 3,51			
Anode 1	220	14,24	13,62				
Anode 2	61	15,90	15,41				
Temp_1 [°C]	33,5	Temp_2[°C]	34,3	Temp_3 [°C]	34,2		
I_1 [A]	0,700	I_2 [A]	0,682	I_3 [A]	0,682		
U [V]	0,801						
Startzeit	✓		Endzeit	✓			
			Dauer [min-]	80			
Netzteil	2						

✓

VersuchNr.	15 7						
SOLL	80	min.	55	°C		A/dm^2	
					0,7	A	
	Nummer	Masse Start [g]	Masse Ende [g]	Fläche Kathode [cm^2]			
Kathode	201	17,80	18,94	4,25 x 3,505			
Anode 1	A 2	12,17	11,55				
Anode 2	A1	13,78	13,26				
Temp_1 [°C]	52,4	Temp_2[°C]	55,8	Temp_3 [°C]	55,9		
I_1 [A]	0,701	I_2 [A]	0,683	I_3 [A]	0,685		
U [V]	0,601						
Startzeit	✓		Endzeit	✓			
			Dauer [min-]	80			
Netzteil	1						

✓

VersuchNr.	158						
SOLL	80	min.	45	°C		A/dm^2	
					0,7	A	
	Nummer	Masse Start [g]	Masse Ende [g]	Fläche Kathode [cm^2]			
Kathode	46	18,19	19,34	4,655 x 3,55			
Anode 1	A 3	12,12	11,48				
Anode 2	A 5	20,51	19,99				
Temp_1 [°C]	40,9	Temp_2[°C]	44,3	Temp_3 [°C]	44,3		
I_1 [A]	0,704	I_2 [A]	0,696	I_3 [A]	0,693		
U [V]	0,595						
Startzeit	✓		Endzeit	✓			
			Dauer [min-]	80			
Netzteil	4						

✓

VersuchNr.	159					
SOLL	15	min.	25	°C		A/dm^2
					1,6	A

	Nummer	Masse Start [g]	Masse Ende [g]	Fläche Kathode [cm^2]
Kathode	203	18,17	18,66	4,35 x 3,50
Anode 1	A 20	14,45	14,18	
Anode 2	701	21,34	21,09	

Temp_1 [°C]	26,8	Temp_2[°C]	27,9	Temp_3 [°C]	28,4
I_1 [A]	1,603	I_2 [A]	1,577	I_3 [A]	1,578
U [V]	1,965				
Startzeit	✓		Endzeit	✓	
			Dauer [min-]	15	
Netzteil	3				

✓

VersuchNr.	160					
SOLL	15	min.	35	°C		A/dm^2
					1,6	A

	Nummer	Masse Start [g]	Masse Ende [g]	Fläche Kathode [cm^2]
Kathode	A 13	15,52	16,00	4,28 x 3,67
Anode 1	702	19,59	19,34	
Anode 2	A 23	12,15	11,90	

Temp_1 [°C]	35,1	Temp_2[°C]	35,1	Temp_3 [°C]	35,3
I_1 [A]	1,601	I_2 [A]	1,554	I_3 [A]	1,551
U [V]	1,737				
Startzeit	✓		Endzeit	✓	
			Dauer [min-]	15	
Netzteil	2				

~~Time correct?~~

✓

VersuchNr.	161					
SOLL	15	min.	55	°C		A/dm^2
					1,6	A

	Nummer	Masse Start [g]	Masse Ende [g]	Fläche Kathode [cm^2]
Kathode	706	17,~~69~~70	18,21	4,34 x 3,495
Anode 1	A 16	16,87	16,58	
Anode 2	A 6	17,12	16,88	

Temp_1 [°C]	55,0	Temp_2[°C]	55	Temp_3 [°C]	54,5
I_1 [A]	1,601	I_2 [A]	1,540	I_3 [A]	1,570
U [V]	1,116				
Startzeit	✓		Endzeit	✓	
			Dauer [min-]	15	
Netzteil	1				

Time correct? Yes!

✓

VersuchNr.	162					
SOLL	15	min.	45	°C		A/dm^2
					1,6	A

	Nummer	Masse Start [g]	Masse Ende [g]	Fläche Kathode [cm^2]
Kathode	A5-2	19,94	20,43	4,68 x 3,585
Anode 1	703	18,04	17,78	
Anode 2	704	16,9[illegible]4	16,68	

Temp_1 [°C]	45,5	Temp_2[°C]	45,4	Temp_3 [°C]	42,8
I_1 [A]	1,600	I_2 [A]	1,579	I_3 [A]	1,582
U [V]	1,312				
Startzeit	/		Endzeit	/	
			Dauer [min-]	15	
Netzteil	4				

VersuchNr.	163					
SOLL	10	min.	25	°C		A/dm^2
					1	A

	Nummer	Masse Start [g]	Masse Ende [g]	Fläche Kathode [cm^2]
Kathode	A4	19,74	19,45	4,2625 x 3,515
Anode 1	A21	11,81	11,72	
Anode 2	A17	16,48	16,38	

Temp_1 [°C]	27,0	Temp_2[°C]	/	Temp_3 [°C]	27,5
I_1 [A]	0,486	I_2 [A]	/	I_3 [A]	0,487
U [V]	1,200				
Startzeit	/		Endzeit	/	
			Dauer [min-]	10	
Netzteil	3				

VersuchNr.	164					
SOLL	10	min.	35	°C		A/dm^2
					1	A

	Nummer	Masse Start [g]	Masse Ende [g]	Fläche Kathode [cm^2]
Kathode	A16	17,09	17,28	4,245 x 3,655
Anode 1	734	19,32	19,22	
Anode 2	733	17,92	17,80	

Temp_1 [°C]	34,3	Temp_2[°C]	/	Temp_3 [°C]	34,2
I_1 [A]	1,002	I_2 [A]	/	I_3 [A]	0,973
U [V]	1,240				
Startzeit	/		Endzeit	/	
			Dauer [min-]	10	
Netzteil	2				

VersuchNr.	165					
SOLL	10	min.	55	°C		A/dm^2
					1	A

	Nummer	Masse Start [g]	Masse Ende [g]	Fläche Kathode [cm^2]
Kathode	731	18,30	18,51	4,28 x 3,44
Anode 1	427	17,52	17,41	
Anode 2	202	20,34	20,24	

Temp_1 [°C]	55,5	Temp_2[°C]	/	Temp_3 [°C]	54
I_1 [A]	1,000	I_2 [A]	/	I_3 [A]	0,971
U [V]	0,820				
Startzeit	/	Endzeit	/		
		Dauer [min-]	10		
Netzteil	1				

VersuchNr.	166					
SOLL	10	min.	45	°C		A/dm^2
					1	A

	Nummer	Masse Start [g]	Masse Ende [g]	Fläche Kathode [cm^2]
Kathode	732	17,13	17,34	4,255 x 3,70
Anode 1	426	17,56	17,45	
Anode 2	452	17,91	17,81	

Temp_1 [°C]	45,6	Temp_2[°C]	/	Temp_3 [°C]	44,5
I_1 [A]	1,003	I_2 [A]		I_3 [A]	0,981
U [V]	0,900				
Startzeit	/	Endzeit	/		
		Dauer [min-]	10		
Netzteil	4				

VersuchNr.	167					
SOLL	80	min.	25	°C		A/dm^2
					1	A

	Nummer	Masse Start [g]	Masse Ende [g]	Fläche Kathode [cm^2]
Kathode	A5	19,59	21,18	4,28 x 3,58
Anode 1	5-2	14,15	13,42	
Anode 2	208	13,05	12,17	

Temp_1 [°C]	24,1	Temp_2[°C]	23,3	Temp_3 [°C]	24,8
I_1 [A]	0,998	I_2 [A]	0,985	I_3 [A]	0,981
U [V]	1,300				
Startzeit	/	Endzeit	/		
		Dauer [min-]	80		
Netzteil	3				

VersuchNr.	168						
SOLL	~~[illegible]~~ 80	min.	35	°C		A/dm^2	
					1	A	

	Nummer	Masse Start [g]	Masse Ende [g]	Fläche Kathode [cm^2]
Kathode	43	17,88	19,45	4,285 x 3,54
Anode 1	710	14,32	13,53	
Anode 2	709	11,42	10,64	

Temp_1 [°C]	31,1	Temp_2[°C]	34	Temp_3 [°C]	34,8
I_1 [A]	1,000	I_2 [A]	0,473	I_3 [A]	0,474
U [V]	1,100				
Startzeit	✓	Endzeit	✓		
		Dauer [min-]	80		
Netzteil	2				

VersuchNr.	169						
SOLL	80	min.	55	°C		A/dm^2	
					1	A	

	Nummer	Masse Start [g]	Masse Ende [g]	Fläche Kathode [cm^2]
Kathode	705	17,65	19,32	4,38 x 3,15
Anode 1	41	15,99	15,18	
Anode 2	707	21,50	20,56	

Temp_1 [°C]	53,5	Temp_2[°C]	55,1	Temp_3 [°C]	55,4
I_1 [A]	0,498	I_2 [A]	0,488	I_3 [A]	0,484
U [V]	0,741				
Startzeit	✓	Endzeit	✓		
		Dauer [min-]	80		
Netzteil	1				

VersuchNr.	170						
SOLL	80	min.	45	°C		A/dm^2	
					1	A	

	Nummer	Masse Start [g]	Masse Ende [g]	Fläche Kathode [cm^2]
Kathode	706	18,85	20,48	4,625 x 3,52
Anode 1	708	13,85	13,03	
Anode 2	46	12,47	11,65	

Temp_1 [°C]	42,2	Temp_2[°C]	43,7	Temp_3 [°C]	43,8
I_1 [A]	1,000	I_2 [A]	0,488	I_3 [A]	0,490
U [V]	0,867				
Startzeit	✓	Endzeit	✓		
		Dauer [min-]	80		
Netzteil	4				

VersuchNr.	171						
SOLL	70	min.	25	°C			A/dm^2
						0,20	A

	Nummer	Masse Start [g]	Masse Ende [g]	Fläche Kathode [cm^2]
Kathode	730	21,56	21,84	4,265 x 3,55
Anode 1	A7	16,21	16,07	
Anode 2	206	13,48	13,34	

Temp_1 [°C]	27,3	Temp_2[°C]	26,5	Temp_3 [°C]	26,5
I_1 [A]	0,201	I_2 [A]	0,202	I_3 [A]	0,203
U [V]	0,320				
Startzeit	/	Endzeit	/		
		Dauer [min-]	70		
Netzteil	3				

VersuchNr.	172						
SOLL	70	min.	35	°C			A/dm^2
						0,20	A

	Nummer	Masse Start [g]	Masse Ende [g]	Fläche Kathode [cm^2]
Kathode	734	24,24	25,28	4,31 x 3,525
Anode 1	A2	16,68	16,19	
Anode 2	200	13,51	12,97	

Temp_1 [°C]	34,3	Temp_2[°C]	34	Temp_3 [°C]	33,5
I_1 [A]	0,~~200~~ 727	I_2 [A]	0,727	I_3 [A]	0,728
U [V]	0,~~[illegible]~~ 828				
Startzeit	/	Endzeit	/		
		Dauer [min-]	20		
Netzteil	2				

VersuchNr.	173						
SOLL	70	min.	55	°C			A/dm^2
						0,20	A

	Nummer	Masse Start [g]	Masse Ende [g]	Fläche Kathode [cm^2]
Kathode	736	15,98	16,25	4,27 x 3,56
Anode 1	221	12,86	12,70	
Anode 2	222	12,35	12,21	

Temp_1 [°C]	54,3	Temp_2[°C]	55,1	Temp_3 [°C]	55,7
I_1 [A]	0,200	I_2 [A]	0,204	I_3 [A]	0,207
U [V]	0,145				
Startzeit	/	Endzeit	/		
		Dauer [min-]	70		
Netzteil	1				

VersuchNr.	174					
SOLL	70	min.	45	°C		A/dm^2
					0,20	A

	Nummer	Masse Start [g]	Masse Ende [g]	Fläche Kathode [cm^2]
Kathode	735	18,92	19,20	4,28 x 3,51
Anode 1	111	13,61	13,46	
Anode 2	61	15,39	15,25	

Temp_1 [°C]	44,7	Temp_2[°C]	43,8	Temp_3 [°C]	44
I_1 [A]	0,201	I_2 [A]	0,206	I_3 [A]	0,206
U [V]	0,232				
Startzeit	/		Endzeit	/	
			Dauer [min-]	70	
Netzteil	4				

VersuchNr.	175					
SOLL	65	min.	25	°C		A/dm^2
					0,825	A

	Nummer	Masse Start [g]	Masse Ende [g]	Fläche Kathode [cm^2]
Kathode	734	25,26	26,33	4,35 x 3,5325
Anode 1	61	15,24	14,69	
Anode 2	206	13,33	12,81	

Temp_1 [°C]	24,4	Temp_2[°C]	26,1	Temp_3 [°C]	27,0
I_1 [A]	0,825	I_2 [A]	0,810	I_3 [A]	0,807
U [V]	1,040				
Startzeit	/		Endzeit	/	
			Dauer [min-]	65	
Netzteil	3				

VersuchNr.	176					
SOLL	65	min.	35	°C		A/dm^2
					0,825	A

	Nummer	Masse Start [g]	Masse Ende [g]	Fläche Kathode [cm^2]
Kathode	736	16,25	17,42	4,29 x 3,565
Anode 1	A2	16,18	15,60	
Anode 2	22	12,21	11,60	

Temp_1 [°C]	35,1	Temp_2[°C]	34,5	Temp_3 [°C]	34,2
I_1 [A]	0,825	I_2 [A]	0,842	I_3 [A]	0,841
U [V]	0,840				
Startzeit	/		Endzeit	/	
			Dauer [min-]	65	
Netzteil	2				

VersuchNr.	177						
SOLL	65	min.	55	°C			A/dm^2
						0,825	A

	Nummer	Masse Start [g]	Masse Ende [g]	Fläche Kathode [cm^2]
Kathode	735	19,20	20,37	4,29 x 3,53
Anode 1	221	12,69	12,13	
Anode 2	111	13,44	12,82	

Temp_1 [°C]	50,8	Temp_2[°C]	54,3	Temp_3 [°C]	55
I_1 [A]	0,825	I_2 [A]	0,856	I_3 [A]	0,854
U [V]	0,628				
Startzeit	✓		Endzeit	✓	
			Dauer [min-]	65	
Netzteil	1				

✓

VersuchNr.	178						
SOLL	65	min.	45	°C			A/dm^2
						0,825	A

	Nummer	Masse Start [g]	Masse Ende [g]	Fläche Kathode [cm^2]
Kathode	730	21,84	22,93	4,285 x 3,575
Anode 1	200	12,95	12,47	
Anode 2	47	16,06	15,44	

Temp_1 [°C]	45,8	Temp_2[°C]	44,0	Temp_3 [°C]	44,1
I_1 [A]	0,827	I_2 [A]	0,821	I_3 [A]	0,821
U [V]	0,771				
Startzeit	✓		Endzeit	✓	
			Dauer [min-]	65	
Netzteil	4				

✓

VersuchNr.	179						
SOLL	45	min.	25	°C			A/dm^2
						0,525	A

	Nummer	Masse Start [g]	Masse Ende [g]	Fläche Kathode [cm^2]
Kathode	411	17,80	18,27	4,335 x 3,55
Anode 1	5-1	16,36	16,11	
Anode 2	41	13,25	13,02	

Temp_1 [°C]	26,5	Temp_2[°C]	27,1	Temp_3 [°C]	27,5
I_1 [A]	0,526	I_2 [A]	0,526	I_3 [A]	0,526
U [V]	0,750				
Startzeit	✓		Endzeit	✓	
			Dauer [min-]	45	
Netzteil	3				

VersuchNr.	180					
SOLL	45	min.	35	°C		A/dm^2
					0,525	A

	Nummer	Masse Start [g]	Masse Ende [g]	Fläche Kathode [cm^2]
Kathode	207	19,84	20,30	4,29 x 3,57
Anode 1	A2	11,55	11,30	
Anode 2	A6	16,86	16,63	

Temp_1 [°C]	34,4	Temp_2[°C]	33,9	Temp_3 [°C]	33,7
I_1 [A]	0,525	I_2 [A]	0,512	I_3 [A]	0,516
U [V]	0,622				
Startzeit	✓	Endzeit	✓		
		Dauer [min-]	45		
Netzteil	2				

VersuchNr.	181					
SOLL	45	min.	55	°C		A/dm^2
					0,525	A

	Nummer	Masse Start [g]	Masse Ende [g]	Fläche Kathode [cm^2]
Kathode	413	16,70	17,18	4,33 x 3,46
Anode 1	211	19,31	19,07	
Anode 2	A5	19,4[illegible]7	19,20	

Temp_1 [°C]	54,5	Temp_2[°C]	55,9	Temp_3 [°C]	55,4
I_1 [A]	0,529	I_2 [A]	0,509	I_3 [A]	0,509
U [V]	0,396				
Startzeit	✓	Endzeit	✓		
		Dauer [min-]	45		
Netzteil	1				

VersuchNr.	182					
SOLL	45	min.	45	°C		A/dm^2
					0,525	A

	Nummer	Masse Start [g]	Masse Ende [g]	Fläche Kathode [cm^2]
Kathode	731	18,50	18,99	4,29 x 3,455
Anode 1	A8	18,87	18,62	
Anode 2	A3	11,46	11,20	

Temp_1 [°C]	43	Temp_2[°C]	44,3	Temp_3 [°C]	43,4
I_1 [A]	0,533	I_2 [A]	0,530	I_3 [A]	0,530
U [V]	0,560				
Startzeit	✓	Endzeit	✓		
		Dauer [min-]	45		
Netzteil	4				

VersuchNr.	183					
SOLL	45	min.	25	°C		A/dm^2
					1,475	A

	Nummer	Masse Start [g]	Masse Ende [g]	Fläche Kathode [cm^2]
Kathode	1/12	17,59	18,91	4,34 x 3,49
Anode 1	803	18,24	17,54	
Anode 2	A 20	14,17	13,52	

Temp_1 [°C]	26,7	Temp_2[°C]		Temp_3 [°C]	30,5
I_1 [A]	1,480	I_2 [A]		I_3 [A]	1,440
U [V]	2,012				
Startzeit			Endzeit		
			Dauer [min-]		
Netzteil	3				

VersuchNr.	184					
SOLL	45	min.	35	°C		A/dm^2
					1,475	A

	Nummer	Masse Start [g]	Masse Ende [g]	Fläche Kathode [cm^2]
Kathode	A3	19,42	20,67	4,345 x 3,555
Anode 1	802	19,82	19,24	
Anode 2	801	17,83	17,09	

Temp_1 [°C]	34	Temp_2[°C]		Temp_3 [°C]	35,0
I_1 [A]	1,426	I_2 [A]		I_3 [A]	1,320
U [V]	1,421				
Startzeit			Endzeit		
			Dauer [min-]		
Netzteil	2				

VersuchNr.	185					
SOLL	45	min.	55	°C		A/dm^2
					1,475	A

	Nummer	Masse Start [g]	Masse Ende [g]	Fläche Kathode [cm^2]
Kathode	A4	19,93	21,26	4,27 x 3,50
Anode 1	A26	16,29	15,67	
Anode 2	800	11,90	11,20	

Temp_1 [°C]	54	Temp_2[°C]		Temp_3 [°C]	55,8
I_1 [A]	1,425	I_2 [A]		I_3 [A]	1,388
U [V]	1,051				
Startzeit			Endzeit		
			Dauer [min-]		
Netzteil	1				

VersuchNr.	186				
SOLL	45	min.	45	°C		A/dm^2
					1,475	A

	Nummer	Masse Start [g]	Masse Ende [g]	Fläche Kathode [cm^2]
Kathode	416	17,28	18,65	4,27 x 3,53
Anode 1	205	16,26	15,63	
Anode 2	116	18,86	18,11	

Temp_1 [°C]	44,1	Temp_2[°C]		Temp_3 [°C]	44,8
I_1 [A]	1,435	I_2 [A]		I_3 [A]	1,257
U [V]	1,260				
Startzeit			Endzeit		
			Dauer [min-]		
Netzteil	4				

VersuchNr.	187					
SOLL	10	min.	25	°C		A/dm^2
					~~0,4~~ 1,275	A

	Nummer	Masse Start [g]	Masse Ende [g]	Fläche Kathode [cm^2]
Kathode	810	19,75	20,14	4,265 x 3,52
Anode 1	222	11,58	11,42	
Anode 2	221	12,11	11,89	

Temp_1 [°C]	30	Temp_2[°C]	30,2	Temp_3 [°C]	30,8
I_1 [A]	1,286	I_2 [A]	1,261	I_3 [A]	1,260
U [V]	1,590				
Startzeit			Endzeit		
			Dauer [min-]		
Netzteil	3				

VersuchNr.	188					
SOLL	10	min.	35	°C		A/dm^2
					1,275	A

	Nummer	Masse Start [g]	Masse Ende [g]	Fläche Kathode [cm^2]
Kathode	732	17,34	17,72	4,25 x 3,59
Anode 1	A7	15,43	15,24	
Anode 2	203	12,46	12,25	

Temp_1 [°C]	34,8	Temp_2[°C]	34,3	Temp_3 [°C]	
I_1 [A]	1,284	I_2 [A]		I_3 [A]	1,272
U [V]	1,581				
Startzeit			Endzeit		
			Dauer [min-]		
Netzteil					

VersuchNr.	189						
SOLL	10	min.	55	°C		A/dm^2	
					1,275	A	

	Nummer	Masse Start [g]	Masse Ende [g]	Fläche Kathode [cm^2]
Kathode	736	17,42	17,82	4,325 x 3,59
Anode 1	61	14,62	14,47	
Anode 2	206	12,79	12,59	

Temp_1 [°C]	55,0	Temp_2[°C]	~~[illegible]~~ 54,9	Temp_3 [°C]	
I_1 [A]	1,273	I_2 [A]		I_3 [A]	1,252
U [V]	0,960				
Startzeit			Endzeit		
			Dauer [min-]		
Netzteil					

VersuchNr.	190						
SOLL	10	min.	45	°C		A/dm^2	
					1,275	A	

	Nummer	Masse Start [g]	Masse Ende [g]	Fläche Kathode [cm^2]
Kathode	736	22,93	23,33	4,29 x 3,56
Anode 1	812	12,80	12,61	
Anode 2	84	15,59	15,39	

Temp_1 [°C]	45,0	Temp_2[°C]	42,0	Temp_3 [°C]	
I_1 [A]	1,273	I_2 [A]		I_3 [A]	1,253
U [V]	1,080				
Startzeit			Endzeit		
			Dauer [min-]		
Netzteil					

VersuchNr.							
SOLL		min.		°C		A/dm^2	
						A	

	Nummer	Masse Start [g]	Masse Ende [g]	Fläche Kathode [cm^2]
Kathode				
Anode 1				
Anode 2				

Temp_1 [°C]		Temp_2[°C]		Temp_3 [°C]	
I_1 [A]		I_2 [A]		I_3 [A]	
U [V]					
Startzeit			Endzeit		
			Dauer [min-]		
Netzteil					

VersuchNr.	141						
SOLL		min.	25	°C		A/dm^2	
					0,22	A	

	Nummer	Masse Start [g]	Masse Ende [g]	Fläche Kathode [cm^2]
Kathode	751	18,98	19,35	4,30x3,455
Anode 1	800	11,18	11,01	
Anode 2	812	12,59	12,40	

Temp_1 [°C]	24,7	Temp_2[°C]	26,2	Temp_3 [°C]	26,8
I_1 [A]	0,222	I_2 [A]	0,226	I_3 [A]	0,224
U [V]	0,380				
Startzeit	[illegible]	Endzeit			
		Dauer [min-]	85		
Netzteil					

VersuchNr.	142						
SOLL		min.	35	°C		A/dm^2	
					0,22	A	

	Nummer	Masse Start [g]	Masse Ende [g]	Fläche Kathode [cm^2]
Kathode	810	20,13	20,49	4,30 x 3,525
Anode 1	888	19,68	19,49	
Anode 2	93	11,19	11,01	

Temp_1 [°C]	31,5	Temp_2[°C]	34,2	Temp_3 [°C]	33,9
I_1 [A]	0,219	I_2 [A]	0,218	I_3 [A]	0,212
U [V]	0,356				
Startzeit		Endzeit			
		Dauer [min-]	84		
Netzteil					

VersuchNr.	143						
SOLL		min.	55	°C		A/dm^2	
					0,22	A	

	Nummer	Masse Start [g]	Masse Ende [g]	Fläche Kathode [cm^2]
Kathode	732	17,73	18,10	4,28 x 3,62
Anode 1	61	14,45	14,26	
Anode 2	206	12,58	12,40	

Temp_1 [°C]	53	Temp_2[°C]	54,8	Temp_3 [°C]	55,4
I_1 [A]	0,220	I_2 [A]	0,225	I_3 [A]	0,226
U [V]	0,200				
Startzeit		Endzeit			
		Dauer [min-]	83		
Netzteil					

VersuchNr.	194					
SOLL		min.	45	°C		A/dm^2
					0,22	A

	Nummer	Masse Start [g]	Masse Ende [g]	Fläche Kathode [cm^2]
Kathode	U 13	17,17	17,54	4,345 x 3,45
Anode 1	200	12,124	12,06	
Anode 2	12	15,23	15,03	

Temp_1 [°C]	45,6	Temp_2[°C]	44,2	Temp_3 [°C]	44,5
I_1 [A]	0,225	I_2 [A]	0,230	I_3 [A]	0,230
U [V]	0,244				
Startzeit			Endzeit		
			Dauer [min-]	82	
Netzteil					

VersuchNr.						
SOLL		min.		°C		A/dm^2
						A

	Nummer	Masse Start [g]	Masse Ende [g]	Fläche Kathode [cm^2]
Kathode				
Anode 1				
Anode 2				

Temp_1 [°C]		Temp_2[°C]		Temp_3 [°C]	
I_1 [A]		I_2 [A]		I_3 [A]	
U [V]					
Startzeit			Endzeit		
			Dauer [min-]		
Netzteil					

VersuchNr.						
SOLL		min.		°C		A/dm^2
						A

	Nummer	Masse Start [g]	Masse Ende [g]	Fläche Kathode [cm^2]
Kathode				
Anode 1				
Anode 2				

Temp_1 [°C]		Temp_2[°C]		Temp_3 [°C]	
I_1 [A]		I_2 [A]		I_3 [A]	
U [V]					
Startzeit			Endzeit		
			Dauer [min-]		
Netzteil					

VersuchNr.	145					
SOLL		min.	25	°C		A/dm^2
					0,579	A

	Nummer	Masse Start [g]	Masse Ende [g]	Fläche Kathode [cm^2]
Kathode	408	14,25	14,89	4,245 x 3,56
Anode 1	A1	15,17	14,83	
Anode 2	A21	11,71	11,41	

Temp_1 [°C]	27,5	Temp_2[°C]		Temp_3 [°C]	28,2
I_1 [A]	0,578	I_2 [A]		I_3 [A]	0,572
U [V]	0,840				
Startzeit		Endzeit			
		Dauer [min-]	55		
Netzteil					

VersuchNr.	146					
SOLL		min.	35	°C		A/dm^2
					0,579	A

	Nummer	Masse Start [g]	Masse Ende [g]	Fläche Kathode [cm^2]
Kathode	907	19,78	20,42	4,28 x 3,45
Anode 1	V6	18,07	17,75	
Anode 2	912	17,43	17,09	

Temp_1 [°C]	33,9	Temp_2[°C]		Temp_3 [°C]	34,1
I_1 [A]	0,5[illegible]	I_2 [A]		I_3 [A]	0,552
U [V]	0,694				
Startzeit		Endzeit			
		Dauer [min-]	55		
Netzteil					

VersuchNr.	147					
SOLL		min.	55	°C		A/dm^2
					0,579	A

	Nummer	Masse Start [g]	Masse Ende [g]	Fläche Kathode [cm^2]
Kathode	906	17,65	18,31	4,27 x 3,48
Anode 1	911	20,63	20,28	
Anode 2	910	15,38	15,05	

Temp_1 [°C]	54,3	Temp_2[°C]		Temp_3 [°C]	55,6
I_1 [A]	0,579	I_2 [A]		I_3 [A]	0,566
U [V]	0,464				
Startzeit		Endzeit			
		Dauer [min-]	55		
Netzteil					

VersuchNr.	198						
SOLL		min.	45	°C			A/dm^2
						0,579	A

	Nummer	Masse Start [g]	Masse Ende [g]	Fläche Kathode [cm^2]
Kathode	905	19,75	20,41	4,63 x 3,58
Anode 1	709	10,62	10,28	
Anode 2	205	15,67	15,30	

Temp_1 [°C]	45	Temp_2[°C]		Temp_3 [°C]	43,9
I_1 [A]	0,572	I_2 [A]		I_3 [A]	0,584
U [V]	0,532				
Startzeit			Endzeit		
			Dauer [min-]	55	
Netzteil					

VersuchNr.	199						
SOLL		min.	25	°C			A/dm^2
						1,4	A

	Nummer	Masse Start [g]	Masse Ende [g]	Fläche Kathode [cm^2]
Kathode	404	21,14	21,58	4,30 x 3,535
Anode 1	809	~~10,2~~ 11,24	11,11	
Anode 2	5-2	13,39	13,16	

Temp_1 [°C]	28	Temp_2[°C]		Temp_3 [°C]	29,8
I_1 [A]	1,451	I_2 [A]		I_3 [A]	1,424
U [V]	1,280				
Startzeit			Endzeit		
			Dauer [min-]	15	
Netzteil					

VersuchNr.	200						
SOLL		min.	35	°C			A/dm^2
						1,4	A

	Nummer	Masse Start [g]	Masse Ende [g]	Fläche Kathode [cm^2]
Kathode	903	16,24	16,71	4,27 x 3,50
Anode 1	208	12,17	11,99	
Anode 2	207	20,22	19,95	

Temp_1 [°C]	34,6	Temp_2[°C]		Temp_3 [°C]	35,1
I_1 [A]	1,400	I_2 [A]		I_3 [A]	1,353
U [V]	1,652				
Startzeit			Endzeit		
			Dauer [min-]		
Netzteil					

VersuchNr.	201						
SOLL		min.	55	°C		A/dm^2
					1,4	A

	Nummer	Masse Start [g]	Masse Ende [g]	Fläche Kathode [cm^2]
Kathode	902	18,41	18,84	4,235 x 3,52
Anode 1	A6	11,62	11,43	
Anode 2	720	13,51	13,28	

Temp_1 [°C]	55,7	Temp_2[°C]		Temp_3 [°C]	54,6
I_1 [A]	1,400	I_2 [A]		I_3 [A]	1,365
U [V]	1,105				
Startzeit		Endzeit			
		Dauer [min-]			
Netzteil					

VersuchNr.	202					
SOLL		min.	45	°C		A/dm^2
					1,4	A

	Nummer	Masse Start [g]	Masse Ende [g]	Fläche Kathode [cm^2]
Kathode	901	17,39	17,86	4,59 x 3,54
Anode 1	708	13,01	12,76	
Anode 2	452	17,79	17,57	

Temp_1 [°C]	43	Temp_2[°C]		Temp_3 [°C]	44,8
I_1 [A]	1,433	I_2 [A]		I_3 [A]	1,401
U [V]	1,100				
Startzeit		Endzeit			
		Dauer [min-]			
Netzteil					

VersuchNr.						
SOLL		min.		°C		A/dm^2
						A

	Nummer	Masse Start [g]	Masse Ende [g]	Fläche Kathode [cm^2]
Kathode				
Anode 1				
Anode 2				

Temp_1 [°C]		Temp_2[°C]		Temp_3 [°C]	
I_1 [A]		I_2 [A]		I_3 [A]	
U [V]					
Startzeit		Endzeit			
		Dauer [min-]			
Netzteil					